Atherosclerotic Plaque Vulnerability in Experimental Models of Atherosclerosis

Dolf Segers

op de weg over pieken en door dalen
vindt men bewijs voor het tegendeel

Atherosclerotic plaque vulnerability in experimental models of atherosclerosis

Atherosclerotic Plaque Vulnerability in Experimental Models of Atherosclerosis

Instabiliteit van Atherosclerotische Plaques in Experimentele Modellen van Atherosclerose

Proefschrift

ter verkrijging van de graad van doctor aan de
Erasmus Universiteit Rotterdam
op gezag van de
rector magnificus

Prof.dr. H.G. Schmidt,

en volgens besluit van het College voor Promoties.

De openbare verdediging zal plaatsvinden op
woensdag 23 november 2011 om 9:30 uur

door

Dolf Segers

geboren te Tilburg

ERASMUS UNIVERSITEIT ROTTERDAM

Doctoral Committee

Promotores: prof.dr.ir. A.F.W. van der Steen
                 prof.dr. R. Krams

Copromotor: dr. M.P.G. de Crom

Overige leden: prof.dr. D.J. Duncker
                 prof.dr. F.G. Grosveld
                 prof.dr. G. Pasterkamp

Contents

shear high adaptive models cellular receptors segment plaques surface mice lesion stress studies human two specific vascular innate atherosclerotic response plaque molecules cholesterol lesions blood chapter Table low macrophages involved role also wall disease chemokines like system e.g may many

atherosclerosis

immune cells mechanisms cytokines genetic immunity activation endothelial

Chapter 1

General Introduction

Introduction

Atherosclerosis is a chronic and often progressive disease of the wall of the arterial vasculature. The term atherosclerosis is derived from the Greek words "athero" meaning gruel or paste and "skleros" meaning stiff or hard. Atherosclerosis is considered a major clinical problem, which underlies most ischemic events of both the heart as well as the brain. It is the result of the Western lifestyle and can start very early in life even in persons without a strong genetic disposition like untreated familial hypercholesteremia[1-3]. From the second decade onwards, the disease progresses more rapidly. The clinical silence of atherosclerosis is often broken between the 3rd and 5th decade, when patients present with ischemic complaints of e.g. heart and brain.

Despite the continuing decrease in cardiovascular disease (CVD) associated death over the last decade, it still is one of the main causes of death in The Netherlands, accounting for 30,7% of total deaths in 2007[4]. As a result, the socio-economic consequences remain huge. It has been estimated that in the European Union annual CVD-associated costs are €169 billion, of which €105 billion are costs directly related to healthcare[5].

Historically, atherosclerosis was simply considered as an accumulation of lipids in the vascular wall. In the late 90's, Russell Ross proposed a major revision of this theory[6], and these days the perspective of atherosclerosis as a complicated lipid-driven inflammatory disease is widely accepted. Lipid metabolism and inflammation mutually influence each other yielding the complete spectrum of atherosclerotic disease progression. This is reflected in the correlation between future cardiovascular events and the combined values of cholesterol, as indicator of lipid status, and CRP, as indicator of systemic inflammatory activity[7, 8]. Since CRP levels reflect systemic inflammatory activity, this notion underscores the role of immunity in human atherosclerosis.

The development of atherosclerosis is strongly associated with conditions like hypertension, diabetes, and hypercholesterolemia and bad life style habits like smoking and lack of physical exercise. These so-called classical risk factors were identified by the Framingham Heart Study[9]. They induce an unbeneficial environment for the inner cellular lining of the arteries, the endothelial cells, which become dysfunctional[10] and loose their barrier function, enabling the circulating cholesterol-containing lipoproteins to pass the endothelial layer[11]. The cholesterol starts to accumulate and it becomes trapped by binding to extracellular matrix. Dysfunctional endothelium also produces chemokines and adhesion molecules, which attract and bind leukocytes to the vascular wall respectively[11], and starts the inflammatory process, which will be discussed later.

```
┌────────────────────────────────────────┐   ┌────────────────────────────────────────┐
│ Intima at highly susceptible sites of arteries │   │ Intima at moderatelysusceptible sites of arteries │
└────────────────────────────────────────┘   └────────────────────────────────────────┘

┌────────────────────────────────────────┐
│        I. isolated macrophage foam cells        │
└────────────────────────────────────────┘

┌────────────────────────────────────────┐
│        II. Multiple foam cell layers formed      │      regression of
└────────────────────────────────────────┘      type I-III changes
                                                 to normal is possible

┌────────────────────────────────────────┐
│     III. Isolated extracellular lipid pools formed   │
└────────────────────────────────────────┘

┌────────────────────────────────────────┐
│     IV. Confluent extracellular lipid pool formed    │
└────────────────────────────────────────┘

┌────────────────────────────────────────┐
│        V. Fibromuscular tissue layers formed      │      fibrosis of type VI
└────────────────────────────────────────┘      adds to type V thickness
                                                 and stiffness and results
   successive type IV episodes may quickly lead to occlusion      in loss of lumen

┌────────────────────────────────────────┐
│      VI. Surface defect, hematoma, thrombosis     │
└────────────────────────────────────────┘

┌────────────────────────────────────────┐
│        VII. Calcifications predominate           │      regression or change of
└────────────────────────────────────────┘      lipid in lesion types IV-VI
                                                 may result in lesion
┌────────────────────────────────────────┐      types VII-VIII
│    VIII. Fibrous tissue changes predominate      │
└────────────────────────────────────────┘
```
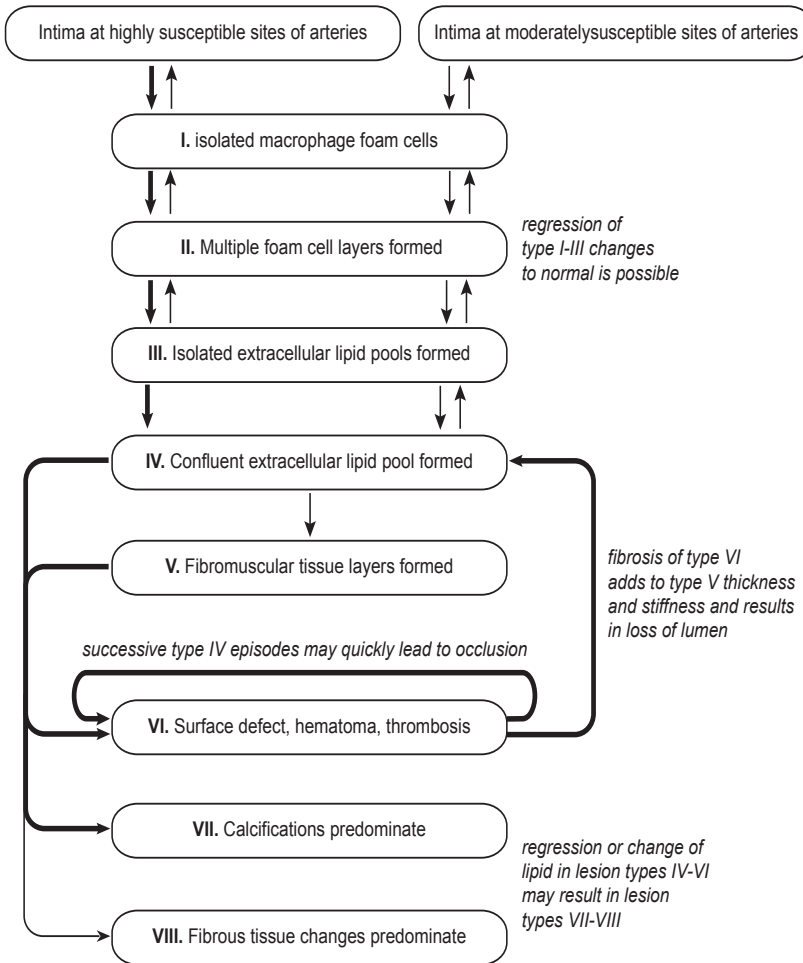
Figure 1. Schematic of the chronological transitions between the lesion types as recommended by the American Heart Association. The stroke of the arrows indicated Wthe likelihood of the transition. Adapted from[14]

Important differences in lesion morphology

Atherosclerotic plaques are not uniform in their presentation. There is a large gradient of lesion morphologies depending on the natural history of the lesion. To structure organization of lesions, a classification system has been developed by the American Heart Association[12, 13], which has been updated[14] and modified[15] recently. The classification recommended by the American Heart Association (AHA) organizes the lesions into 6 groups (Type I-VI) and is displayed in Figure 1.

In general, plaques may be regarded as either early or mature lesions. Early lesions consist of the AHA Type I-III plaques. These are always small and clinically silent, despite the fact that lesions size usually does not predict its composition, luminal obstruction or clinical relevance[14]. As a result, all mature lesions (AHA type IV-VI) are capable of inducing luminal obstruction to the point of clinical symptoms or even a fatal event. Nevertheless, the AHA Type IV-V lesions are most often associated with clinical presentation. These plaques are characterized by a large necrotic pool of lipids and cellular debris covered by a fibrous cap consisting of collagen and smooth muscle cells. The amount of collagenous structures present in these caps is essential for its stability. When the cap thins, it becomes prone to rupture or erosion, which will result in intraluminal thrombosis and possible instant occlusion of the artery, refraining downstream tissues of oxygen supply. These rupture-prone lesions are often called unstable or vulnerable plaques and are believed to be the main cause of myocardial infarctions[16].

Inflammation driven by integrated innate and adaptive immune mechanisms

Although our awareness of the complexity of the immune system is expanding continuously, the principles of immune regulation of inflammation are increasingly well understood. Also, since the immune system plays such a central role in atherosclerosis, an overview of these fundamentals is essential. The figures and tables cover and summarize the contents of this part, while the references include more comprehensive reviews and detailed studies on the different subjects.

Figure 2 outlines the generic inflammatory cascade, which appears to be remarkably applicable to the events observed in the arterial wall upon initiation and progression of atherosclerotic lesions. Central to the initiation of this cascade is the recognition of exogenous or (altered) endogenous molecules by cells of both innate and adaptive immunity. Activation of cells in both arms leads to an integrated response, triggering the pathogenic vascular effects characteristic of the disease. In the following paragraphs, we focus in particular on these early steps of recognition and the ensuing cellular response, and apply these to the specific conditions of atherosclerosis, since recent developments in this area have led to exciting new insights in the pathogenesis of inflammatory diseases, including atherosclerosis.

Innate versus adaptive immunity

Table 1 globally compares innate with adaptive immunity. The principal difference between the two arms of the immune system is the nature of the cellular receptors involved in recognition of potentially pathogenic molecules and the triggering of these cells, which leads to cellular activation. Receptors of adaptive immunity, expressed only by T- and B-lymphocytes, are generated by recombination of
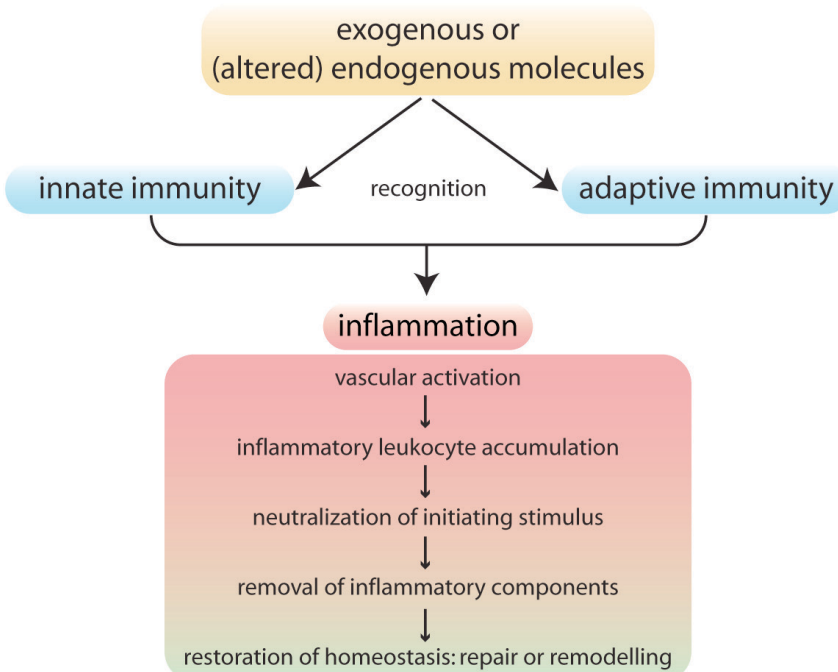
Figure 2. The inflammatory cascade in atherosclerosis, involving collaboration of innate and adaptive immunity, follows a common pathway.

The inflammatory response is triggered by recognition of specific molecules by cells of innate and adaptive immunity that lead to their activation. The ensuing inflammatory cascade is initiated by lipid uptake in the vessel wall, which facilitates accumulation of leukocytes. These mobile defense forces attempt to neutralize and remove the initial trigger. If successful, inflammation subsides and homeostasis can be restored by tissue repair. Semi-successful elimination triggers tissue remodeling, allowing partial functionality. Adapted from[79].

gene segments, while receptors of innate immunity are encoded as such within the genome, not requiring genetic recombination. Leukocytes involved in innate immunity such as monocytes, macrophages (Mf), dendritic cells (DC) and granulocytes express a large variety of receptors recognizing molecules of pathogens. For example, they can express receptors for bacterial compounds such as lipopolysaccharide (LPS) and for viral RNA (see also Tables 2 and 3, for receptors and ligands, respectively). The specificity of these receptors is fixed by the nature of their static genetic encoding. In general, all body cells can make use of several innate immune mechanisms involving such receptors. However, the leukocytes of innate immunity are unique in the fact that they provide a mobile response and are specialized in expressing various host defense mechanisms upon triggering. As a consequence of their mobility and functional specialization, these
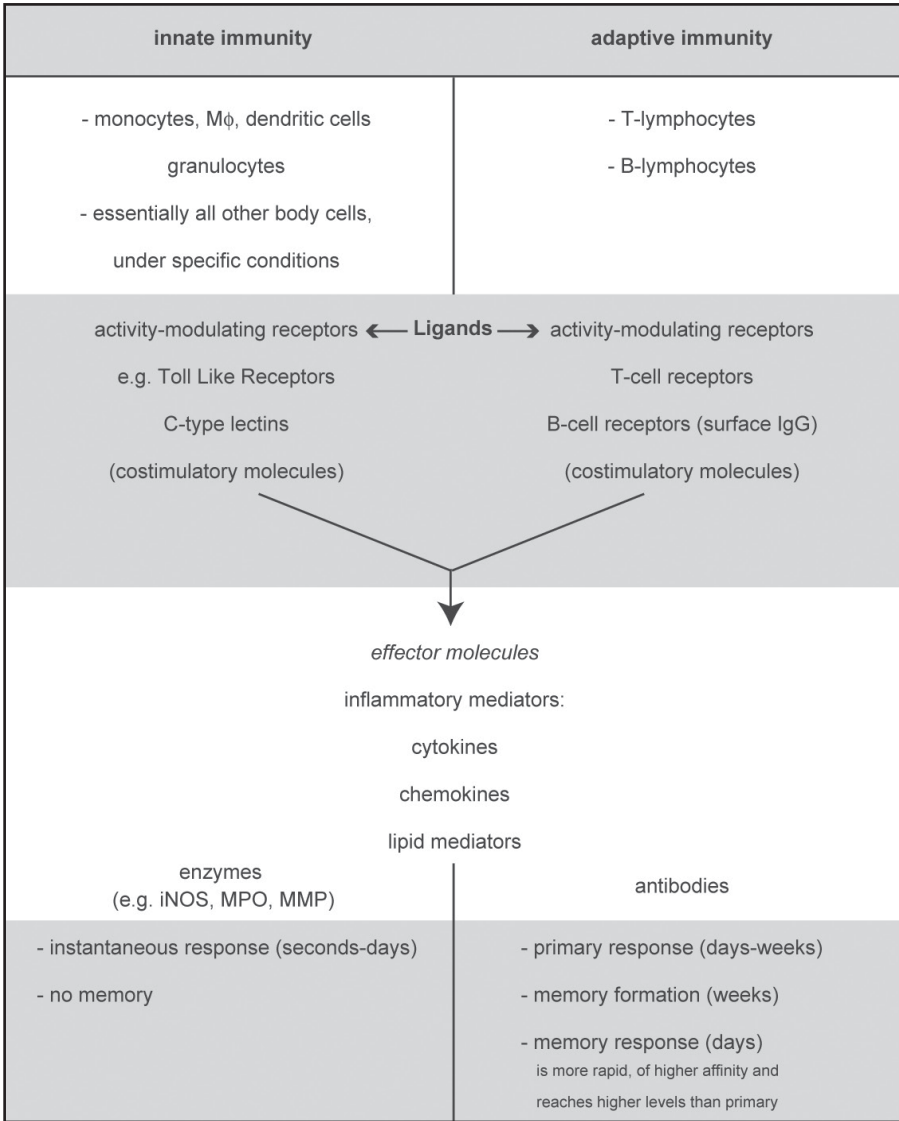
innate immunity	adaptive immunity
- monocytes, Mφ, dendritic cells granulocytes - essentially all other body cells, under specific conditions	- T-lymphocytes - B-lymphocytes
activity-modulating receptors ⟵ **Ligands** ⟶ activity-modulating receptors e.g. Toll Like Receptors T-cell receptors C-type lectins B-cell receptors (surface IgG) (costimulatory molecules) (costimulatory molecules)	

effector molecules

inflammatory mediators:

cytokines

chemokines

lipid mediators

enzymes (e.g. iNOS, MPO, MMP)	antibodies

- instantaneous response (seconds-days)
 	
- no memory
	- primary response (days-weeks)
	
	- memory formation (weeks)
	
	- memory response (days)
	  is more rapid, of higher affinity and
	  reaches higher levels than primary

Table 1. *Global comparison of innate and adaptive immunity.*
Cells involved in innate or adaptive immunity employ distinct receptors to recognize ligands that trigger cellular activation. Interaction of stimulated cells of either pathway leads to further activation and release of inflammatory mediators and effector molecules, which are partially specific for each response type. Since efficacy of the adaptive immune response depends on proliferation of antigen-specific lymphocytes, the kinetics of innate and adaptive responses are essentially different.

cells can rapidly accumulate at affected tissue sites in case of injury or infection and create an effective response.

In contrast to innate immunity, adaptive immunity is exclusively restricted to T- and B-lymphocytes. These cells employ intricate mechanisms to rearrange gene building blocks, thus constructing novel receptors. Such receptors are cell-specific (clonotypic) and the expressing cells are subsequently selected for optimal recognition of an antigenic ligand and clonal expansion. The T-cell receptor expressed on the surface of the T lymphocyte specifically recognizes pathogenic or self-peptides presented by major histocompatibility (MHC) class II (for the CD4+ T helper cells) or MHC class I (for the CD8+ cytotoxic T-cells). MHC molecules are the scaffolds expressed by antigen presenting cells (APC), which expose peptides to lymphocytes, controlling responses in infection and transplantation. B-lymphocytes use their unique cell surface immunoglobulin as antigen-specific receptor and, after activation, secrete these as antibodies that are able to recognize epitopes on intact proteins.

The innate response to potentially harmful substances provides immediate protection (seconds to hours), while the adaptive response takes longer to develop (days), but has the unique properties of very high specificity and memory formation, with a stronger and higher affinity response upon second exposure (i.e. the principle of vaccination). Although the definition of adaptive versus innate immunity is clear-cut (yes or no genetic recombination to form receptors), these two arms of the immune system are completely integrated and intertwined, since they depend on mutual activation for an optimal response (see middle part of Table 1). Moreover, T and B-lymphocytes express several innate receptors in addition to their cell-specific antigen receptor. Upon activation by recognition of cognate ligands, cells of both innate and adaptive immunity produce soluble signaling molecules, including cytokines and chemokines (Table 1). In addition, they express sets of costimulatory molecules on their surface guiding cellular interactions and modulating the ultimate response to the initial pathogenic stimulus. So, although the definition of the two separate arms is clear, innate and adaptive immunity work coordinately and jointly. Much of this coordination and integration is brought about by APC, in particular Mf and DC. The cells of the Mf/DC lineage are specialists in immune regulation by virtue of their high level expression of the relevant surface molecules and the ability to migrate and thus convey environmental information to and from the adaptive immune system. This environmental information is particularly sensed by a variety of innate antigen receptors that have been discovered over the last years and which appear to belong to large families of partially unknown molecules (Table 2).

innate immunity receptors	adaptive immunity receptors
receptors as such encoded in the genome	receptors generated by genetic recombination

scavenger receptors
   (e.g. CD36, SR-A1/2, CD68, LDL-R)
toll-like receptors
NOD-like receptors
C-type lectins
immunoglobulin Fc receptors
complement receptors
	T cell receptors (TCR)
	estimated potential repertoire:
	   ~10^{18} different R
	   actually present: ~10^7
	
	B cell receptors (BCR/immunoglobulins)
	estimated potential repertoire:
	   ~10^{11} different R
	   actually present: ~10^7

Table 2. *Major receptors used in innate and adaptive immunity.*
Cells involved in innate and adaptive immune responses use essentially distinct receptors to recognize potentially harmful substances. Binding of foreign or endogenous ligands to such receptors may have very diverse effects, depending on the status of the cells involved and on the molecular pathway(s) connected to the respective receptors.

Atherosclerosis: innate and adaptive immunity out of control?

The role of the immune system in atherosclerosis has gained acceptance in the last two decades because of a series of experiments performed mainly by human pathologists in parallel to experimental vascular biologists. Pathologists showed that in addition to foamy Mf, also T-cells, B-cells and DC are present in human atherosclerotic plaques[17-20] (Figure 3). Since MHC class-II and co-stimulatory molecules like CD40, CD80 and CD86 were also expressed in plaques obtained at autopsy[21-25], important requirements for local activation of adaptive immune mechanisms are fulfilled. Evidence suggests that activated T-cells in both human and mouse plaques are of oligoclonal origin[26, 27], implying selective activation by a limited number of antigenic epitopes. The expression of Toll-like receptors (TLR) in human plaques, especially in vulnerable plaques, allows the activation of the innate immune system not only by microbial ligands, but also by potential endogenous ligands such as modified LDL and heat shock proteins[28, 29].

These human studies were paralleled by studies in experimental atherosclerosis models, in particular those focusing on chemokines and cytokines, both soluble mediators of inflammation. Cytokines are key players in the inflammatory response. They are centrally involved in orchestrating the initiation, propagation and regulation of the inflammatory response. Many cytokines involved in atherosclerosis, exerting both pro-inflammatory as well as anti-inflammatory effects. A summary of cytokines in atherosclerosis have been recently reviewd in[30]. Chemokines, a combination of the words chemotactic cytokines, are a family of proteins that play an important role in atherosclerosis[31]. They control the
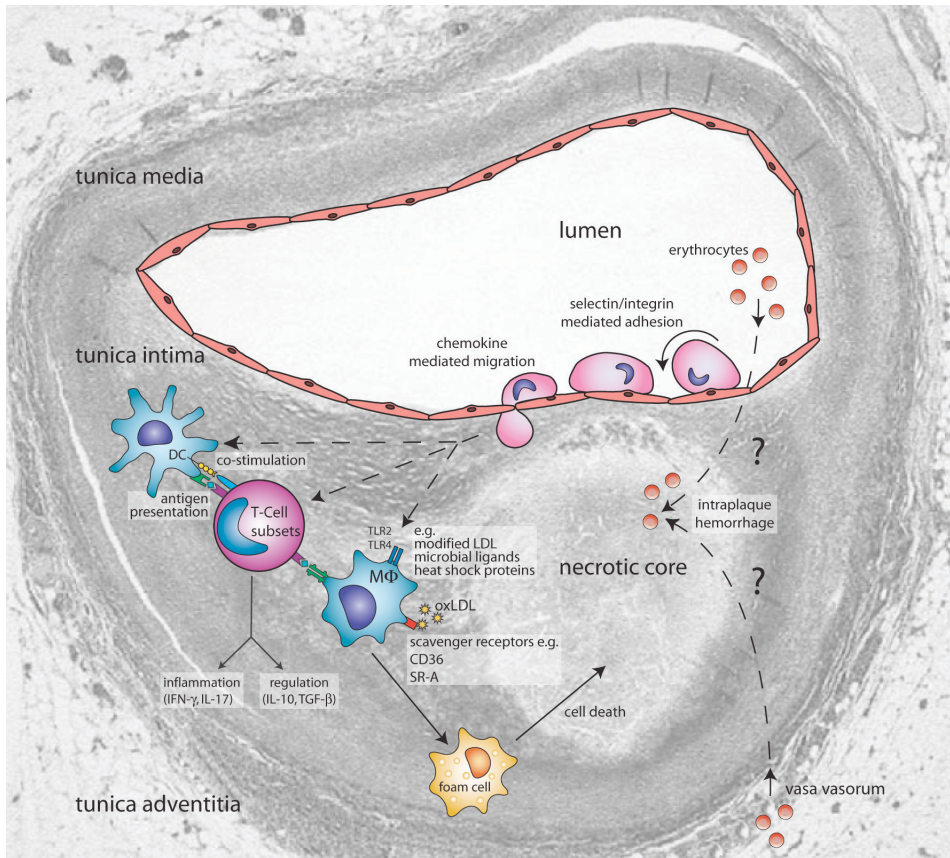
Figure 3. *Immune mechanisms in atherosclerosis projected onto a vulnerable plaque section*.
This schematic view displays selected mechanisms discussed in the general introduction, with special emphasis on immune modulatory therapy. The histological section displays a lumen-narrowing plaque, which consists of a large necrotic core covered by a thin fibrous cap. This is a typical example of a vulnerable plaque. In brief, monocytes and lymphocytes roll over, and adhere to the dysfunctional vascular endothelium, and subsequently migrate into the vascular wall. Next, monocytes will differentiate into dendritic cells and macrophages. Macrophage uptake of oxLDL results in the formation of foam cells, which form a major constituent of the growing plaque. Demise of foam cells by necrosis or apoptosis gives rise to a necrotic core. Activation of T-cells by macrophages and dendritic cells results in the differentiation of T-cells into distinct subsets that either promote inflammation (Th1, Th2, Th-IL-17) or limit the inflammatory process (Treg). Also, the neovascularization in the plaque and the vasa vasorum of the plaque is displayed, which possibly leads to intraplaque hemorrhages. Please note that the cartoon components are not drawn to scale with respect each other, nor to the underlying section. This plaque section was previously published in[80]. Adapted with permission from The American College of Cardiology Foundation.

Mouse Model	Effect on lesion size	Effect on plaque composition	Reference
CCR2-/- LDLr-/-	Atherosclerosis ↓	Macrophages ↓	83
CCR2-/- Apoe-/-	Neointima ↓	not described	84
CCR2-/- BM > Apoe3-Leiden	Atherosclerosis ↓	Macrophages ↓, NS	58
CCR5-/- Apoe-/-	Aortic root ↓ Aorta ↓	Mononuclear cells ↓ T cells ↓	85
CCR5-/- Apoe-/-	Neointima ↓	IL-10 expression SMC ↑	86
CCL5-/- BM > Apoe-\-	Aortic root ↓	Macrophages ↓	87
Treating LDLr-/- with CCR5/ CXCR3 inhibitor TAK-779	Aortic root ↓ Brachiocephalic artery ↓	Macrophages ↓ T cells ↓	88
CX3CL1-/- Apoe-/-	Brachiocephalic artery ↓ Aortic root ↔	Macrophages ↓ Macrophages ↓	89
CX3CL1-/- Apoe-/-	Proximal & thoracic aorta ↓	Macrophages ↓	39, 40
CX3CL1-/- LDLr-/-	Brachiocephalic artery ↓ Aortic root ↓	Macrophages ↓ Macrophages ↓	89
CX3CL1-/- CCR2-/- Apoe-/-	Proximal aortic root ↓ Aorta ↓	Monocyte recruitment ↓ Monocyte recruitment ↓	90
CCL2, CX3CR1 and CCR5 inhibition	Aortic root ↓	Circulating Ly6C-lo ↓	91
CXCR3-/- Apoe-/-	Abdominal aorta ↓	Regulatory T cells ↑	92
CXCR3 antagonist in LDLr-/-	Aortic root ↓	Macrophages & T cells ↓	93
CXCL10-/- Apoe-/-	Aortic arch ↓	Macrophages ↓ CD4+ CXCR3+ T cells ↓	94

Table 3. *Overview of literature regarding chemokines described in this thesis.*

This table summarizes the effects of chemokine modulation and the effects on lesions size and composition of the chemokines that are further discussed in this thesis. For a more extended overview of other chemokines we refer to two recently published literature reviews[36, 37]. NS=not significant, SMC=smooth muscle cell, BM=bone marrow transplant.

recruitment, growth and activation of leukocytes through their cognate G-protein coupled receptors, which are present on the endothelium or target leukocytes. Four chemokine subgroups have been described so far (CC, CXC, CX3 and XC), identified on the configuration of the first two cysteines in the protein. Some chemokines (like CXCL10) are known to bind to glycosaminoglycans present on the (endothelial) cell surface or the extracellular matrix[32-35]. This is important to generate a chemokine gradient, e.g. under arterial vascular flow conditions, which is essential for leukocyte recruitment and migration to target tissues. In Table 3, the chemokines further discussed in this thesis are summarized. The role of all chemokines relevant in atherosclerosis in murine models were extensively recently reviewed in[36] and in[37]. Inhibition of various chemokines reduces plaque formation to different degrees[31, 38-44]. In addition, production of pro-inflammatory cytokines by activated immune cells has a pro-atherogenic effect, while the anti-inflammatory cytokine IL-10 limits atherosclerosis[45-48]. Inhibition of pro-inflammatory compounds clearly mediates a reduction in atherosclerosis[49-51]. These findings on the role of the immune system in atherosclerosis have all been excellently and extensively reviewed recently, with emphasis on general aspects[52], innate immunity [52-56], adaptive immunity [57] and immunomodulation [57].

The role of innate immunity in atherosclerosis

The monocyte-macrophage lineage is considered to play a central role in innate immunity as well as in atherosclerosis. For example, studies in mice deficient for Chemokine (C-C motif) receptor 2 (CCR2), the monocyte receptor which mediates transmigration into the vessel wall by MCP-1, show a reduction in atherosclerosis, indicating that monocyte-derived cells, presumably (activated) Mf aggravate atherosclerosis. Although studies in MCP-1 deficient mice further confirmed these early findings, recent studies indicate that the MCP1-CCR2 axis is particularly important during early atherosclerosis and that additional stimuli are necessary for advanced plaque formation[58]. It is becoming increasingly clear that the monocyte-macrophage lineage is a highly heterogeneous group of inflammatory cells. This results in specific roles and functions attributed to highly specified subgroups of these cells[59], and may have its consequences for their role in atherosclerosis. The most simplistic distinction that can be made is the division into classically and alternatively activated macrophages. The first will result into pro-inflammatory macrophages, producing matrix degrading enzymes and pro-inflammatory cytokine, resulting in a strong inflammatory response. The second will mature into more resident-type macrophages, responsible for tissue homeostasis and repair. The (patho-)physiological role of these subsets and the relevance for disease are not fully understood. Nevertheless, some groups have reported on the relevance of these subsets of monocyte-macrophages in atherosclerosis. Tacke et al showed that immature Ly6Chi monocytes are dependant on different

innate immunity ligands		adaptive immunity ligands	
microbial	*endogenous*	*microbial*	*endogenous*
lipopolysaccharide (LPS)	HSP60	potentially any	potentially any
lipoteichoic acid (LTA)	HSP70	type of microbial	type of
peptidoglycan (PGN)	oxLDL	antigen present	self-compound
PGN fragments	fibronectin domain A	in the vessel wall,	HSP60
lipopeptides	hyaluronic acid fragments	especially HSP65 (the	HSP65
CpG dinucleotides	heparan sulphate	homologue to human	oxLDL
double stranded RNA	posttranslational	HSP60)	
single stranded RNA	modifications		
flagellin			
heat shock proteins			
(HSP)			

Table 4. *Ligands for receptors of innate and adaptive antigen receptors relevant for atherosclerosis.* Identification of ligands for innate receptors is complicated by the fact that minute amounts of contaminating or co-purifying compounds may be the true ligand and not the main constituent of a preparation. For instance, LPS preparations often contain peptidoglycan, while LPS is a notorious contaminant of many tools and preparations in laboratory and clinical settings. Identification of endogenous ligands for innate antigen receptors has been specifically plagued by this problem. For a complete overview of TLR ligands, see[81]. An overview and extensive discussion of other innate receptors and ligands is written by[82].

chemokines to enter the lesion compared to more mature Ly6Clo monocytes[60]. This is interesting since the former is believed to mature into inflammatory macrophages, whereas the latter evolves into more resdident-like macrophages[61], though the effects on atherosclerosis have not been investigated so far.

An important way of macrophage stimulation is by TLR ligation, in particular TLR4 and TLR2, (reviewed in[62]). Lack of TLR-signaling in pro-atherogenic backgrounds of the mouse gives rise to decreased disease severity. In line with the mouse studies, some epidemiological data suggest that altered TLR function, caused by gene polymorphisms, protects from atherosclerosis (discussed in[63]). This might be due to changed ligation of TLR by pathogens and their derived products like LPS. Hence, these receptors have been mentioned as a connecting factor between atherosclerosis and other parameters, including circulating plasma endotoxins, Chlamydia pneumoniae infections and periodontal disease (Porphyromonas gingivalis). Taken together, these findings suggest that the fast and efficient reactions against bacterial pathov gens may increase progression of atherosclerosis.

The importance of the innate immune system in atherosclerosis is also demonstrated by the ubiquitous presence in the plaques of the macrophage scavenger receptors, which include CD36, SR-B1, SR-A, and less known receptors such as FEEL-1,

SR-PSOX and CD163. The scavenger receptors are low affinity receptors with broad ligand specificity, which play a role in the uptake of oxidized low density lipoprotein, oxLDL (CD36, SR-B1, SR-A and SR-PSOX) and the uptake of hemoglobin (CD163). They lack feedback inhibition of activity by intracellular cholesterol levels and as such load macrophages with oxLDL and play a key role in foam cell formation, one of the hallmarks of atherogenesis.

In conclusion, the innate system is capable of rapid activation of the monocyte-macrophage cell lineage through a variety of mechanisms, thereby contributing to atherosclerosis by driving proinflammatory mechanisms. This has led to a theory of repeated activation of innate immunity in atherogenesis by some authors [56, 64, 65].

The role of adaptive immunity in atherosclerosis

It is clear from the above-mentioned studies that the immune system plays a dominant role in atherogenesis. In addition to innate mechanisms, adaptive immunity also plays a role in atherogenesis. Important components of adaptive responses are expressed in plaques, including MHC class II, co-stimulatory molecules and Th1 cytokine profiles[52, 56]. Many studies, mainly performed in ApoE or LDL-receptor deficient mice, show that inhibition of a specific part of adaptive immunity inhibits atherogenesis. Ligands relevant in the activation of adaptive immunity are listed in Table 4. More recently, the view has emerged that adaptive immunity may be particularly important in the regulation of plaque phenotype, i.e. stable vs. vulnerable plaque, which may rupture and lead to myocardial or cerebral infarction[66]. Vulnerable plaques display a specific cellular composition[15], including many inflammatory cells and little stabilizing connective tissue. It is presently unknown how this plaque composition develops, but inhibition of (certain components of) adaptive immunity has been shown to induce a decrease in atherosclerosis[65, 67, 68]. Therefore, a major conclusion from this research is, that the activation of adaptive immunity is associated with the severity of atherosclerosis (Table 5).

As adaptive immunity needs an antigenic trigger to become activated, studies focused on the identification of specific antigens and epitopes involved in atherogenesis. Several candidates were put forward: oxLDL, Chlamydia, endogenous HSP60 and microbial HSP65. Especially the first candidate, oxLDL, is of importance as it may be regarded as a modified self-protein. Consequently, it has been suggested that atherosclerosis is an autoimmune disease[56]. Currently, the discussion is lively and of great importance as identification of such antigens and epitopes in principle allows for development of vaccines against atherosclerosis. Such a vaccine should induce immune responses generating protective antibodies or, alternatively, long-lasting immune tolerance.

plaque	functions	cell type
fatty streak stable plaque	inflammation	macrophage, foam cell
	tissue remodeling	macrophage, foam cell
	lipid handling	macrophage, foam cell
	antigen presentation	macrophage, foam cell
vulnerable plaque	inflammation	inflammatory macrophage
	lipid handling	inflammatory macrophage
	antigen presentation	inflammatory macrophage, DC
		B lymphocyte
	vessel wall remodeling	(inflammatory) macrophage
	transportation of antigens to local lymph nodes	DC
	cytokine production	B and T lymphocytes
	cytotoxicity	T lymphocytes
	growth factor secretion	T lymphocytes

Table 5. *Main roles of different immune cells in the atherosclerotic plaque at distinct stages of development.* This figure focuses on leukocytes, but other cell types are involved with atherogenesis as well. For instance, there is good evidence that smooth muscle cells can also develop into foam cells upon lipid ingestion. In addition to plaque stage, also location of leukocytes within the plaque is potentially important: it has been suggested that Mf producing proteolytic enzymes in the shoulder of the plaque codetermine plaque rupture.

Animal models in atherosclerosis

Gaining detailed insight in the (molecular) mechanisms in atherosclerosis can only be done in animal models. It enables us to study multiple time points, interfere in biological pathways and perform surgical interventions on a non-therapeutical basis. In atherosclerosis research mice and rabbits are the most commonly used animals. Generally, mice are very well protected from atherosclerosis due to a beneficial cholesterol spectrum in the blood. It contains high levels of the athero-protective HDL cholesterol and low levels of LDL and VLDL, whereas in humans the spectrum is opposite and pro-atherogenic. The C57BL6 strain of inbred mice is relatively susceptible for atherosclerosis, since their cholesterol profile is less beneficial. By feeding them with an atherogenic diet, development of atherosclerosis can be augmented to such extend that resulting advanced lesions are useful to study disease mechanisms. Over the years many variants of murine
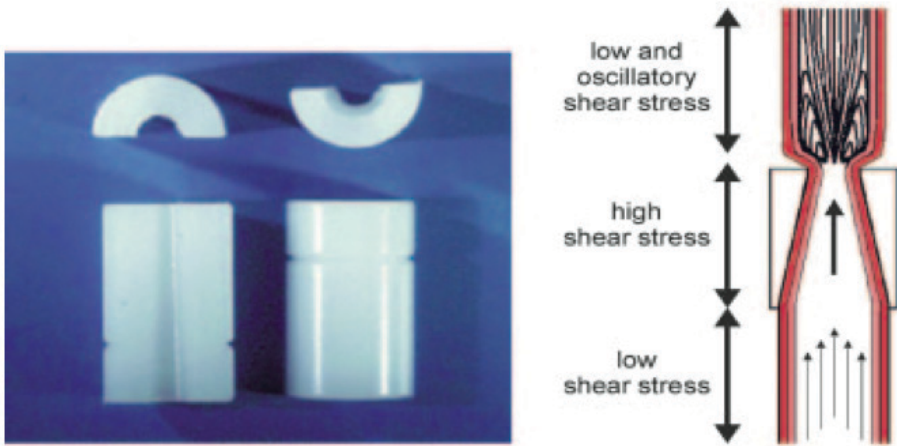
Figure 4. *Design of the shear stress modifier published by Cheng et al[72]*

Cast model. (A; left panel) The cast consists of 2 longitudinal halves of a cylinder with a conical lumen. (B; right panel) The theoretical design with induction of large vortices downstream of the cast in the carotid artery. Additionally, the conical lumen induces a stenosis of the vessel, causing a gradual increase in vascular shear stress in the cast area. Because of the stenosis, a region of low shear stress is created upstream of the cast.

models for atherosclerosis have been proposed and widely used, most commonly based on two genetically engineered strains: Apolipoprotein E deficient (ApoE-/-)[69] and the LDL-receptor deficient mice[70]. Within each of the two variants, many models have been developed, e.g. based on surgical interventions, specific vascular locations, and also many further genetically engineered mice with either increased of decreased functions. Using mice has many benefits over using rabbits. Mice can be quickly bred, thereby offering many genetic engineering possibilities. Besides, the availability of histological, cellular and molecular analysis techniques are almost endless. Last but not least, they are cost-effective. Rabbits on the other hand, are especially suited for studies using (intravascular) imaging techniques, such as catheter based ultrasound, mainly due to their size. However, to induce atherosclerosis in rabbits it is necessary to inflict physical vascular damage by denuding the endothelial layer added to a high cholesterol diet. Also, the analytical and genetic possibilities are limited and costs of keeping and maintaining rabbit colonies are much higher than in mice.

Shear stress and atherosclerosis

Although the classical risk factors of atherosclerosis are of systemic nature, it has long been observed that plaques are not evenly distributed along the arterial tree. In fact, atherosclerotic lesions appear at specific predilection sites. These sites are

at or near side branches or bifurcations, where blood flow is non-uniform, or at the lesser curvature of bends, where blood velocity is relatively low. The effect of blood flow on the vessel wall is mediated through fluid shear stress, which alters the physiological response of endothelial cells. Shear stress in general is a force that is applied parallel or tangentially to the face of a material, as opposed by a normal force (e.g. blood pressure), which is applied perpendicular to a surface. Fluid shear stress arises from the friction between a fluid and the solid boundary along which the fluid moves, and is induced by the difference in movement of the two layers and the 'roughness' (or viscosity) between these layers. Therefore, fluid shear stress (from here onwards called shear stress) also arises at the interplay between blood (the fluid) and the endothelial layer (the solid boundary), where it induces a shearing deformation of the endothelial cells, which can be sensed. For example, when cultured endothelial cells are exposed to shear stress in vitro, they will display a response dependant on the shear stress pattern. High shear stress results in an atheroprotective response e.g. by expression of endothelial nitric oxide synthase (eNOS)[71, 72], whereas low and oscillatory shear stress are pro-atherosclerotic by expression of e.g. leukocyte adhesion factors VCAM-1 and ICAM-1[73, 74] and downregulation of eNOS[75]. The first causative evidence between shear stress and atherosclerosis in vivo was published by Cheng et al, who developed a novel method to assess the response of the vessel wall to changes in shear stress[72]. Around the common carotid artery, which is normally exposed to high shear stress, they placed a plastic cylinder with a gradually narrowing lumen (Figure 4). As a result, the vascular segment upstream of the device was now exposed to lowered shear stress, whereas a small part of the segment downstream was sensing oscillatory shear stress with reversal of flow. The segment inside the cylinder was exposed to high shear stress. When this method was applied in atherosclerosis-susceptible ApoE-/- mice, it resulted in plaque formation in both the upstream and downstream segments, whereas the part inside the device remained free of lesions[76]. Next, they assessed the morphology of the lesions and found that a plaque with characteristics of an unstable plaque had developed in the low shear stress segment. This lesion consisted of a large necrotic core, a thin cap of collagen and little smooth muscle cells. In the oscillatory shear stress segment on the other hand, a stable lesion had developed, containing more collagen and smooth muscle cells. Also, there was less matrix-degrading enzymatic activity compared to the low shear stress lesion.

Aim and outline of this thesis

As mentioned before, the morphological qualities of an atherosclerotic plaque lay at the basis of (future) clinical consequences. Lesions with a vulnerable composition are prone to rupture, resulting in thrombosis and subsequent vascular occlusion. There is strong evidence that the shear forces of flowing blood inflicting on the endothelial cells influence the development of plaque vulnerability. However, the (immunological) mechanisms involved in this shear stress mediated vulnerable plaque development are currently unclear. In this thesis we aimed to clarify some of the immunological mechanisms involved, working towards future therapeutic interventions in treatment and prevention of unstable plaque rupture. Since it is very difficult to perform such mechanistic studies in humans, we studied experimental atherosclerosis in two specific animal models. It has been shown in humans that plaque ruptures are not equally distributed along the length of a lesion, but that ruptures occur more often in the upstream part of an atherosclerotic lesion[77, 78]. In **chapter 2**, we describe a novel technique in rabbits to assess the spatial distribution of the main lesion components in a 3-dimensional fashion, explaining the upstream localization of plaque ruptures. In **chapter 3** we tested the hypothesis that activated macrophages are the prime source of matrix-degrading proteases and that smooth muscle cells are the main producers of collagen in a shear stress driven model of murine atherosclerosis. In **chapter 4** we evaluated the differences in chemokine expression patterns between the stable and unstable lesions in the shear stress driven murine model. In **chapter 5**, we describe the effects of specific inhibition of CXCL10 on the plaque stability in atherosclerosis-susceptible mice. CXCL10 is one of the chemokines that was indentified to be specifically upregulated in the segment developing into the unstable lesion in chapter 4. In this chapter we also report on the association between human carotid artery lesion phenotype and its concentration of plaque CXCL10.

In **chapter 6** we report on the current work and (preliminary) results of a whole-genome expression analysis of plaque tissue, comparing tissue from the low and oscillatory shear stress segments during the development of the two different plaque phenotypes.

Finally the obtained results are summarized and discussed in **chapter 7** of this thesis.

References

1. Stary HC. Macrophages, macrophage foam cells, and eccentric intimal thickening in the coronary arteries of young children. Atherosclerosis. 1987;64:91-108

2. Pesonen E, Norio R, Hirvonen J, Karkola K, Kuusela V, Laaksonen H, Mottonen M, Nikkari T, Raekallio J, Viikari J, et al. Intimal thickening in the coronary arteries of infants and children as an indicator of risk factors for coronary heart disease. Eur Heart J. 1990;11 Suppl E:53-60

3. Kaprio J, Norio R, Pesonen E, Sarna S. Intimal thickening of the coronary arteries in infants in relation to family history of coronary artery disease. Circulation. 1993;87:1960-1968

4. Kerncijfers sterfte en doodsoorzaken.

5. Leal J, Luengo-Fernández R, Gray A, Petersen S, Rayner M. Economic burden of cardiovascular diseases in the enlarged european union. Eur Heart J. 2006;27:1610-1619

6. Ross R. Atherosclerosis--an inflammatory disease. N Engl J Med. 1999;340:115-126

7. Hingorani AD, Shah T, Casas JP, Humphries SE, Talmud PJ. C-reactive protein and coronary heart disease: Predictive test or therapeutic target? Clin Chem. 2009;55:239-255

8. Casas JP, Shah T, Hingorani AD, Danesh J, Pepys MB. C-reactive protein and coronary heart disease: A critical review. J Intern Med. 2008;264:295-314

9. Wilson PW, D'Agostino RB, Levy D, Belanger AM, Silbershatz H, Kannel WB. Prediction of coronary heart disease using risk factor categories. Circulation. 1998;97:1837-1847

10. Brunner H, Cockcroft JR, Deanfield J, Donald A, Ferrannini E, Halcox J, Kiowski W, Luscher TF, Mancia G, Natali A, Oliver JJ, Pessina AC, Rizzoni D, Rossi GP, Salvetti A, Spieker LE, Taddei S, Webb DJ. Endothelial function and dysfunction. Part ii: Association with cardiovascular risk factors and diseases. A statement by the working group on endothelins and endothelial factors of the european society of hypertension. J Hypertens. 2005;23:233-246

11. Simionescu M. Implications of early structural-functional changes in the endothelium for vascular disease. Arterioscler Thromb Vasc Biol. 2007;27:266-274

12. Stary HC, Chandler AB, Dinsmore RE, Fuster V, Glagov S, Insull W, Rosenfeld ME, Schwartz CJ, Wagner WD, Wissler RW. A definition of advanced types of atherosclerotic lesions and a histological classification of atherosclerosis. A report from the committee on vascular lesions of the council on arteriosclerosis, american heart association. Arterioscler Thromb Vasc Biol. 1995;15:1512-1531

13. Stary HC, Chandler AB, Glagov S, Guyton JR, Insull W, Rosenfeld ME, Schaffer SA, Schwartz CJ, Wagner WD, Wissler RW. A definition of initial, fatty streak, and

intermediate lesions of atherosclerosis. A report from the committee on vascular lesions of the council on arteriosclerosis, american heart association. Arterioscler Thromb. 1994;14:840-856

14. Stary HC. Natural history and histological classification of atherosclerotic lesions: An update. Arterioscler Thromb Vasc Biol. 2000;20:1177-1178

15. Virmani R, Kolodgie FD, Burke AP, Farb A, Schwartz SM. Lessons from sudden coronary death: A comprehensive morphological classification scheme for atherosclerotic lesions. Arterioscler Thromb Vasc Biol. 2000;20:1262-1275

16. Virmani R, Burke AP, Farb A, Kolodgie FD. Pathology of the vulnerable plaque. J Am Coll Cardiol. 2006;47:C13-18

17. Bobryshev YV, Lord RS. Mapping of vascular dendritic cells in atherosclerotic arteries suggests their involvement in local immune-inflammatory reactions. Cardiovasc Res. 1998;37:799-810.

18. Waltner-Romen M, Falkensammer G, Rabl W, Wick G. A previously unrecognized site of local accumulation of mononuclear cells. The vascular-associated lymphoid tissue. J Histochem Cytochem. 1998;46:1347-1350

19. Hakkinen T, Karkola K, Yla-Herttuala S. Macrophages, smooth muscle cells, endothelial cells, and t-cells express cd40 and cd40l in fatty streaks and more advanced human atherosclerotic lesions. Colocalization with epitopes of oxidized low- density lipoprotein, scavenger receptor, and cd16 (fc gammariii). Virchows Arch. 2000;437:396-405.

20. Lord R, Bobryshev Y. Hallmarks of atherosclerotic lesion development with special reference to immune inflammatory mechanisms. Cardiovasc Surg. 2002;10:405

21. de Boer OJ, Hirsch F, van der Wal AC, van der Loos CM, Das PK, Becker AE. Costimulatory molecules in human atherosclerotic plaques: An indication of antigen specific t lymphocyte activation. Atherosclerosis. 1997;133:227-234.

22. Salazar-Fontana LI, Bierer BE. T-lymphocyte coactivator molecules. Curr Opin Hematol. 2001;8:5-11

23. Bruemmer D, Riggers U, Holzmeister J, Grill M, Lippek F, Settmacher U, Regitz-Zagrosek V, Fleck E, Graf K. Expression of cd40 in vascular smooth muscle cells and macrophages is associated with early development of human atherosclerotic lesions. Am J Cardiol. 2001;87:21-27

24. Laman JD, de Smet BJ, Schoneveld A, van Meurs M. Cd40-cd40l interactions in atherosclerosis. Immunol Today. 1997;18:272-277.

25. Lutgens E, Daemen MJ. Cd40-cd40l interactions in atherosclerosis. Trends Cardiovasc Med. 2002;12:27-32.

26. Paulsson G, Zhou X, Tornquist E, Hansson GK. Oligoclonal t cell expansions in atherosclerotic lesions of apolipoprotein e-deficient mice. Arterioscler Thromb Vasc Biol. 2000;20:10-17

27. De Palma R, Del Galdo F, Abbate G, Chiariello M, Calabro R, Forte L, Cimmino G, Papa MF, Russo MG, Ambrosio G, Giombolini C, Tritto I, Notaristefano S, Berrino L, Rossi F, Golino P. Patients with acute coronary syndrome show oligoclonal t-cell recruitment within unstable plaque: Evidence for a local, intracoronary immunologic mechanism. Circulation. 2006;113:640-646

28. Xu XH, Shah PK, Faure E, Equils O, Thomas L, Fishbein MC, Luthringer D, Xu XP, Rajavashisth TB, Yano J, Kaul S, Arditi M. Toll-like receptor-4 is expressed by macrophages in murine and human lipid-rich atherosclerotic plaques and upregulated by oxidized ldl. Circulation. 2001;104:3103-3108.

29. Laman JD, Schoneveld AH, Moll FL, van Meurs M, Pasterkamp G. Significance of peptidoglycan, a proinflammatory bacterial antigen in atherosclerotic arteries and its association with vulnerable plaques. Am J Cardiol. 2002;90:119-123.

30. Kleemann R, Zadelaar S, Kooistra T. Cytokines and atherosclerosis: A comprehensive review of studies in mice. Cardiovasc Res. 2008;79:360-376

31. Reape TJ, Groot PH. Chemokines and atherosclerosis. Atherosclerosis. 1999;147:213-225.

32. Proudfoot AEI, Handel TM, Johnson Z, Lau EK, LiWang P, Clark-Lewis I, Borlat F, Wells TNC, Kosco-Vilbois MH. Glycosaminoglycan binding and oligomerization are essential for the in vivo activity of certain chemokines. Proc Natl Acad Sci USA. 2003;100:1885-1890

33. Ranjbaran H, Wang Y, Manes TD, Yakimov AO, Akhtar S, Kluger MS, Pober JS, Tellides G. Heparin displaces interferon-gamma-inducible chemokines (ip-10, i-tac, and mig) sequestered in the vasculature and inhibits the transendothelial migration and arterial recruitment of t cells. Circulation. 2006;114:1293-1300

34. Luster AD, Greenberg SM, Leder P. The ip-10 chemokine binds to a specific cell surface heparan sulfate site shared with platelet factor 4 and inhibits endothelial cell proliferation. J Exp Med. 1995;182:219-231

35. Campanella G, Grimm J, Manice L, Colvin R, Medoff B, Wojtkiewicz G, Weissleder R, Luster A. Oligomerization of cxcl10 is necessary for endothelial cell presentation and in vivo activity. The Journal of Immunology. 2006;177:6991

36. Zernecke A, Shagdarsuren E, Weber C. Chemokines in atherosclerosis. An update. Arterioscler Thromb Vasc Biol. 2008:ATVBAHA.107.161174v161171

37. Zernecke A, Weber C. Chemokines in the vascular inflammatory response of atherosclerosis. Cardiovasc Res. 2010;86:192-201

38. Lutgens E, Gorelik L, Daemen MJ, de Muinck ED, Grewal IS, Koteliansky VE, Flavell RA. Requirement for cd154 in the progression of atherosclerosis. Nat Med. 1999;5:1313-1316.

39. Combadiere C, Potteaux S, Gao JL, Esposito B, Casanova S, Lee EJ, Debre P, Tedgui A, Murphy PM, Mallat Z. Decreased atherosclerotic lesion formation in cx3cr1/apolipoprotein e double knockout mice. Circulation. 2003;107:1009-1016

40. Lesnik P, Haskell CA, Charo IF. Decreased atherosclerosis in cx3cr1-/- mice reveals a role for fractalkine in atherogenesis. J Clin Invest. 2003;111:333-340

41. Burke-Gaffney A, Brooks AV, Bogle RG. Regulation of chemokine expression in atherosclerosis. Vascul Pharmacol. 2002;38:283-292

42. Bursill CA, Channon KM, Greaves DR. The role of chemokines in atherosclerosis: Recent evidence from experimental models and population genetics. Curr Opin Lipidol. 2004;15:145-149

43. Veillard NR, Kwak B, Pelli G, Mulhaupt F, James RW, Proudfoot AE, Mach F. Antagonism of rantes receptors reduces atherosclerotic plaque formation in mice. Circ Res. 2004;94:253-261

44. Inoue S, Egashira K, Ni W, Kitamoto S, Usui M, Otani K, Ishibashi M, Hiasa K, Nishida K, Takeshita A. Anti-monocyte chemoattractant protein-1 gene therapy limits progression and destabilization of established atherosclerosis in apolipoprotein e-knockout mice. Circulation. 2002;106:2700-2706

45. Hansson GK. Immune mechanisms in atherosclerosis. Arterioscler Thromb Vasc Biol. 2001;21:1876-1890.

46. Hansson GK. Regulation of immune mechanisms in atherosclerosis. Ann N Y Acad Sci. 2001;947:157-165; discussion 165-156.

47. Frostegard J, Ulfgren AK, Nyberg P, Hedin U, Swedenborg J, Andersson U, Hansson GK. Cytokine expression in advanced human atherosclerotic plaques: Dominance of pro-inflammatory (th1) and macrophage-stimulating cytokines. Atherosclerosis. 1999;145:33-43.

48. Tedgui A, Mallat Z. Anti-inflammatory mechanisms in the vascular wall. Circ Res. 2001;88:877-887.

49. Merhi-Soussi F, Kwak BR, Magne D, Chadjichristos C, Berti M, Pelli G, James RW, Mach F, Gabay C. Interleukin-1 plays a major role in vascular inflammation and atherosclerosis in male apolipoprotein e-knockout mice. Cardiovasc Res. 2005;66:583-593

50. Hauer AD, Uyttenhove C, de Vos P, Stroobant V, Renauld JC, Van Berkel TJ, van Snick J, Kuiper J. Blockade of interleukin-12 function by protein vaccination attenuates atherosclerosis. Circulation. 2005;112:1054-1062

51. Chi H, Messas E, Levine RA, Graves DT, Amar S. Interleukin-1 receptor signaling mediates atherosclerosis associated with bacterial exposure and/or a high-fat diet in a murine apolipoprotein e heterozygote model: Pharmacotherapeutic implications. Circulation. 2004;110:1678-1685

52. Hansson GK, Libby P, Schonbeck U, Yan ZQ. Innate and adaptive immunity in the pathogenesis of atherosclerosis. Circ Res. 2002;91:281-291

53. Binder CJ, Chang MK, Shaw PX, Miller YI, Hartvigsen K, Dewan A, Witztum JL. Innate and acquired immunity in atherogenesis. Nat Med. 2002;8:1218-1226.

54. Taylor PR, Gordon S. Monocyte heterogeneity and innate immunity. Immunity. 2003;19:2-4

55. Gough PJ, Gordon S. The role of scavenger receptors in the innate immune system. Microbes Infect. 2000;2:305-311

56. Wick G, Knoflach M, Xu Q. Autoimmune and inflammatory mechanisms in atherosclerosis. Annu Rev Immunol. 2004;22:361-403

57. Hansson GK. Vaccination against atherosclerosis: Science or fiction? Circulation. 2002;106:1599-1601

58. Guo J, de Waard V, Van Eck M, Hildebrand RB, van Wanrooij EJ, Kuiper J, Maeda N, Benson GM, Groot PH, Van Berkel TJ. Repopulation of apolipoprotein e knockout mice with ccr2-deficient bone marrow progenitor cells does not inhibit ongoing atherosclerotic lesion development. Arterioscler Thromb Vasc Biol. 2005;25:1014-1019

59. Gordon S, Taylor P. Monocyte and macrophage heterogeneity. Nat Rev Immunol. 2005;5:953-964

60. Tacke F, Alvarez D, Kaplan T, Jakubzick C, Spanbroek R, Llodra J, Garin A, Liu J, Mack M, van Rooijen N, Lira S, Habenicht A, Randolph G. Monocyte subsets differentially employ ccr2, ccr5, and cx3cr1 to accumulate within atherosclerotic plaques. J Clin Invest. 2007;117:185-194

61. Mantovani A, Sica A, Sozzani S, Allavena P, Vecchi A, Locati M. The chemokine system in diverse forms of macrophage activation and polarization. Trends Immunol. 2004;25:677-686

62. Tobias P, Curtiss LK. Thematic review series: The immune system and atherogenesis. Paying the price for pathogen protection: Toll receptors in atherogenesis. J Lipid Res. 2005;46:404-411

63. Schroder NW, Schumann RR. Single nucleotide polymorphisms of toll-like receptors and susceptibility to infectious disease. Lancet Infect Dis. 2005;5:156-164

64. Espinola-Klein C, Rupprecht HJ, Blankenberg S, Bickel C, Kopp H, Rippin G, Victor A, Hafner G, Schlumberger W, Meyer J. Impact of infectious burden on extent and long-term prognosis of atherosclerosis. Circulation. 2002;105:15-21.

65. Epstein SE, Zhu J, Burnett MS, Zhou YF, Vercellotti G, Hajjar D. Infection and atherosclerosis: Potential roles of pathogen burden and molecular mimicry. Arterioscler Thromb Vasc Biol. 2000;20:1417-1420.

66. Hansson GK. Inflammation, atherosclerosis, and coronary artery disease. N Engl J Med. 2005;352:1685-1695

67. Laurat E, Poirier B, Tupin E, Caligiuri G, Hansson GK, Bariety J, Nicoletti A. In vivo downregulation of t helper cell 1 immune responses reduces atherogenesis in apolipoprotein e-knockout mice. Circulation. 2001;104:197-202.

68. Andersson J, Libby P, Hansson GK. Adaptive immunity and atherosclerosis. Clin Immunol. 2010;134:33-46

69. Piedrahita JA, Zhang SH, Hagaman JR, Oliver PM, Maeda N. Generation of mice carrying a mutant apolipoprotein e gene inactivated by gene targeting in embryonic stem cells. Proc Natl Acad Sci U S A. 1992;89:4471-4475

70. Ishibashi S, Brown MS, Goldstein JL, Gerard RD, Hammer RE, Herz J. Hypercholesterolemia in low density lipoprotein receptor knockout mice and its reversal by adenovirus-mediated gene delivery. J Clin Invest. 1993;92:883-893

71. Ziegler T, Silacci P, Harrison VJ, Hayoz D. Nitric oxide synthase expression in endothelial cells exposed to mechanical forces. Hypertension. 1998;32:351-355

72. Cheng C, van Haperen R, de Waard M, van Damme LC, Tempel D, Hanemaaijer L, van Cappellen GW, Bos J, Slager CJ, Duncker DJ, van der Steen AF, de Crom R, Krams R. Shear stress affects the intracellular distribution of enos: Direct demonstration by a novel in vivo technique. Blood. 2005;106:3691-3698

73. Sampath R, Kukielka GL, Smith CW, Eskin SG, McIntire LV. Shear stress-mediated changes in the expression of leukocyte adhesion receptors on human umbilical vein endothelial cells in vitro. Ann Biomed Eng. 1995;23:247-256

74. Walpola PL, Gotlieb AI, Cybulsky MI, Langille BL. Expression of icam-1 and vcam-1 and monocyte adherence in arteries exposed to altered shear stress. Arterioscler Thromb Vasc Biol. 1995;15:2-10

75. Ziegler T, Bouzourene K, Harrison VJ, Brunner HR, Hayoz D. Influence of oscillatory and unidirectional flow environments on the expression of endothelin and nitric oxide synthase in cultured endothelial cells. Arterioscler Thromb Vasc Biol. 1998;18:686-692

76. Cheng C, Tempel D, van Haperen R, van der Baan A, Grosveld F, Daemen MJ, Krams R, de Crom R. Atherosclerotic lesion size and vulnerability are determined by patterns of fluid shear stress. Circulation. 2006;113:2744-2753

77. Pregowski J, Tyczynski P, Mintz GS, Kim SW, Witkowski A, Satler L, Kruk M, Waksman R, Maehara A, Weissman NJ. Intravascular ultrasound assessment of the spatial distribution of ruptured coronary plaques in the left anterior descending coronary artery. Am Heart J. 2006;151:898-901

78. Wang JC, Normand SL, Mauri L, Kuntz RE. Coronary artery spatial distribution of acute myocardial infarction occlusions. Circulation. 2004;110:278-284

79. Henson PM. Dampening inflammation. Nat Immunol. 2005;6:1179-1181

80. Falk E. Pathogenesis of atherosclerosis. J Am Coll Cardiol. 2006;47:C7-12

81. Akira S, Uematsu S, Takeuchi O. Pathogen recognition and innate immunity. Cell. 2006;124:783-801

82. Taylor PR, Martinez-Pomares L, Stacey M, Lin HH, Brown GD, Gordon S. Macrophage receptors and immune recognition. Annu Rev Immunol. 2005;23:901-944

83. Gu L, Okada Y, Clinton SK, Gerard C, Sukhova GK, Libby P, Rollins BJ. Absence of monocyte chemoattractant protein-1 reduces atherosclerosis in low density lipoprotein receptor-deficient mice. Mol Cell. 1998;2:275-281

84. Boring L, Gosling J, Cleary M, Charo IF. Decreased lesion formation in ccr2-/- mice reveals a role for chemokines in the initiation of atherosclerosis. Nature. 1998;394:894-897

85. Braunersreuther V, Zernecke A, Arnaud C, Liehn EA, Steffens S, Shagdarsuren E, Bidzhekov K, Burger F, Pelli G, Luckow B, Mach F, Weber C. Ccr5 but not ccr1 deficiency reduces development of diet-induced atherosclerosis in mice. Arterioscler Thromb Vasc Biol. 2007;27:373-379

86. Zernecke A, Liehn EA, Gao JL, Kuziel WA, Murphy PM, Weber C. Deficiency in ccr5 but not ccr1 protects against neointima formation in atherosclerosis-prone mice: Involvement of il-10. Blood. 2006;107:4240-4243

87. Weber C, Koenen RR. Fine-tuning leukocyte responses: Towards a chemokine 'interactome'. Trends Immunol. 2006;27:268-273

88. van Wanrooij EJ, Happe H, Hauer AD, de Vos P, Imanishi T, Fujiwara H, van Berkel TJ, Kuiper J. Hiv entry inhibitor tak-779 attenuates atherogenesis in low-density lipoprotein receptor-deficient mice. Arterioscler Thromb Vasc Biol. 2005;25:2642-2647

89. Teupser D, Pavlides S, Tan M, Gutierrez-Ramos J, Kolbeck R, Breslow J. Major reduction of atherosclerosis in fractalkine (cx3cl1)-deficient mice is at the brachiocephalic artery, not the aortic root. Proc Natl Acad Sci U S A. 2004;101:17795-17800

90. Saederup N, Chan L, Lira SA, Charo IF. Fractalkine deficiency markedly reduces macrophage accumulation and atherosclerotic lesion formation in ccr2-/- mice. Evidence for independent chemokine functions in atherogenesis. Circulation. 2007

91. Combadière C, Potteaux S, Rodero M, Simon T, Pezard A, Esposito B, Merval R, Proudfoot A, Tedgui A, Mallat Z. Combined inhibition of ccl2, cx3cr1, and ccr5 abrogates ly6c(hi) and ly6c(lo) monocytosis and almost abolishes atherosclerosis in hypercholesterolemic mice. Circulation. 2008;117:1649-1657

92. Veillard N, Steffens S, Pelli G, Lu B, Kwak B, Gerard C, Charo I, Mach F. Differential influence of chemokine receptors ccr2 and cxcr3 in development of atherosclerosis in vivo. Circulation. 2005;112:870-878

93. van Wanrooij EJ, de Jager SC, van Es T, de Vos P, Birch HL, Owen DA, Watson RJ, Biessen EA, Chapman GA, Van Berkel TJ, Kuiper J. Cxcr3 antagonist nbi-74330 attenuates atherosclerotic plaque formation in ldl receptor-deficient mice. Arterioscler Thromb Vasc Biol. 2008;28:251-257

94. Heller EA, Liu E, Tager AM, Yuan Q, Lin AY, Ahluwalia N, Jones K, Koehn SL, Lok VM, Aikawa E, Moore KJ, Luster AD, Gerszten RE. Chemokine cxcl10 promotes atherogenesis by modulating the local balance of effector and regulatory t cells. Circulation. 2006;113:2301-2312

gelatinolytic blood data two Figure accumulation measured described performed segment plaques MMP vascular heterogeneity MΦ fraction spatially studies activity SMC co–localization indicated inflammatory foamy total types oxLDL technique vessel subsets associated present similar smooth cells sections mM cross study vivo plaque demonstrated artery analysis histological cell upstream may area arterial

Chapter 2

Gelatinolytic Activity in Atherosclerotic Plaques is Highly Localized and is Associated with Both Macrophages and Smooth Muscle Cells

D. Segers, F. Helderman, C. Cheng, L.C. van Damme, D. Tempel,
E. Boersma, P.W. Serruys, R. de Crom, A.F.W. van der Steen, P. Holvoet,
and R. Krams

Abstract

Background

Atherosclerosis is considered an inflammatory disease. Recent studies provided evidence for a predominant upstream location of plaque inflammation. The present study introduces a novel technique that evaluates the underlying mechanism of this spatial organization.

Methods and Results

In hypercholesteremic rabbits, atherosclerosis of the infra-renal aorta was induced by a combination of endothelial denudation and a high cholesterol diet (2% cholesterol; 2 months). At sacrifice, aortic vessel segments were dissected and reconstructed with a new technique, which preserved the original intravascular ultrasound derived lumen geometry. This enabled us to study the spatial relation of histological markers, like macrophages (MF), smooth muscle cells (SMC), lipids, gelatinolytic activity and oxidized LDL (oxLDL). Results show a predominant upstream localization of macrophages and gelatinase activity. Co-localization studies indicated that gelatinase activity was associated with MF and SMC. Further analysis revealed that this was caused by subsets of SMC and MF which were associated with oxLDL accumulation.

Conclusion

Upstream localization of a vulnerable plaque phenotype is probably due to an accumulation of oxLDL, which activates/induces subsets of SMC and MF to gelatinase production.

Introduction

Atherosclerosis is nowadays considered a lipid driven inflammatory disease. Inflammation has been associated with plaque progression, plaque rupture, thrombosis and subsequent myocardial infarction[1-4]. Several studies indicated that plaque inflammation is unevenly distributed over its length, with a predominant upstream presence of inflammatory cells and/or a location in the plaque shoulders[3,5-9]. These observations indicate a spatially oriented mechanism, which to date has not received much attention. In order to study the underlying mechanism of such a highly spatially localizing mechanism, there is a need for a precise, quantitative technique, enabling the study of plaque heterogeneity in experimental atherosclerosis. The first aim of the present study is to present a 3D histological technique permitting the study of plaque heterogeneity in more detail as before.

Both plaque progression and plaque rupture have been associated with a larger infiltration of macrophages (MF), irrespective of the underlying plaque morphology[10,11]. Activated MF produce numerous factors, including matrix-metalloproteinases (MMP)[12]. MMP belong to a family of zinc activated proteases modulating the extracellular matrix in the vascular wall[13-15]. The activity of some family members induces weak spots in the extracellular matrix, thereby introducing a condition sensitive to plaque rupture[12,16-18]. However, only a relatively small fraction of MF can be measured in the entire plaque[19] and therefore the process of plaque weakening may either be very localized, or other cell types may be involved in the process. Indeed, several studies have indicated that, besides MF, endothelial cells and smooth muscle cells (SMC) may produce MMP when brought into an inflammatory, atherogenic environment[20-22]. Recently, a new technique has been introduced to measure gelatinolytic activity in histological cross sections with a high spatial resolution[23,24]. We have adopted this method for vascular tissue and incorporated it into the 3D histological reconstructions. Our second aim was to evaluate whether MMP are active either very locally or that multiple cell types are involved in experimental atherosclerosis in vivo, by combining above techniques.

Low-density lipoproteins (LDL) accumulate in the vessel wall, where they may become oxidized (oxLDL). OxLDL is known to be involved in many processes related to atherosclerosis, including stimulation of macrophage infiltration and foam cell formation, stimulation of vascular smooth muscle cell migration and proliferation, and endothelial cell apoptosis[25-29]. Recent studies indicated that oxLDL is associated with plaque instability[29]. This observation might be explained by the modulation of activation of some MMP family members by oxLDL[15]. However, most of the oxLDL related studies have been conducted on isolated cells in vitro, which are devoid of the complex environment of the atherosclerotic vessel wall, thereby identifying the need to study the role of oxLDL in vivo. It is presently unknown whether oxLDL is distributed heterogeneously within the

plaque or if it is associated locally with Gelatinolytic activity in plaques in vivo. Therefore, the third aim of the present study was to evaluate if oxLDL might be the cause of the spatially restricted accumulation of activated MF in plaques in vivo.

Methods

Instrumentation

Three days before baseline measurements, male New Zealand White rabbits (n=8; weight=3.6±0.2 kg; Harlan, The Netherlands) were fed a high (2%) cholesterol diet for a 2-month period. At experimentation, rabbits were anaesthetized with an intramuscular injection of ketamine (Sanaket 10%, 25 mg/kg, Anisane BV, Raamsdonkveer, Holland) and a subcutaneous injection of medetomidine (Domitor, 0,5 mg/kg, Orion, Espoo, Finland). The marginal ear artery was canulated for arterial pressure measurement with a fluid-filled catheter (Amatek U.S. Gauge, Feasterville, USA) and for arterial blood withdrawal. A 4 French (Fr) guiding catheter was advanced from the left femoral artery up to the level of the renal artery ostium. Following angiography, a 40 MHz intravascular ultrasound (IVUS) catheter (CVUS, Boston Scientific, Maastricht, The Netherlands) was advanced through the guiding catheter and located 1 cm upstream of the lower of the two renal arteries. Subsequently, a motorized pull back was performed at a speed of 0.5 mm/sec spanning an arterial segment of 7 cm, which was recorded on high-resolution videotapes. Endothelial denudation was performed within this predefined segment by twisting and pulling back an inflated 3 Fr Fogarty balloon (Applied Cardiac Systems, Inc. Laguna Hills, USA) over a length of 5 centimeters.

Follow-up

After 8 weeks of follow-up, rabbits were anesthetized as described above. Next, the right femoral artery was dissected for the introduction of a 4 Fr sheath. An angiographic overview of the infra-renal aorta was performed and radiopaque markers were located subcutaneously to indicate the previously denuded region. Subsequently, the IVUS pullback was repeated at the location of the previously denuded segment. Following, the abdomen was opened and a longitudinal marker and two transverse markers were placed externally on aortic vessel wall, the lumen was filled with OCT compound (Tissue-Tek, Sakura Finetek Inc. Torrance, USA) and the arterial segment of interest was dissected, collected and snap-frozen in liquid nitrogen. The distance between both transverse markers was measured before and after excision and used to calculate a correction factor for shrinkage due to arterial elasticity.

All experiments were performed in accordance with institutional regulations and

the "Guiding for the care and use of laboratory animals" published by the US as approved by the Council of the American Physiological Society.

Plasma lipids

Lipid profiles were measured according to well-established enzymatic calorimetric methods (Roche Diagnostics, Pleasanton, USA). Cholesterol levels were determined at 8 weeks follow-up in the present hypercholesteremic group and in a normocholesteremic control group, which consisted of sex and age-matched rabbits.

Intravascular ultrasound

The high-resolution videotaped IVUS data were digitized at intervals of 0.5 mm with a resolution of 800 x 600 pixels and stored on a standard PC. Next, the lumen and the acoustic interface between media and the adventitial layer were traced semi-automatically by a well-validated software package[30], following the lumen area and media bounded area were calculated from these contours. The difference between these two was defined as the wall area.

Tissue harvesting and histological analysis

From the excised 5 cm aortic segment, tissue blocks were prepared every 2 mm with an in-house developed cutting device. This resulted in approximately 20-25 blocks per blood vessel, depending on shrinkage extend. Immunohistochemistry was performed on 5 mm cryosections obtained from the middle of the 2 mm tissue blocks. Sections were stained for MF (RAM-11, Dako Diagnostics BV, Glostrup, DK), smooth muscle cells (a-actin, Dako Diagnostics BV, Glostrup, DK) and for oxidized LDL (epitope against ApoB100; [31]) and lipids (Oil Red O; Sigma, Rotterdam, The Netherlands). Following staining, sections were digitized using a high-resolution CCD camera (Zeiss Axiocam HR, Jena, Germany) and quantitatively analyzed using commercial image analysis software (Clemex Technologies Inc, Longueuil, Canada).

In situ zymography

Gelatinolytic activity was demonstrated in unfixed cryosections using DQ-gelatin as a substrate (EnzChek; Molecular Probes, Eugene, OR). Sections were air-dried for 60 min, while during that period DQ-gelatin was dissolved in a concentration of 1 mg/ml in Milli-Q and then diluted 1:10 in 1% (w/v) low gelling temperature agarose (Sigma, Rotterdam, The Netherlands) in PBS. Subsequently, 25 µl of this mixture was placed on each cryosection and incubated for two hours at room temperature following placement of a cover slip. Fluorescence was detected with a confocal microscope (Zeiss, LSM 510 Meta, Jena, Germany) using an argon laser for excitation at 488 nm and emission collection at 512–542 nm, applying appropriate filters, background and autofluorescence correction. A detailed

testing for specificity of the in situ zymography was described in literature[23] and is described in the supplemental data section as well.

3D histology

The 3D reconstruction of histological cross sections consisted of the following steps: i) acquisition of quantitative image analysis data from histological sections, ii) rotation of sections on basis of an externally placed longitudinal marker, which was still present following histological processing, iii) stacking of image data, correction for shrinkage in longitudinal and radial direction and iv) rotation of the entire stack of data with respect to the renal artery and mapping of histology on 3D IVUS reconstructions. Details of the 3D reconstruction, including several tests are described in the supplemental data.

Data analysis and statistics

As a first approach, we averaged each histological variable (plaque area, MF, SMC, lipids, Gelatinolytic activity and oxLDL) per cross section and displayed the longitudinal heterogeneity per blood vessel. Subsequently, plaque areas of each blood vessel were shifted such that maximal plaque areas of all vessels were aligned. The shift for each individual blood vessel was applied to all its histological variables, which were eventually spatially averaged. To study spatial differences in relation of the histological variables described above in relation to plaque area, spatial averages were calculated upstream and downstream of the maximum plaque area for each individual animal. Differences between these averages were then evaluated by an exact Wilcoxon signed ranks test.

To further explore underlying mechanisms, we performed co-localization studies of the reordered data as well as linear regression analyses. Co-localization was defined as the existence of two variables in the same radial segment. The numbers of co-localized pixels were counted per histological variable and divided by the number of total elements in the segment of interest. Differences between co-localization of MF-gelatinolytic activity and SMC-gelatinolytic activity and of MF-oxLDL and SMC-oxLDL were tested. In addition, the amount of MF as a fraction of total MF, and SMC as a fraction of total SMC were calculated and differences in co-localization were tested, as described above. Detailed explanation of the image segmentation is described in the data supplement.

The authors of this article had full access to all of the data in the study and take responsibility for the integrity of the data and the accuracy of the data analysis.

Results
Animal characteristics

Systolic, diastolic and mean arterial blood pressures were 88±1 mmHg, 60±3 mmHg, and 69±1 mmHg, respectively. These values remained unchanged during the experimental procedures. The 2% cholesterol rich diet significantly increased

total plasma cholesterol (from 1.4±0.2 mM to 33.4±15.7 mM); HDL (from 0.7±0.1 mM to 14.5±2.7 mM) and LDL (from 0.2±0.1 to 30.9±10.8 mM). Triglyceride levels remained unchanged.

Longitudinal plaque heterogeneity displays an upstream location of inflammatory cells, Gelatinolytic activity and a vulnerable phenotype.
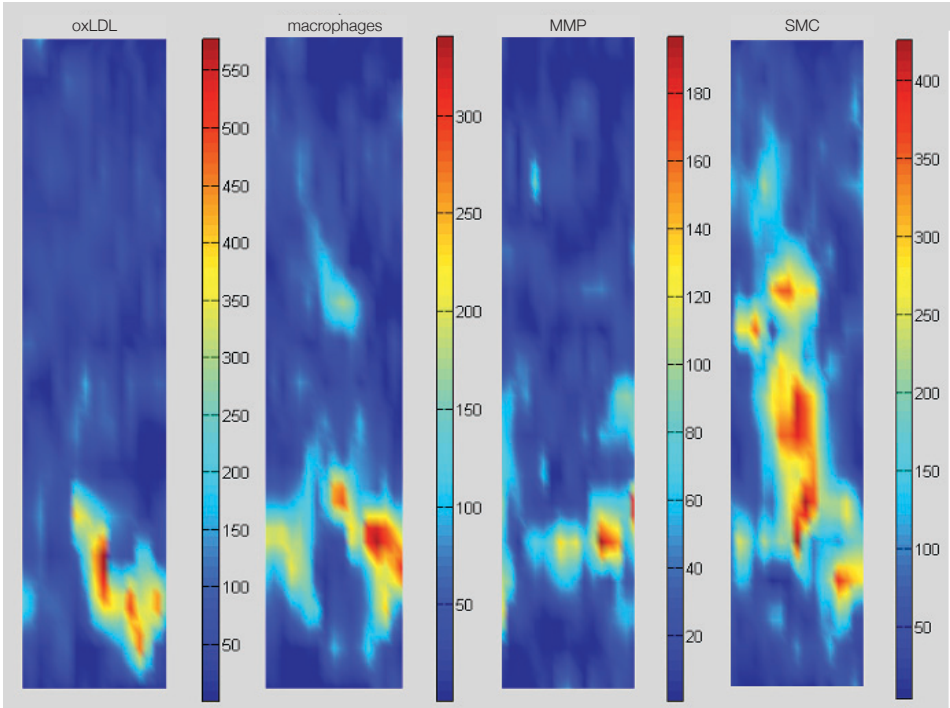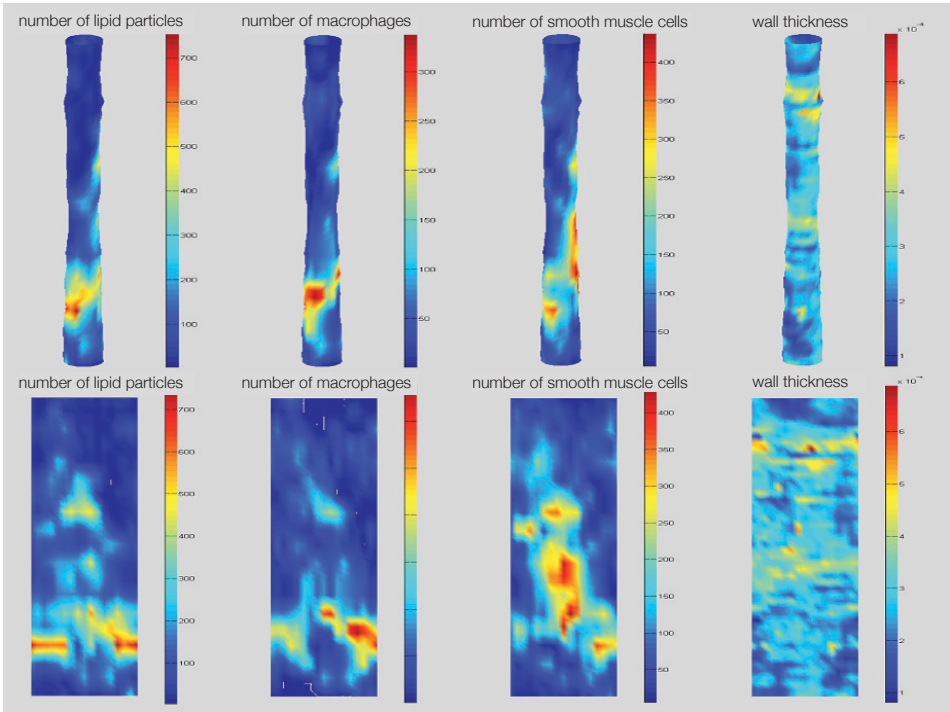
In plaques generated in the aorta of a representative hypercholesteremic rabbit, longitudinal plaque heterogeneity of lipid particles, MF and SMC was clearly present (Figure 1). Surprisingly, a similar upstream accumulation of gelatinolytic activity and oxLDL were measured (Figure 2). When the data were shifted and spatially averaged (see above) the predominant accumulation of MF was demonstrated for all animals (Figure 3). Distribution of each variable with plaque area, revealed a higher accumulation of MF upstream (11.6%) of the plaque, as compared to downstream of the plaque (7.9% p=0.016). In contrast, a more diffuse distribution of vascular SMC (26.6% vs 27.1%) and lipids (2.9% vs. 2.5%) was measured. As a consequence, a local vulnerability index (modified from Shiomi et al[32]) displayed a maximum upstream of maximal plaque area as compared to downstream (3.2 versus 2.8, p=0.039, Figure 4) This higher vulnerability upstream is similar to observations in the carotid arteries of patients[7].

In vivo gelatinolytic activity is co-localized with both smooth muscle cells and macrophages

Inspection of histological cross sections revealed that both SMC and MF were associated with gelatinolytic-activity (Figure 5). Quantitative analysis confirmed these findings, as the total amount of gelatinolytic associated with SMC and MF was 85±10%, distributed into an equal SMC - gelatinolytic fraction of 42±7% and MF - gelatinolytic fraction of 43±9% (Figure 6). While this pointed to a similar contribution of SMC and MF to overall gelatinolytic activity, these fractions represents only a minor fraction of overall MF (23±7%) and SMC (22±7%) content, which was similar for both cell types. When we re-examined the cross section containing gelatinolytic producing vascular SMC and MF, we identified foamy SMC and foamy MF (Figure 5; right panels).

OxLDL identifies subsets of gelatinolytic producing smooth muscle cells and macrophages

Inspection of histological cross sections revealed that both SMC and MF were associated with oxLDL accumulation (Figure 5). These single observations were confirmed by quantitative analysis, as co-localization of MF and SMC with oxLDL was 98±10%, with a contribution of 54±9% of SMC co-localizing with oxLDL and 44±7% of MF with oxLDL that was not different (Figure 6). These co-localization studies identified similar subset of SMC (28±4%) and a subset of MF (28±8%) that were spatially associated with oxLDL.

number of lipid particles   number of macrophages   number of smooth muscle cells   wall thickness

number of lipid particles   number of macrophages   number of smooth muscle cells   wall thickness

oxLDL   macrophages   MMP   SMC

Left page top panel

Figure 1.

3D vascular lumen reconstructions of a rabbit aorta, which was obtained by combining Intravascular Ultrasound (IVUS) with histological data. The upper panel shows the histology projected on the 3D IVUS lumen reconstruction, while the bottom panel shows the same data on a flat plane. From left to right are displayed: lipid distribution, macrophage distribution, smooth muscle cell distribution, and IVUS derived wall thickness distribution. Flow direction is from the bottom to the top. Note the predominant upstream location of inflammatory markers.

Left page bottom panel

Figure 2.

3D reconstructions of the same aorta as presented in figure 1. Presented are histological markers projected on a flat plane only. From left to right are displayed: oxidized LDL distribution, macrophage distribution, the distribution of metalloproteinase gelatinolytic activity, and smooth muscle cell distribution. Flow direction is from the bottom to the top. Note the predominant upstream location of all components, similar as presented in figure 1.

Plaque area

Macrophages

Smooth muscle cells
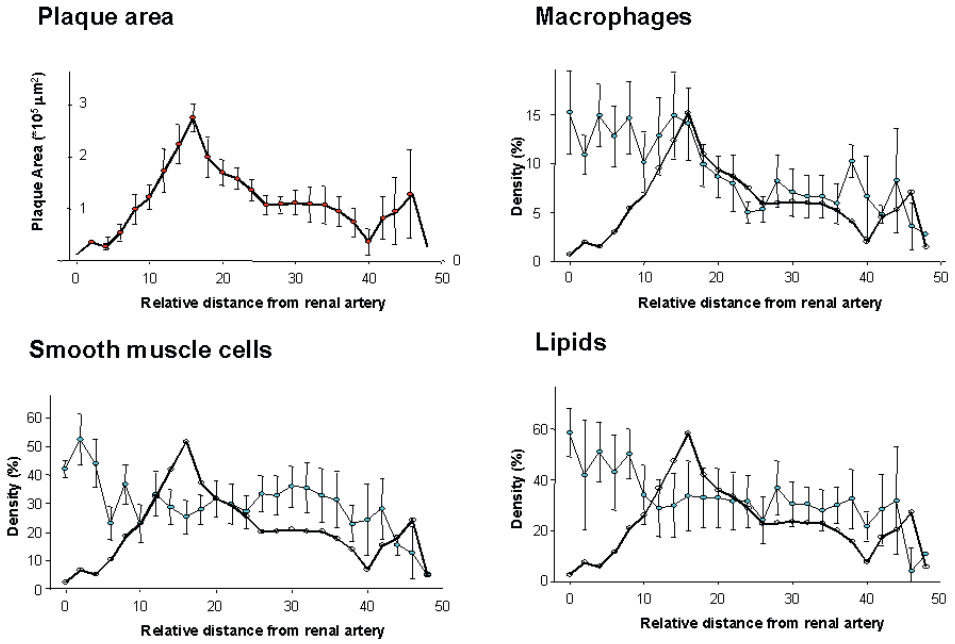
Lipids

Figure 3.

Longitudinal heterogeneity of plaque area (panel A), macrophage (panel B), smooth muscle cell (panel C) and lipid distribution (panel D). Displayed in each figure is the longitudinal plaque area distribution as averaged for all rabbits, note that all variables are located predominantly upstream of the plaque.
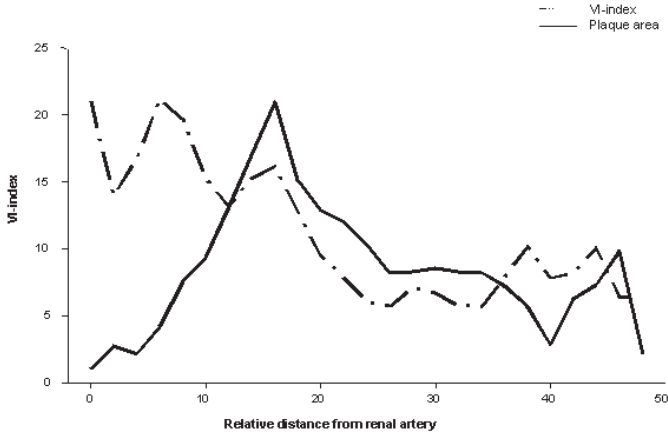
VI-index
Plaque area

Figure 4.

Local distribution of the vulnerability index adapted from Shiomi[32], displayed as a function of longitudinal location in a series of atherosclerotic rabbit aortas (n=10). A high value signifies a more vulnerable phenotype, while a low value signifies a more stable phenotype. It is clearly shown that the highest values are displayed upstream of the plaque.

Discussion

Atherosclerosis is considered a lipid driven inflammatory disease. Several studies indicated a strong heterogeneity of the inflammatory process[11,33,34], consisting either of an accumulation of inflammatory cells in the shoulders and/or upstream of the plaque[7]. Not much attention has been paid to this heterogeneity in experimental atherosclerosis, probably due to the lack of a suitable technique to study such phenomena in animals.

With a new 3D reconstruction technique for histology, we were able to show that the inflammatory component in the atherosclerotic plaque was spatially located upstream of the maximal cross-sectional plaque area, similar as reported for human conditions[7]. In addition, we demonstrated that gelatinolytic activities were also spatially confined to the same region and were associated with MF and SMC. This tight spatial localization of gelatinases enabled us to study co-localization with other cell types. We found that, not only MF, but also SMC contributed significantly to gelatinolytic activity in vivo. Previous studies indicated that SMC in culture produce pro-MMP-2 after stimulation, and at the same time reduce their TIMP production leading to a higher MMP-2 activity[35]. Furthermore, macrophages stimulated with oxLDL decrease their TIMP-1 release and increase pro-MMP-9 release, leading to MMP-9 activation[22]. The imbalance between TIMP and pro-MMP release may explain the high gelatinase activity found in the present study. Thus, from the present findings, one may postulate that local weak spots in the extracellular matrix occur upstream of the plaque because of a highly localized gelatinolytic concentration produced by a both (foamy) MF's and (foamy) SMC.

The reason why such a localized accumulation of cells in atherosclerotic plaques occurs is presently unknown, but several lines of evidence indicate that oxLDL is involved. OxLDL has been measured in (vulnerable) plaques, where it modulates macrophage accumulation and foam cell formation through the expression of adhesion factors and MCP-1 secretion, migration of SMC and apoptosis of SMC and endothelial cells[27-29,36] Furthermore, several studies identified a modulating effect of oxLDL on MMP activation by MF and SMC in vitro[37-41]. Therefore we tested whether oxLDL co-localized with MF and SMC. Only 25% of either cell type were associated with oxLDL, but these two cell types accounted for all oxLDL co-localization and all gelatinolytic-activity in our plaques. This indicates that the total oxLDL is taken up by SMC and MF in approximately similar amounts, but this uptake is performed by subsets of both cell types.

Highly evolutionary preserved subsets of monocytes have been identified in the blood of humans and mice[42,43], which results in a different macrophage
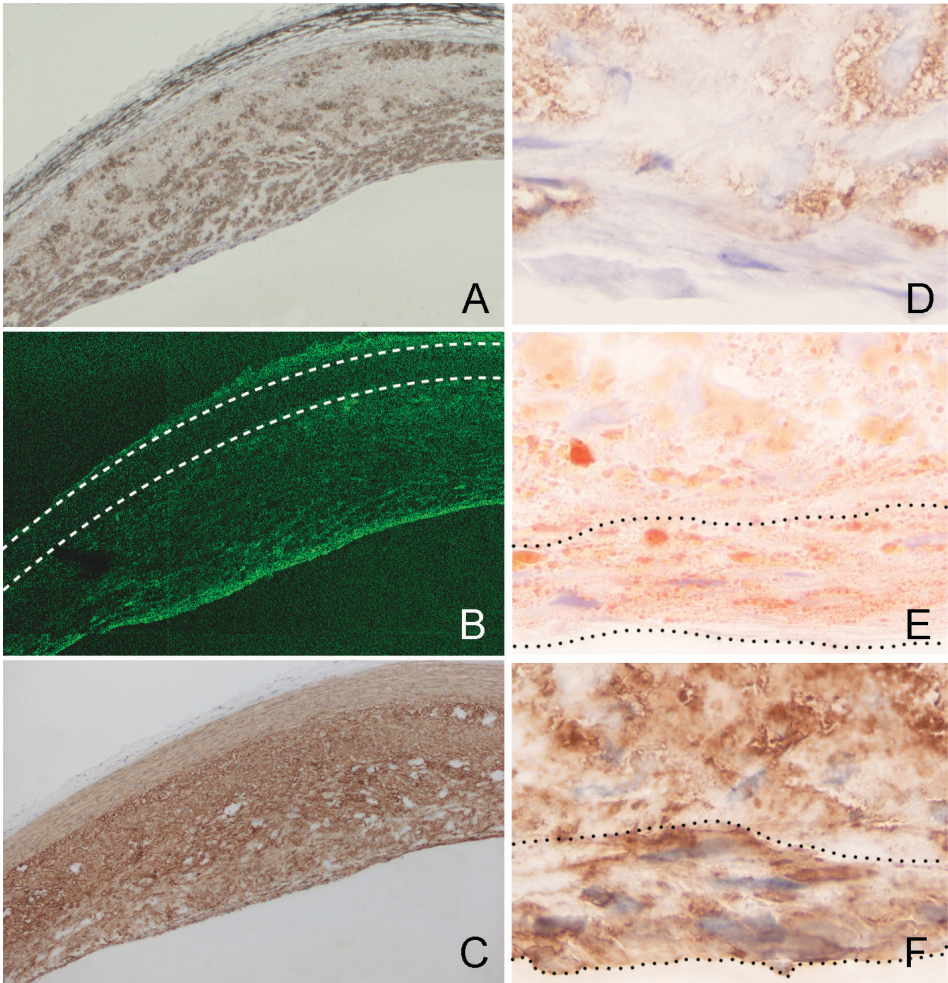
Figure 5.

Near consecutive cross sections of a single atherosclerotic rabbit aorta at low magnification showing macrophage accumulation (panel A), gelatinolytic activity (panel B, the dashed white line indicates the tunica media) and smooth muscle cell distribution (panel C). Note that near the cap the gelatinolytic activity is high. At this location both smooth muscle cells and macrophages are identified. A 100 X magnification of near consecutive cross sections indicates that foam cells (Oil Red O staining; panel E) belong to the macrophage fraction (RAM-11; panel D) and to the smooth muscle cell fraction (a-actin: panel F). The dashed black lines indicate an area where foamy smooth muscle cells are present.

Gelatinolytic activity

oxLDL accumulation
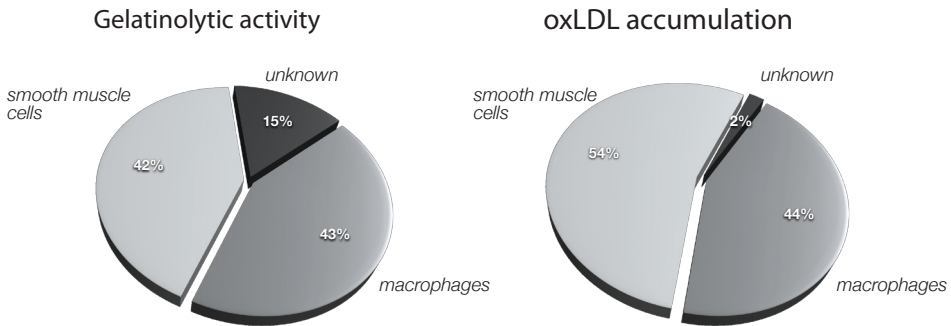
Figure 6.

Pie diagrams of gelatinolytic activity (left panel) and oxLDL accumulation distribution, with respect to smooth muscle cells and macrophages. The distribution is calculated as a percentage of SMC or macrophages co-localized with gelatinase activity or oxLDL, divided by total gelatinolytic or total oxLDL, respectively. Unknown refers to the amount of either gelatinolytic activity or to the oxLDL accumulation not associated with either smooth muscle cells or macrophages. oxLDL: oxidized LDL.

phenotypes as maturation occurs [43,44]. These circulating subsets express different chemokine receptors [43,45] and different scavenger receptors [43,44]. These studies may offer an explanation for the finding of a subset of MF with a preferential location upstream of the plaque combined with a particular predominance to foam cell differentiation.

Subsets of SMC may change into foam cells and therefore their role in atherogenesis may have been underestimated[46,47]. Recently, it was demonstrated that discrete clones of SMC exist in human vessels, which differentially accumulate cholesteryl esters when exposed to oxidized lipoproteins [47,48]. Once turned into foamy SMC, they start to produce cytokines and express chemokine receptors [49] providing an explanation for their tight co-localization within the plaque. The fact that foamy SMC and foamy MF are located in similar vessel segments might be explained by the evidence that MF secrete factors enhancing uptake of cholesteryl ester by vascular SMC[50]. The association of foamy SMC subsets, foamy macrophage subsets and gelatinolytic activity in atherosclerotic plaques in vivo has, to the best of our knowledge not been described before.

In conclusion, a specific spatial co-localization of MF, lipids and SMC was demonstrated upstream of the plaque, similar as found in patients with proven upstream plaque ruptures. This upstream plaque composition is characterized by an accumulation of (subsets of) MF and SMC, oxLDL and gelatinolytic activity. We hypothesize that activation of these subsets by oxLDL induces gelatinolytic activity, followed by breakdown of the extracellular matrix and subsequent weakening of the plaque. The unexpected important role of a subset of SMC in this process warrants further studies.

References

1. Davies MJ, Richardson PD, Woolf N, Katz DR, Mann J. Risk of thrombosis in human atherosclerotic plaques: role of extracellular lipid, macrophage, and smooth muscle cell content. Br Heart J. 1993;69:377-81.

2. Schaar JA, Muller JE, Falk E, Virmani R, Fuster V, Serruys PW, Colombo A, Stefanadis C, Ward Casscells S, Moreno PR, Maseri A, van der Steen AF. Terminology for high-risk and vulnerable coronary artery plaques. Report of a meeting on the vulnerable plaque, June 17 and 18, 2003, Santorini, Greece. Eur Heart J. 2004;25:1077-82.

3. van der Wal AC, Becker AE. Atherosclerotic plaque rupture--pathologic basis of plaque stability and instability. Cardiovasc Res. 1999;41:334-44.

4. Naghavi M, Libby P, Falk E, Casscells SW, Litovsky S, Rumberger J, Badimon JJ, Stefanadis C, Moreno P, Pasterkamp G, Fayad Z, Stone PH, Waxman S, Raggi P, Madjid M, Zarrabi A, Burke A, Yuan C, Fitzgerald PJ, Siscovick DS, de Korte CL, Aikawa M, Juhani Airaksinen KE, Assmann G, Becker CR, Chesebro JH, Farb A, Galis ZS, Jackson C, Jang IK, Koenig W, Lodder RA, March K, Demirovic J, Navab M, Priori SG, Rekhter MD, Bahr R, Mehran R, Colombo A, Boerwinkle E, Ballantyne C, Insull W, Jr., Schwartz RS, Vogel R, Serruys PW, Hansson GK, Faxon DP, Kaul S, Drexler H, Greenland P, Muller JE, Virmani R, Ridker PM, Zipes DP, Shah PK, Willerson JT. From vulnerable plaque to vulnerable patient: a call for new definitions and risk assessment strategies: Part I. Circulation. 2003;108:1664-72.

5. Falk E, Shah P, Fuster V. Coronary plaque disruption. Circulation.1995;92:657-71.

6. Lovett JK, Rothwell PM. Site of carotid plaque ulceration in relation to direction of blood flow: an angiographic and pathological study. Cerebrovasc Dis. 2003;16:369-75.

7. Dirksen MT, van der Wal AC, van den Berg FM, van der Loos CM, Becker AE. Distribution of inflammatory cells in atherosclerotic plaques relates to the direction of flow. Circulation. 1998;98:2000-3.

8. Tricot O, Mallat Z, Heymes C, Belmin J, Leseche G, Tedgui A. Relation between endothelial cell apoptosis and blood flow direction in human atherosclerotic plaques. Circulation. 2000;101:2450-3.

9. Schminke U, Motsch L, Hilker L, Kessler C. Three-dimensional ultrasound observation of carotid artery plaque ulceration. Stroke. 2000;31:1651-5.

10. van der Wal AC, Becker AE, van der Loos CM, Tigges AJ, Das PK. Fibrous and lipid-rich atherosclerotic plaques are part of interchangeable morphologies related to inflammation: a concept. Coron Artery Dis. 1994;5:463-9.

11. Pasterkamp G, Schoneveld AH, Hijnen DJ, de Kleijn DP, Teepen H, van der Wal AC, Borst C. Atherosclerotic arterial remodeling and the localization of macrophages and matrix metalloproteases 1, 2 and 9 in the human coronary artery. Atherosclerosis. 2000;150:245-53.

12. Galis ZS, Khatri JJ. Matrix metalloproteinases in vascular remodeling and atherogenesis: the good, the bad, and the ugly. Circ Res. 2002;90:251-62.

13. Richardson PD. Biomechanics of plaque rupture: progress, problems, and new frontiers. Ann Biomed Eng. 2002;30:524-36.

14. Jones CB, Sane DC, Herrington DM. Matrix metalloproteinases. A review of their structure and role in acute coronary syndrome. Cardiovasc Res. 2003;59:812-23.

15. Newby AC, Southgate KM, Davies M. Extracellular matrix degrading metalloproteinases in the pathogenesis of arteriosclerosis. Basic Res Cardiol. 1994;89 Suppl 1:59-70.

16. Galis ZS, Sukhova GK, Kranzhofer R, Clark S, Libby P. Macrophage foam cells from experimental atheroma constitutively produce matrix-degrading proteinases. Proc Natl Acad Sci U S A. 1995;92:402-6.

17. Libby P, Ridker PM, Maseri A. Inflammation and atherosclerosis. Circulation. 2002;105:1135-43.

18. Libby P. Atherosclerosis: the new view. Sci Am. 2002;286:46-55.

19. Pasterkamp G, Schoneveld AH, van der Wal AC, Hijnen DJ, van Wolveren WJ, Plomp S, Teepen HL, Borst C. Inflammation of the atherosclerotic cap and shoulder of the plaque is a common and locally observed feature in unruptured plaques of femoral and coronary arteries. Arterioscler Thromb Vasc Biol. 1999;19:54-8.

20. Cho A, Reidy MA. Matrix metalloproteinase-9 is necessary for the regulation of smooth muscle cell replication and migration after arterial injury. Circ Res. 2002;91:845-51.

21. Schonbeck U, Mach F, Sukhova GK, Murphy C, Bonnefoy JY, Fabunmi RP, Libby P. Regulation of matrix metalloproteinase expression in human vascular smooth muscle cells by T lymphocytes: a role for CD40 signaling in plaque rupture? Circ Res. 1997;81:448-54.

22. Xu XP, Meisel SR, Ong JM, Kaul S, Cercek B, Rajavashisth TB, Sharifi B, Shah PK. Oxidized low-density lipoprotein regulates matrix metalloproteinase-9 and its tissue inhibitor in human monocyte-derived macrophages. Circulation. 1999;99:993-8.

23. Mook OR, Van Overbeek C, Ackema EG, Van Maldegem F, Frederiks WM. In situ localization of gelatinolytic activity in the extracellular matrix of metastases of colon cancer in rat liver using quenched fluorogenic DQ-gelatin. J Histochem Cytochem. 2003;51:821-9.

24. Yan SJ, Blomme EA. In situ zymography: a molecular pathology technique to localize endogenous protease activity in tissue sections. Vet Pathol. 2003;40:227-36.

25. Mertens A, Verhamme P, Bielicki JK, Phillips MC, Quarck R, Verreth W, Stengel D, Ninio E, Navab M, Mackness B, Mackness M, Holvoet P. Increased low-density lipoprotein oxidation and impaired high-density lipoprotein antioxidant defense are associated with increased macrophage homing and atherosclerosis in

dyslipidemic obese mice: LCAT gene transfer decreases atherosclerosis. Circulation. 2003;107:1640-6.

26. Asmis R, Begley JG. Oxidized LDL promotes peroxide-mediated mitochondrial dysfunction and cell death in human macrophages: a caspase-3-independent pathway. Circ Res. 2003;92:e20-9.

27. de Vries HE, Buchner B, van Berkel TJ, Kuiper J. Specific interaction of oxidized low-density lipoprotein with macrophage-derived foam cells isolated from rabbit atherosclerotic lesions. Arterioscler Thromb Vasc Biol. 1999;19:638-45.

28. Huang YH, Ronnelid J, Frostegard J. Oxidized LDL induces enhanced antibody formation and MHC class II- dependent IFN-gamma production in lymphocytes from healthy individuals. Arterioscler Thromb Vasc Biol. 1995;15:1577-83.

29. Nishi K, Itabe H, Uno M, Kitazato KT, Horiguchi H, Shinno K, Nagahiro S. Oxidized LDL in carotid plaques and plasma associates with plaque instability. Arterioscler Thromb Vasc Biol. 2002;22:1649-54.

30. Krams R, Wentzel JJ, Oomen JA, Schuurbiers JC, Andhyiswara I, Kloet J, Post M, de Smet B, Borst C, Slager CJ, Serruys PW. Shear stress in atherosclerosis, and vascular remodelling. Semin Interv Cardiol. 1998;3:39-44.

31. Holvoet P, Vanhaecke J, Janssens S, Van de Werf F, Collen D. Oxidized LDL and malondialdehyde-modified LDL in patients with acute coronary syndromes and stable coronary artery disease. Circulation. 1998;98:1487-94.

32. Shiomi M, Ito T, Hirouchi Y, Enomoto M. Stability of atheromatous plaque affected by lesional composition: study of WHHL rabbits treated with statins. Ann N Y Acad Sci. 2001;947:419-23.

33. Hansson GK. Regulation of immune mechanisms in atherosclerosis. Ann N Y Acad Sci. 2001;947:157-65; discussion 165-6.

34. Stemme S, Faber B, Holm J, Wiklund O, Witztum JL, Hansson GK. T lymphocytes from human atherosclerotic plaques recognize oxidized low density lipoprotein. Proc Natl Acad Sci U S A. 1995;92:3893-7.

35. Tummalapalli CM, Tyagi SC. Responses of vascular smooth muscle cell to extracellular matrix degradation. J Cell Biochem. 1999;75:515-27.

36. Varadhachary AS, Monestier M, Salgame P. Reciprocal induction of IL-10 and IL-12 from macrophages by low-density lipoprotein and its oxidized forms. Cell Immunol. 2001;213:45-51.

37. Kalela A, Koivu TA, Hoyhtya M, Jaakkola O, Lehtimaki T, Sillanaukee P, Nikkari ST. Association of serum MMP-9 with autoantibodies against oxidized LDL. Atherosclerosis. 2002;160:161-5.

38. Moreau M, Brocheriou I, Petit L, Ninio E, Chapman MJ, Rouis M. Interleukin-8 mediates downregulation of tissue inhibitor of metalloproteinase-1 expression in cholesterol-loaded human macrophages: relevance to stability of atherosclerotic plaque. Circulation. 1999;99:420-6.

39. Haug C, Lenz C, Diaz F, Bachem MG. Oxidized low-density lipoproteins stimulate extracellular matrix metalloproteinase Inducer (EMMPRIN) release by coronary smooth muscle cells. Arterioscler Thromb Vasc Biol. 2004;24:1823-9.

40. Auge N, Maupas-Schwalm F, Elbaz M, Thiers JC, Waysbort A, Itohara S, Krell HW, Salvayre R, Negre-Salvayre A. Role for matrix metalloproteinase-2 in oxidized low-density lipoprotein-induced activation of the sphingomyelin/ceramide pathway and smooth muscle cell proliferation. Circulation. 2004;110:571-8.

41. Huang Y, Song L, Wu S, Fan F, Lopes-Virella MF. Oxidized LDL differentially regulates MMP-1 and TIMP-1 expression in vascular endothelial cells. Atherosclerosis. 2001;156:119-25.

42. Leenen PJ, de Bruijn MF, Voerman JS, Campbell PA, van Ewijk W. Markers of mouse macrophage development detected by monoclonal antibodies. J Immunol Methods. 1994;174:5-19.

43. Sunderkotter C, Nikolic T, Dillon MJ, Van Rooijen N, Stehling M, Drevets DA, Leenen PJ. Subpopulations of mouse blood monocytes differ in maturation stage and inflammatory response. J Immunol. 2004;172:4410-7.

44. Draude G, von Hundelshausen P, Frankenberger M, Ziegler-Heitbrock HW, Weber C. Distinct scavenger receptor expression and function in the human CD14(+)/CD16(+) monocyte subset. Am J Physiol. 1999;276:H1144-9.

45. Grage-Griebenow E, Flad HD, Ernst M. Heterogeneity of human peripheral blood monocyte subsets. J Leukoc Biol. 2001;69:11-20.

46. Llorente-Cortes V, Otero-Vinas M, Berrozpe M, Badimon L. Intracellular lipid accumulation, low-density lipoprotein receptor-related protein expression, and cell survival in vascular smooth muscle cells derived from normal and atherosclerotic human coronaries. Eur J Clin Invest. 2004;34:182-90.

47. Argmann CA, Sawyez CG, Li S, Nong Z, Hegele RA, Pickering JG, Huff MW. Human smooth muscle cell subpopulations differentially accumulate cholesteryl ester when exposed to native and oxidized lipoproteins. Arterioscler Thromb Vasc Biol. 2004;24:1290-6.

48. Li S, Sims S, Jiao Y, Chow LH, Pickering JG. Evidence from a novel human cell clone that adult vascular smooth muscle cells can convert reversibly between noncontractile and contractile phenotypes. Circ Res. 1999;85:338-48.

49. Lucas AD, Bursill C, Guzik TJ, Sadowski J, Channon KM, Greaves DR. Smooth muscle cells in human atherosclerotic plaques express the fractalkine receptor CX3CR1 and undergo chemotaxis to the CX3C chemokine fractalkine (CX3CL1). Circulation. 2003;108:2498-504.

50. Vijayagopal P, Glancy DL. Macrophages stimulate cholesteryl ester accumulation in cocultured smooth muscle cells incubated with lipoprotein-proteoglycan complex. Arterioscler Thromb Vasc Biol. 1996;16:1112-21.

plaque lesion collagen LSS model disruptions findings cap LSS-induced significant found may mice gelatinase disruption lower MHC HSP-47 analysis evidence distribution segment well upstream activation expression observed macrophage II cells part unstable atherosclerotic shear class presence compared fibrous rupture plaques segments production low downstream activity macrophages vs Figure lesions stress

Chapter 3

Atherosclerotic Plaque Vulnerability in a Mouse Model of Atherosclerosis is Predominantly Located in the Upstream Segment of the Lesion

D. Segers, R.Krams, R. de Crom, P.J.M. Leenen.
Submitted

Abstract

Background

We previously developed a mouse model for vulnerable atherosclerotic plaque induced by a low shear stress pattern. In the present study we characterized various vulnerability-determining factors in this model, addressing the question how these factors compared to the well-described features of human vulnerable plaque.

Methods and Results

In ApoE-/- mice, we induced unstable plaque using a flow-altering device around the carotid artery for 9 weeks. Lesion compositions were evaluated in two equally sized plaque segments. We found frequent disruptions of the plaque, but only in the upstream segment. This was accompanied by increased macrophage activation compared to the downstream segment (MHC class II staining; 15.3% vs. 6.9%, p<0.01). Collagen presence tended to be lower upstream, whereas production in this segment was higher. Surprisingly, collagen-degrading gelatinase activity was highest in the downstream segment.

Conclusion

In the present study we show that plaque disruptions are frequent in the low shear stress-induced plaque and the colocalization with activated macrophages suggests that they might be important in this respect. The upstream localization of disruptions is in accordance with findings in humans. We believe that, when the limitations of this model are respected, it may prove valuable for pathogenic and pre-clinical studies of unstable atherosclerosis and that results can be interpreted as relevant for human disease.

Introduction

Rupture of atherosclerotic plaques is a relatively common occurrence causing significant morbidity and mortality. Vulnerability to rupture is associated with specific morphological presentation of lesions(1, 2). These plaques display a large core of lipid deposits and necrotic cell debris, which is covered by a thin cap of fibrous material, mainly collagen. The production of matrix-degrading enzymes like matrix metalloproteinases (MMP) by especially macrophages, results in the loss of collagen and subsequent thinning of the cap(3). Once the cap can no longer withstand the forces imposed upon it, the cap may rupture, exposing the plaque content to the blood. This leads to a strong coagulation response and subsequent formation of a thrombus, which may instantly occlude the artery at the rupture site and refrain the downstream tissues from oxygen supply or embolize and occlude vessels further downstream with similar consequences.

Recently, we developed a mouse model in which the histological characteristics of unstable atherosclerosis are mimicked(4). This model was based on the induction of different profiles of shear stress, i.e. the parallel force applied upon the endothelial cell layer by the flowing blood, in a straight arterial segment in ApoE knockout mice(5). Thus, we could provide convincing experimental evidence for the long-suggested concept that arterial segments exposed to low shear stress (LSS) or oscillatory shear stress (OSS) are more susceptible to atherosclerosis. These assumptions were based on the observation that inner curvatures of large arteries (LSS pattern) and near side branches and arterial bifurcations (OSS pattern) are predilection sites of atherosclerotic plaque development, reviewed in(6). Furthermore, we observed in this model that LSS-induced atherosclerotic plaques developed an unstable phenotype, in contrast to the OSS-induced plaques(4). This difference in plaque composition appeared to be causally related to the differential production of chemokines(7). In particular, fractalkine is produced to a larger extend in the LSS-induced plaque.

In humans, a large amount of clinical evidence has indicated that the unstable regions and rupture sites are predominantly located in the proximal segment of the plaque(8, 9). Since we now have a model available mimicking the morphology of an unstable human plaque, we aimed to take the analysis a step further and to determine how the instability is distributed over the lesion in this model. Therefore, we characterized various vulnerability-determining factors in low shear stress-induced atherosclerotic plaque, which allowed us to compare these to the well-described features of human plaque.

Materials and Methods

Animals and surgical procedures

Apolipoprotein-E deficient mice (female, 15-20 weeks of age, n=13) were obtained from the Jackson Laboratories (Bar Harbor, ME, USA), and fed a high fat, high cholesterol diet consisting of 15% (wt/wt) cocoa butter and 0.25% (wt/wt) cholesterol (Diet W, Hope Farms, Woerden, The Netherlands). Two weeks after this diet was initiated, the mice were anesthetized with 2% isoflurane and instrumented with a shear stress-altering device around the right common carotid artery, as described previously(4). Briefly, this device gradually narrows the vessel lumen to ~70% of its original diameter. As a consequence, shear stress is lowered upstream (low shear stress, LSS) of the device, then gradually increases inside the device and is oscillating (oscillatory shear stress, OSS) just downstream of the device(5). Mice were kept on the high fat, high cholesterol diet for the remainder of the experiment. The device remained in situ until sacrifice after 9 weeks.

All animal experiments were approved by the institutional animal ethical committee and performed in compliance with institutional and national guidelines.

Tissue preparation, staining and analysis

Following sacrifice, mice were perfused systemically with PBS. Next, the common carotid artery was isolated, embedded in OCT compound (Tissue-Tek, Sakura, Japan), and snap-frozen in isopropanol on dry ice. For histology, 8 μm serial cryosections were cut covering the entire length of the lesion and stained for general plaque morphology (hematoxilin-eosin), lipids (Oil Red O), collagen (Picrosirius Red), macrophages (anti-CD68, AbD-Serotec, Oxford, UK), macrophage activation (anti-Major Histocompatibility Complex (MHC) class II, clone M5/114, ATCC TIB-120), smooth muscle cells (anti-SMC α-actin, Sigma-Aldrich, The Netherlands) and collagen production (anti-HSP-47, MBL International, Woburn, MA, USA). Following staining, high-resolution images ware obtained using an Olympus BX-40 microscope or a Zeiss LSM5 Meta confocal microscope (Zeiss Jena, Germany). Collagen stainings were assessed using crossed circular polarization filters.

For in situ zymography a PBS solution of DQ™ gelatin (1 mg/ml) (Invitrogen, Paisley, UK) in 1% agarose (Sigma Chemical Co., Zwijndrecht, The Netherlands) was applied to the slides and incubated for 2 hours at room temperature. Gelatinase activity was detected following incubation by assessing the fluorescent signal using confocal microscopy.

To calculate lesion size and cellular content relative to the plaque area all images were analyzed after digitalization by automated image analysis software (Clemex Technologies Inc, Canada) applying thresholding of the stained areas as before(4).

Statistical analysis

Prism 5 (GraphPad Software, La Jolla, Ca, USA) was used for all statistical analyses. Histological data of the LSS-induced plaque were divided into two equally sized segments, representing the upstream and downstream part of the plaque, respectively (Figure 1). These two segments were compared to each other. For each staining an average was calculated per segment, which was then used in the analysis. Each average resulted from approximately 5 equally spread sections. Differences between segments were tested by a paired t-test when data met the normality assumptions. If not, a nonparametric Wilcoxon matched-pairs test was used. Correlation analysis was performed by the Spearman nonparametric correlation test. Data are presented as mean ± SEM. A p-value of <0.05 was considered statistically significant.
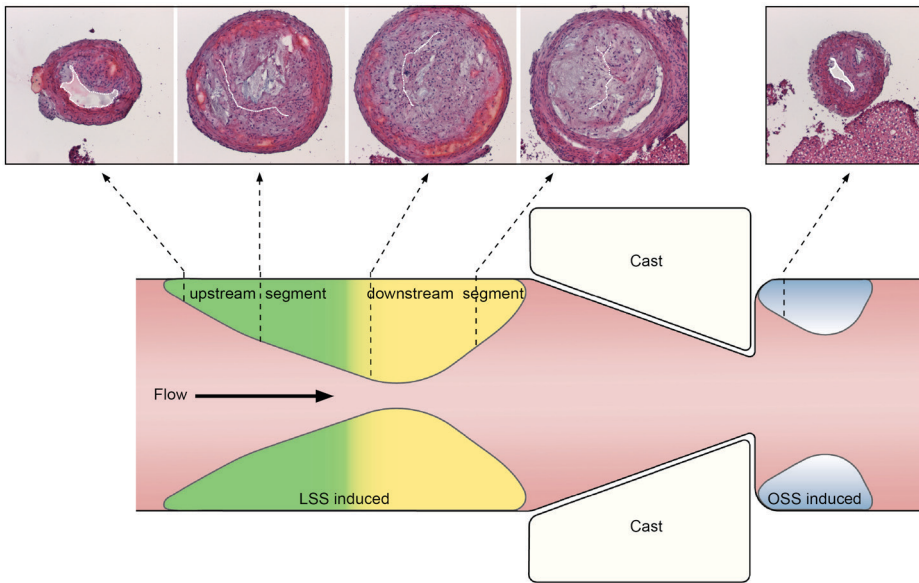
Figure 1. *Disruptions of atherosclerotic plaque induced by low shear stress are located in the upstream part of the lesion.*

Displayed are serial sections of representative H&E-stained plaque from a single mouse. Lesions disruptions can be identified by the pink-reddish color inside the plaque, which indicates the presence of erythrocytes/blood. The white lines on the sections mark the location of the lumen, which collapsed during dissection due to the elasticity of the artery wall and the loss of pressure at the luminal side. The cartoon below shows a graphical representation of the model used, and the approximated location of the sections above indicated by the dashed arrows.

Results

By systematic analysis of various vulnerability-associated factors on serial cross-sections of LSS-induced plaques, we aimed to clarify the distribution of these factors over the length of the plaque and their relevance for plaque instability.

Upstream parts of the LSS plaque show evidence of plaque disruption

In 53% (7/13) of the mice evaluated in this study we found evidence of plaque disruption. This ranged from a minor amount of erythrocytes (15%), to large hemorrhages (15%). In 3 cases (23%) we found major newly formed canals. These were filled with blood, even after systemically and extensively flushing the animals during sacrifice, indicating that they were not continuous with the vascular lumen. These canals appeared to arise from the upstream part of the plaque and on average extended to approximately two third of the plaque's longitudinal length (Figure 1). All three types of disruption, i.e. erythrocyte deposits, large hemorrhages and canal formation, were found in the area close to the tunica media and sometimes in the middle part of the plaque, but never directly adjacent to the collagenous cap. Longitudinally, disruptions were located in the upstream segment. Importantly, we never observed any signs of plaque disruption in the OSS plaque segment.

Macrophages are equally distributed in the low shear stress-induced lesion, but are highly immune-activated in the upstream location

Macrophages are the hallmark leukocytes in atherosclerotic plaques and are considered to be prime cells in plaque dynamics and therefore important for the findings above. We compared the relative occurrence of macrophages in the upstream and downstream parts the LSS plaque (Figures 2A and 3). We found that there are equal amounts of macrophages in either half of the LSS lesion (27.4% ± 2.8% vs. 23.9% ± 2.2%), as indicated by the presence of CD68. In the OSS segment the amount is significantly lower (8.7%), confirming previous findings in this model.

As CD68 is a general macrophage marker, not reflecting the immunological activity of the cells, we measured the expression of MHC class II as a general indicator for macrophage activation(10) (Figures 2B and 3). Remarkably, despite the equal amounts of macrophages in the two LSS segments, we found MHC class II to be much higher expressed in the upstream half of the lesion (15.3% ± 3.0% vs. 6.9% ± 1.9%, p<0.01). When evaluating the distribution of MHC class II cross-sectionally, we noticed that cells close to the luminal border of the lesion more often expressed this marker, suggesting that these were recent immigrants into the plaque (Figure 3).
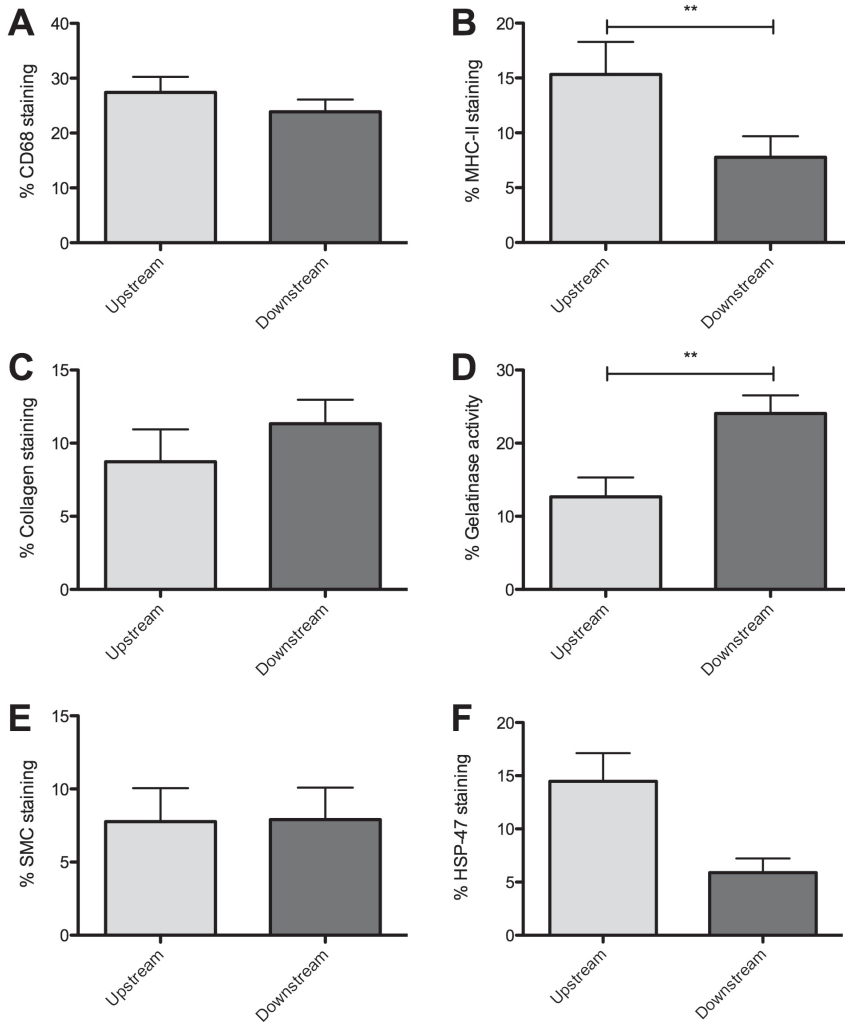
Figure 2. *Characteristics associated with an unstable plaque phenotype are unequally distributed along the plaque length.* A flow-altering device around the common carotid artery of ApoE-/- mice induced different shear stress profiles, resulting in unstable atherosclerotic lesions in the low shear stress (LSS)-induced plaques, whereas the plaques induced by oscillatory shear stress (OSS) are stable. We divided the LSS plaque into an upstream and a downstream segment and compared vulnerability-determining factors with each other. We found differences in CD68 (A) and MHC class II (B) and matrix-degrading gelatinase activity (D) between the different segments. Also, we found a trend of collagen (C) in the upstream segment. We also tested for SMC α-actin (E) and HSP-47 (F), the latter tended was increased in upstream segments of the LSS plaque. These differences did not reach statistical significance, probably due to the limited number of samples available for analysis.
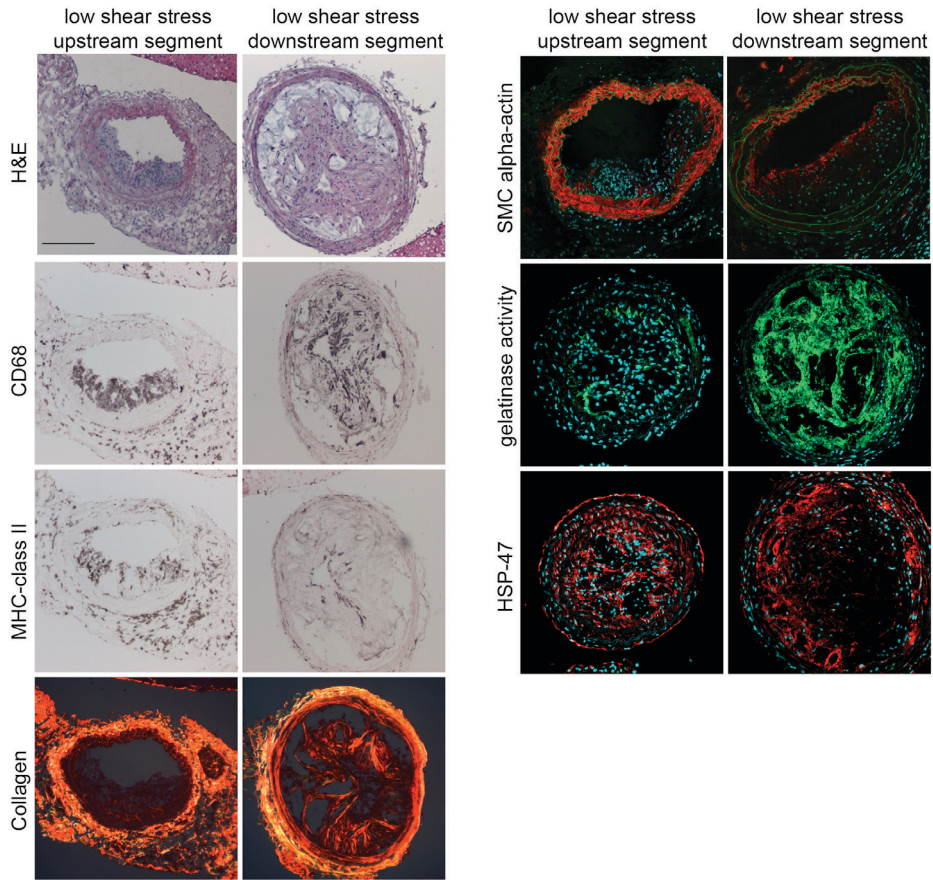
Figure 3. *Histological representation of the longitudinal expression of markers associated with plaque instability.* These images show representative histological sections taken along the length of a low shear stress plaque and the oscillatory shear stress plaque. Compare with Figure 1 for the approximate location in the lesion from which the sections originate. All photographs have been made with the same magnification (100x). A scale bar is provided in the lower right corner of the upper left figure and represents 100 μm.

Collagen tends to be lower in the upstream segment of low shear stress induced lesions

The most important matrix component determining the stability of a lesion is collagen. When comparing the amount of collagen between the two LSS segments, we found no statistically significant difference between the two LSS segments (Figures 2C and 3). Nevertheless, there is a clear trend showing a 23% lower collagen content in the upstream segment (8.7% ± 2.2 vs. 11.3% ± 1.6, p=0.17). We confirmed that the OSS segment contained a significantly higher amount of collagen (29.4%) compared to both LSS segments, as was found before(4).
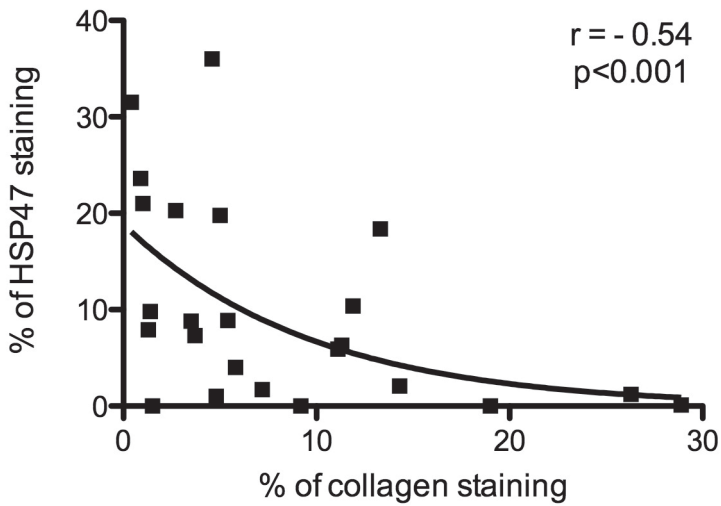
Figure 4. *HSP-47 is inversely related to collagen expression.* High expression of HSP-47, a chaperone protein indicative of collagen production, correlates with low presence of collagen in LSS-induced plaques. We histologically quantified the expression of HSP-47 and collagen in adjacent sections and used the Spearman non-parametric correlation test to test for correlation. We found that low collagen presence in plaque is associated with high expression of the collagen production marker HSP-47.

Matrix-degrading gelatinase activity is most prominent in the downstream segment of the lesion and is partly dissociated from macrophage activation.

Since destabilization of atherosclerotic lesions is partly explained by matrix degradation mediated by macrophage-derived proteases, we performed in situ zymography to show gelatinase activity in the lesions. The highest gelatinase activity was observed in the downstream part (24.1% ± 2.5% vs. 12.7% ± 2.7%, p<0.01) (Figures 2D and 3), indicating that it is not fully related to macrophage activation as evidenced by MHC class II expression. Smooth muscle cells can also produce these matrix-degrading proteases, but the expression of SMC alpha-actin was equally distributed (7,8% ± 2.3 vs. 7.9% ± 2.2%)(Figures 2E and 3).

Collagen production tends to be higher in the upstream segment of the LSS plaque segment

The unexpected distribution of gelatinase activity, inspired us to investigate collagen production as well. Therefore, we measured the expression of the chaperone molecule Heat Shock Protein 47 (HSP-47), which presence closely reflects collagen production(11). We found that HSP-47 expression was almost threefold higher in the upstream segment compared to the downstream segment
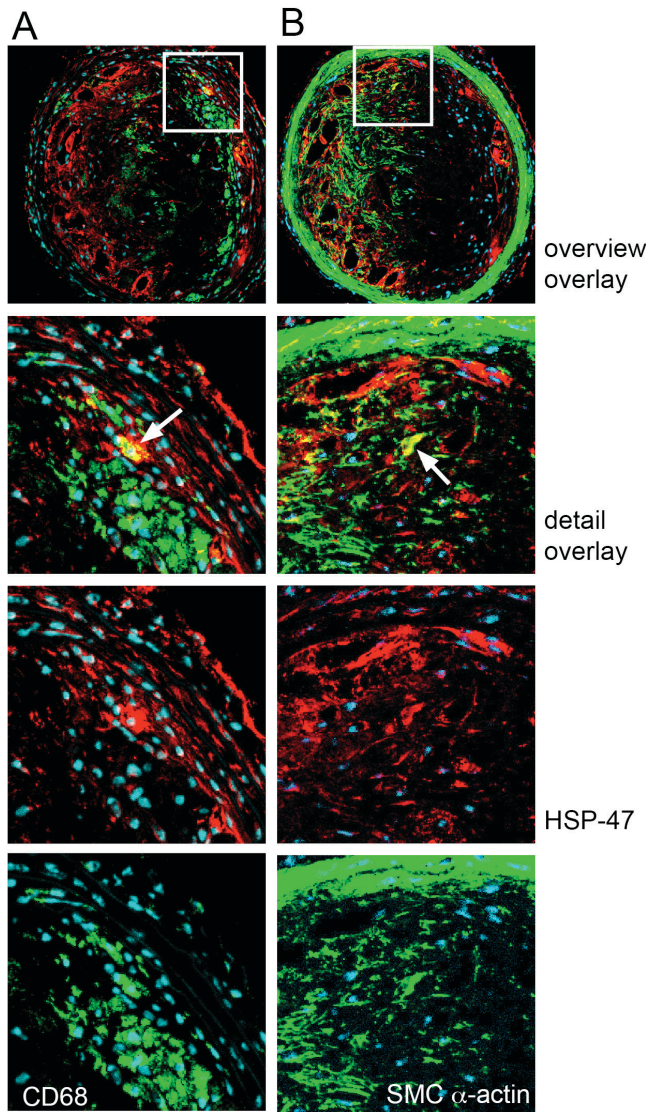
Figure 5. *Colocalization of HSP-47 with cellular components of a plaque.* Expression of HSP-47, a collagen production-associated chaperone, only occasionally co-localizes with macrophages and SMC. Fluorescent double stainings were performed of HSP-47 with (A) macrophages (anti-CD68) and (B) SMC (anti-SMC α-actin) to find the cellular source of the production of collagen. Only occasionally we found single cells that expressed both markers (indicated by white arrows). White boxes in the overview pictures indicate the location of the enlargements. HSP-47 staining is displayed in red; CD68 and SMC α-actin are displayed in green (panel A and B, respectively). Nuclei are stained by DAPI and displayed in blue.

(14.5% ± 2.7% vs. 5.9 ± 1.3%)(Figures 2F and 3). However, these differences were borderline statistically significant (p=0.06), due to the limited amount of available samples (n=4). Despite the small sample size, this finding suggests that the presence of collagen fibers and the expression of HSP-47 are inversely related. This notion is indeed confirmed by correlation analysis (Spearman r = -0.54, p<0.001) (Figure 4). When assessing the distribution of HSP-47 on a cross-sectional level, we noticed that HSP-47 expression was found throughout the entire lesion in the upstream part of the LSS segment, whereas in the downstream part most HSP-47 was found near the medial border of the plaque (Figure 3). To establish the source of the HSP-47, we also performed double staining with SMC α-actin and CD68 (Figure 5). We found that both α-actin-positive SMC and CD68-positive macrophages express HSP-47, but that the bulk of HSP-47 did not match with either marker.

Discussion

The aim of this study was to characterize the various vulnerability-determining factors in LSS-induced atherosclerotic plaques in mice and relate these findings to their location in the plaque. To determine plaque vulnerability we assessed the following features: evidence of plaque disruption, the presence, production and degradation of collagen, the activation of macrophages, and the presence of SMC. We found frequent plaque disruptions only in the upstream part, which associated with macrophage activation. Collagen presence in this segment appeared to be slightly lower than in the downstream part, and, surprisingly, this was accompanied by an increased level of collagen synthesis and a lower level of degradation. Our main findings are summarized in Figure 6 and will be further discussed below.

We observed that disruptions of the unstable plaque, as indicated by intraplaque hemorrhages, occur predominantly in the upstream half of the lesion and never occur in the stable OSS-induced plaque. This reflects the localization of plaque ruptures in humans, which has been shown extensively to be more prominent in the proximal part of the lesion(8, 9, 12). Interestingly, disruptions in our model are exclusively located near the medial border of the lesions and appear as dissections of plaques from the elastic media or as canalization of basal plaque layers. In contrast to the situation in human, we have never observed rupture of the fibrous cap near the luminal side of the lesion, nor have we found evidence of previous ruptures by deposition of erythrocyte particles at this location. Notably, most plaque disruptions arise from the growing, proximal end of the plaque, but continue deep into the length of the plaque.

In order to study the role of activated macrophages in the process of destabilization in our model, we evaluated the distribution of the general macrophage activation

marker MHC-class II, which is known to be up-regulated by different activating stimuli, including pro-inflammatory cytokines and modified LDL that also induce gelatinase expression(10, 13). We found that expression of MHC class II was much higher in the upstream segment compared to the downstream LSS segment. Also, we noticed that most MHC class II-positive cells were found just below the endothelial cell layer, suggesting that these cells were recent immigrants into the plaque by transendothelial migration. The cellular morphology and location associated with MHC class II expression suggests that macrophages are the most likely candidates for MHC class II expression in our samples, especially since it is spatially related to CD68 expression, observed in adjacent sections. However, it must be noted that other plaque cell types, like endothelial cells, may express MHC class II as well(14). In contrast, near the sites of plaque disruption we found little or only very diffuse staining of MHC class II, implying remnant staining of deceased macrophages rather than viable activated cells, or the downregulation of MHC class II on plaque-resident cells. The latter is in accordance with the recently described finding that macrophages exposed to intraplaque hemorrhage adopt an atheroprotective phenotype, accompanied by a downregulation of MHC class II(15).

We also studied the distribution of collagen and compared up and downstream segments of the unstable LSS-induced plaque. We found that there is no statistically significant difference in the distribution of collagen along the plaque, although there is a clear trend to less collagen in the upstream location. In general, our findings show that LSS-induced plaques, at 9 weeks after induction, have an unstable phenotype, while OSS-induced plaques may be considered stable, in accordance with results obtained previously in this model by Cheng et al[1].

The accumulation of lesion-stabilizing collagen is the net result of the balance between (prior) collagen production and its degradation by proteolytic processes. Surprisingly, the expression of collagen synthesis-associated HSP-47 was highest in the collagen-low upstream segment. HSP-47 is known to reside selectively in the endoplasmic reticulum of collagen-producing cells(16, 17). Here it uniquely binds type 1 procollagen and functions as a molecular chaperone protein, crucial in the folding and secretion of type 1 collagen, the predominant type in human atherosclerotic lesions(2, 18). Accordingly, HSP-47 is being expressed in the fibrous regions of advanced plaques in mice(19), as well as in humans(20).

We found that gelatinase activity was highest in the downstream segment of the LSS plaque, remarkably not matching the site with the disrupted lesions. Activated macrophages are regarded as culprits in destabilizing plaques, as they are a major source of matrix-degrading enzymes(21). Macrophages may express collagen-degrading gelatinases (MMP2 and MMP9) upon activation by proinflammatory cytokines(22) or oxidized LDL(23). Both MMPs are expressed in mouse(24) and human lesions(25, 26) and are known for their potential to degrade the fibrous
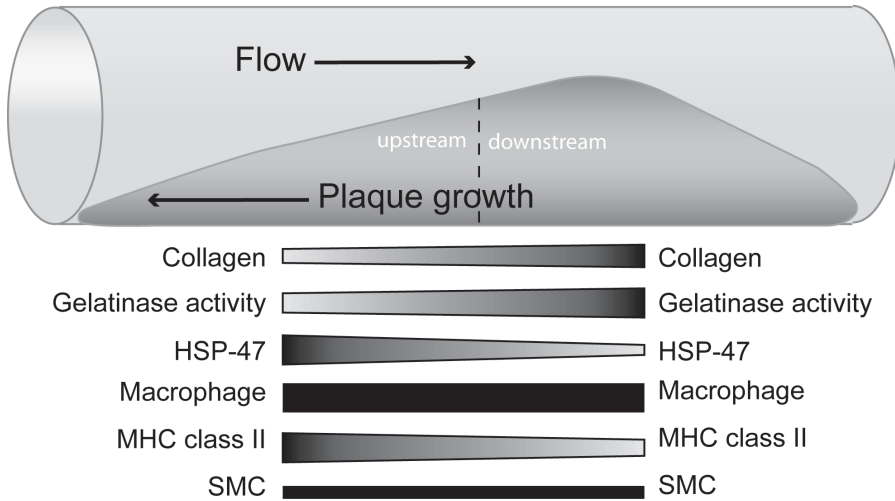
Figure 6. *Summary of study results.*

This figure summarizes the results of the histological analysis. It depicts a plaque with an upstream (left) and downstream segment (right), with below the expression of the histological parameters. A bar with decreasing thickness represents a decrease in expression and vice versa.

cap(27). Macrophage activation as indicated by MHC class II expression and gelatinase activity were shown to be partly longitudinally dissociated, which leaves the question open what cell type is then primarily responsible for the enhanced production of gelatinases in the downstream LSS segment. It was shown before by us(28) and others(26) that α-actin-positive SMC may produce these enzymes as well. Co-localization of gelatinase activity and α-actin is present in our specimens, although most of it does not co-localize with either macrophage CD68 or α-actin. A possible explanation for these findings is that MMPs will be excreted into to extracellular matrix and therefore may dissociate from their producing cells.

Together, our findings show a clear uneven distribution of plaque disruptions along the lesion in our model of low shear stress-induced atherosclerosis. The upstream location of disruptions is accompanied by macrophage activation as indicated by high expression of MHC class II and a trend towards decreased collagen presence. Unexpectedly, in segments with plaque disruption, collagen degradation seems to be lower and collagen production seems increased (Figure 7). We believe that the plaque growth rate might be an important factor in the development of an unstable phenotype at the upstream segment of the LSS-induced plaque. Due to rapid growth in the upstream direction there is little time to produce strong collagen-rich fibrous caps, resulting on proneness to disruption. The high expression of HSP-47 evidences the efforts to produce sufficient collagen.

A remaining question is how well our model represents plaque vulnerability in humans. Clearly, significant similarities as well as differences were observed. The most obvious difference is the time needed to develop (unstable) disease, which is decades in humans vs. weeks in mice. Another major difference is the fact that this model does not display acute rupture of the fibrous cap. A detailed discussion about the possibility and significance of (signs of) plaque rupture in mouse models in general can be found elsewhere (29, 30). However, despite these differences, the morphological similarities between the lesions induced in our model and unstable human lesions are plentiful and therefore support the model's usefulness. The lesions show hallmark characteristics defined by the American Heart Association(1, 2) like: confluent cores of lipids, cores of necrotic cell debris, fibrous caps, as well as positive remodeling of the vessel wall. An additional significant advantage of this model is that it is based upon the concept of shear stress variations, which have shown to be important in humans as well(31-33). Furthermore, the model has been shown to be highly reproducible in the hands of multiple investigators, evidenced by the reproduction of previously found results(4, 7) in the current study.

In summary, in this study we show that the vulnerability of atherosclerotic plaque induced by a low shear stress flow pattern is located predominantly in the upstream lesion segment. This is associated with activation of macrophages and a relatively low collagen content, but partly dissociated from gelatinase activity. This upstream vulnerability results frequently in disruption of the lesion, occurring primarily at the tunica media rather than at the collagenous cap. We believe that, when its limitations are respected, this model may be valuable for pathogenic and pre-clinical studies of unstable atherosclerosis.

References

1 Stary HC. Natural history and histological classification of atherosclerotic lesions: an update. Arterioscler Thromb Vasc Biol 2000; 20(5):1177-1178.

2 Stary HC, Chandler AB, Dinsmore RE, et al. A definition of advanced types of atherosclerotic lesions and a histological classification of atherosclerosis. A report from the Committee on Vascular Lesions of the Council on Arteriosclerosis, American Heart Association. Arterioscler Thromb Vasc Biol 1995; 15(9):1512-1531.

3 Newby AC. Metalloproteinases and vulnerable atherosclerotic plaques. Trends in Cardiovascular Medicine 2007; 17(8):253-258.

4 Cheng C, Tempel D, van Haperen R, et al. Atherosclerotic lesion size and vulnerability are determined by patterns of fluid shear stress. Circulation 2006; 113(23):2744-2753.

5 Cheng C, van Haperen R, de Waard M, et al. Shear stress affects the intracellular distribution of eNOS: direct demonstration by a novel in vivo technique. Blood 2005;

106(12):3691-3698.

6 Helderman F, Segers D, de Crom R, et al. Effect of shear stress on vascular inflammation and plaque development. Curr Opin Lipidol 2007; 18(5):527-533.

7 Cheng C, Tempel D, van Haperen R, et al. Shear stress-induced changes in atherosclerotic plaque composition are modulated by chemokines. J Clin Invest 2007; 117(3):616-626.

8 Wang JC, Normand SL, Mauri L, et al. Coronary artery spatial distribution of acute myocardial infarction occlusions. Circulation 2004; 110(3):278-284.

9 Cheruvu PK, Finn AV, Gardner C, et al. Frequency and distribution of thin-cap fibroatheroma and ruptured plaques in human coronary arteries: a pathologic study. J Am Coll Cardiol 2007; 50(10):940-949.

10 Gordon S. Alternative activation of macrophages. Nat Rev Immunol 2003; 3(1):23-35.

11 Lamandé SR, Bateman JF. Procollagen folding and assembly: the role of endoplasmic reticulum enzymes and molecular chaperones. Semin Cell Dev Biol 1999; 10(5):455-464.

12 Pregowski J, Tyczynski P, Mintz GS, et al. Intravascular ultrasound assessment of the spatial distribution of ruptured coronary plaques in the left anterior descending coronary artery. Am Heart J 2006; 151(4):898-901.

13 Cho HJ, Shashkin P, Gleissner CA, et al. Induction of dendritic cell-like phenotype in macrophages during foam cell formation. Physiol Genomics 2007; 29(2):149-160.

14 Labarrere CA, Pitts D, Nelson DR, et al. Coronary artery disease in cardiac allografts: association with arteriolar endothelial HLA-DR and ICAM-1 antigens. Transplant Proc 1995; 27(3):1939-1940.

15 Boyle JJ, Harrington HA, Piper E, et al. Coronary intraplaque hemorrhage evokes a novel atheroprotective macrophage phenotype. Am J Pathol 2009; 174(3):1097-1108.

16 Dafforn TR, Della M, Miller AD. The molecular interactions of heat shock protein 47 (Hsp47) and their implications for collagen biosynthesis. J Biol Chem 2001; 276(52):49310-49319.

17 Nagai N, Hosokawa M, Itohara S, et al. Embryonic lethality of molecular chaperone hsp47 knockout mice is associated with defects in collagen biosynthesis. J Cell Biol 2000; 150(6):1499-1506.

18 Katsuda S, Okada Y, Minamoto T, et al. Collagens in human atherosclerosis. Immunohistochemical analysis using collagen type-specific antibodies. Arterioscler Thromb 1992; 12(4):494-502.

19 Zhou J, Werstuck GH, Lhoták S, et al. Association of multiple cellular stress pathways with accelerated atherosclerosis in hyperhomocysteinemic apolipoprotein E-deficient mice. Circulation 2004; 110(2):207-213.

20 Rocnik E, Chow LH, Pickering JG. Heat shock protein 47 is expressed in fibrous regions of human atheroma and Is regulated by growth factors and oxidized low-density lipoprotein. Circulation 2000; 101(11):1229-1233.

21 Newby A. Metalloproteinase Expression in Monocytes and Macrophages and its Relationship to Atherosclerotic Plaque Instability. Arterioscler Thromb Vasc Biol 2008; 28:2108-2114.

22 Sarén P, Welgus HG, Kovanen PT. TNF-alpha and IL-1beta selectively induce expression of 92-kDa gelatinase by human macrophages. J Immunol 1996; 157(9):4159-4165.

23 Xu XP, Meisel SR, Ong JM, et al. Oxidized low-density lipoprotein regulates matrix metalloproteinase-9 and its tissue inhibitor in human monocyte-derived macrophages. Circulation 1999; 99(8):993-998.

24 Deguchi JO, Aikawa M, Tung CH, et al. Inflammation in atherosclerosis: visualizing matrix metalloproteinase action in macrophages in vivo. Circulation 2006; 114(1):55-62.

25 Galis ZS, Sukhova GK, Lark MW, et al. Increased expression of matrix metalloproteinases and matrix degrading activity in vulnerable regions of human atherosclerotic plaques. J Clin Invest 1994; 94(6):2493-2503.

26 Brown DL, Hibbs MS, Kearney M, et al. Identification of 92-kD gelatinase in human coronary atherosclerotic lesions. Association of active enzyme synthesis with unstable angina. Circulation 1995; 91(8):2125-2131.

27 Shah PK, Falk E, Badimon JJ, et al. Human Monocyte-Derived Macrophages Induce Collagen Breakdown in Fibrous Caps of Atherosclerotic Plaques: Potential Role of Matrix- Degrading Metalloproteinases and Implications for Plaque Rupture. Circulation 1995; 92(6):1565-1569.

28 Segers D, Helderman F, Cheng C, et al. Gelatinolytic activity in atherosclerotic plaques is highly localized and is associated with both macrophages and smooth muscle cells in vivo. Circulation 2007; 115(5):609-616.

29 Jackson CL. Defining and defending murine models of plaque rupture. Arterioscler Thromb Vasc Biol 2007; 27(4):973-977.

30 Schwartz SM, Galis ZS, Rosenfeld ME, et al. Plaque rupture in humans and mice. Arterioscler Thromb Vasc Biol 2007; 27(4):705-713.

31 Caro CG. Discovery of the role of wall shear in atherosclerosis. Arterioscler Thromb Vasc Biol 2009; 29(2):158-161.

32 Jeremias A, Huegel H, Lee DP, et al. Spatial orientation of atherosclerotic plaque in non-branching coronary artery segments. Atherosclerosis 2000; 152(1):209-215.

33 Kimura BJ, Russo RJ, Bhargava V, et al. Atheroma morphology and distribution in proximal left anterior descending coronary artery: in vivo observations. J Am Coll Cardiol 1996; 27(4):825-831.
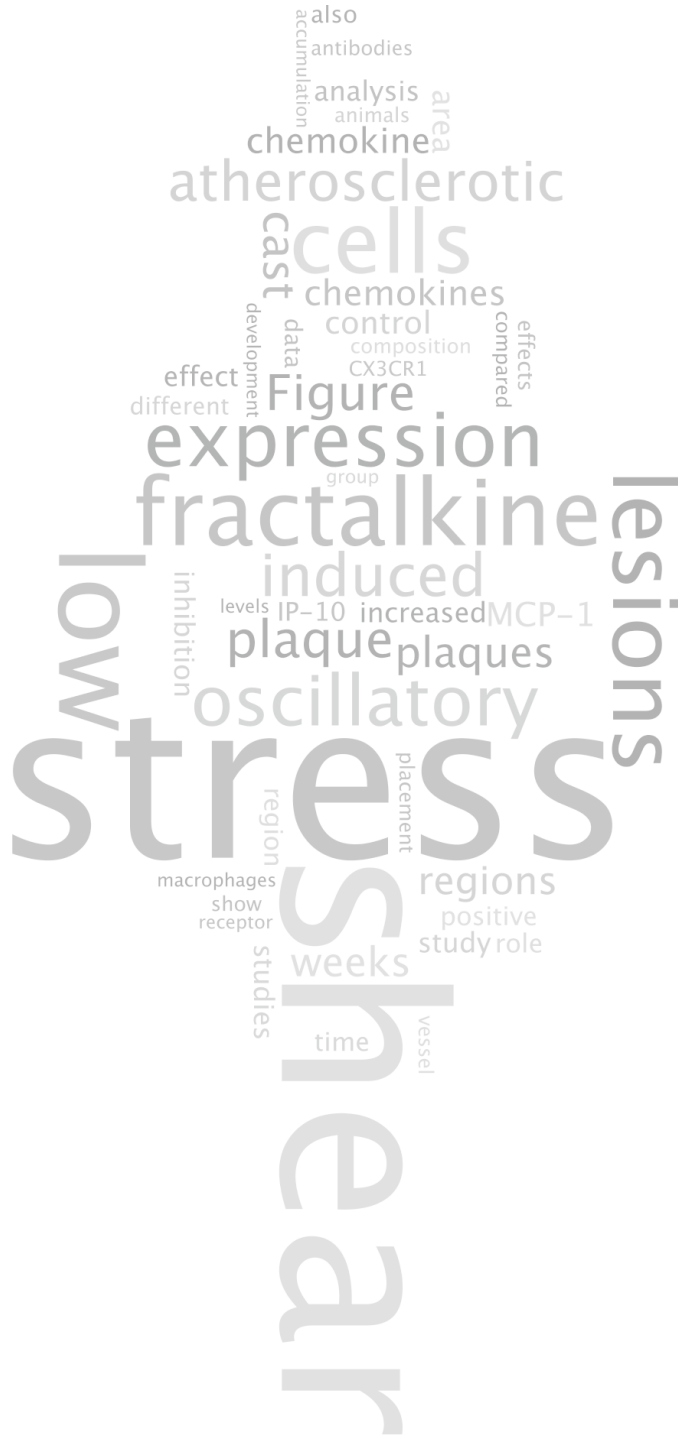
Chapter 4

Shear Stress-Induced Changes in Atherosclerotic Plaque Composition are Modulated by Chemokines

C. Cheng, D. Tempel, R. van Haperen, H.C. de Boer, D. Segers, M. Huisman, A.J. van Zonneveld, P.J. Leenen, A.F.W. van der Steen, P.W. Serruys, R. de Crom, R. Krams.

Abstract

Background
We previously found that low shear stress induces atherosclerotic plaques with characteristics that include increased lipid and MMP content, and decreased vascular smooth muscle and collagen content. The mechanism is currently unknown. In the present study we evaluated the role of chemokines in this process.

Methods and Results
Using an extra-vascular device, we induced regions of low, high, and low/oscillatory shear stress (LSS, HSS, and OSS, respectively) in the carotid artery. Shear stress alterations induced expression of interferon γ inducible protein-10 (IP10) in the LSS region, whereas monocyte chemoattractant protein-1 (MCP1) and the mouse homologue of growth regulated oncogene alpha (GRO-α) were equally upregulated in both LSS and OSS regions, one week after shear stress alterations. After 3 weeks, specific upregulation of GRO-α and IP10 was observed in LSS regions. After 9 weeks, lesions with thinner fibrous caps and larger necrotic cores were found in the LSS region compared to the OSS region. Equal levels of MCP1 expression were observed in both regions, while expression of fractalkine was found in the LSS region only. Results were confirmed on protein level by immunohistochemistry data. Blockage of fractalkine inhibited plaque growth, decreased lipid and CD68 accumulation, decreased the intimal necrotic core area, increased VSMCs and collagen content, and increased the fibrous cap thickness of atherosclerotic lesions in the LSS region.

Conclusion
We conclude that LSS or OSS triggers expression of chemokines involved in atherogenesis. Upregulation of fractalkine during LSS induced atherogenesis is critical in determining the phenotype of the atherosclerotic lesion.

Introduction

Shear stress, which is the drag force per unit area acting on the endothelium as a result of blood flow, plays a critical role in plaque location and progression (1, 2). Both low shear stress and oscillatory shear stress have been implied as pro-atherogenic in observational studies in humans and animals (1, 3, 4). Using a newly developed method to study cause-effect relationships of shear stress in vivo (5), we were able to demonstrate that low shear stress and oscillatory shear stress are both important stimuli for the induction of atherosclerosis (6). Remarkably, low shear stress induces the development of large-sized lesions with less lipids and MMP activity, and increased VSMCs and collagen content compared to the by oscillatory shear stress triggered lesions.

Several studies indicated the role of inflammatory cells in the pathogenesis of plaques with a vulnerable phenotype (7-11). Furthermore, it has been postulated that rupture of vulnerable plaques is associated with activation of macrophages and of the adaptive immune system, leading to metalloproteinase activity and collagen breakdown (9, 12, 13). Accumulation of inflammatory cells occurs through a series of events consisting of rolling, arrest and migration (14, 15). Capture and initial rolling is induced by the interaction of several proteins, while arrest occurs predominantly by integrin-ligand interactions (16-18). The strength of the intergrin-ligand interaction is regulated through changes in avidity and affinity of the integrins (19). Shear stress plays an important role in this process as it counteracts the adhesion of the rolling cells (20, 21), and affects the density of adhesion factors (22, 23). Both in low shear and oscillatory shear stress fields, these two factors enhance the uptake of inflammatory cells.

Recent studies indicate that avidity and affinity of integrins, are modulated by chemokines (17, 24). Chemokines are a family of small, secreted proteins consisting of C, C-C, C-X3-C and C-X-C subgroups based on the positioning of cysteine residues in their backbones (25). Data demonstrating a role for low or oscillatory shear stress in the regulation of chemokines come from a limited number of in vitro studies. These studies show a shear stress dependent expression of monocyte chemoattractant protein-1 (MCP-1/CCL2) (26, 27), and growth regulated oncogene alpha (GRO-α /CXCL8) (28). Chemokine specificity determines the type of inflammatory cells that migrate into the vessel wall. Hence, they might also modulate the phenotype of atherosclerotic lesion that develops in response to shear stress. The role of shear stress regulated chemokine expression during atherogenesis still needs to be investigated. Therefore, the aim of the study is to characterize the chemokine expression pattern in shear stress induced plaque formation.

Results

The effect of low shear stress and oscillatory shear stress on the development of atherosclerotic lesions

Cast placement around the common carotid artery reduced shear stress upstream, and induced oscillatory shear stress downstream from the cast (5, 29). To study the effects of these shear stress fields on atherogenesis, a time series was performed (time points 1, 3, and 9 weeks, N = 5 mice per time point). No statistically significant differences in intimal/media ratio were observed between the different shear stress areas after 1 week of cast placement due to minimal atherogenesis (Figure 1A, B). At 3 weeks, the intimal/media ratio in the low shear stress region was significantly larger than in the control region (Figure 1B), but the difference between oscillatory shear stress regions and control regions did not reach statistical significance. Evaluation of the intimal/media ratio at 9 weeks showed lesions in the low shear stress area that were larger in size compared to those in oscillatory shear stress (5 fold) and control (66 fold) regions. The intimal/media ratio in the oscillatory shear stress region was also larger (14 fold) than in the control region at this time point. Furthermore, lesions that developed under low shear stress conditions contained large necrotic cores underneath a thin fibrous cap, whereas the lesions in the oscillatory shear stress had a more "stable" morphology. These findings are in accordance with earlier obtained data (6).

Gene expression of specific chemokines characterizes low shear stress induced plaque development

To investigate the effect of low shear stress and oscillatory shear stress on chemokine expression under pro-atherogenic conditions, we screened the linearly amplified pools of antisense RNA from vessel segments exposed to the different shear stress conditions after 1, 3, and 9 weeks of cast placement in apoE-/- mice. Because no plaques were present in the low or oscillatory shear stress regions after 1 week of cast placement (Figure 1A, B), the results obtained from this time point show the effect of shear stress alteration on the vessel wall without an existing atherosclerotic lesion. In addition, the 3 weeks time point serves to study the effect of shear stress on the carotid artery with an early atherosclerotic lesion. Finally, at 9 weeks after cast placement, the specific chemokine expression of advanced lesions is analyzed. We compared the response of the chemokines MCP-1, GRO-α/KC, RANTES, eotaxin-1, ELC, SDF-1α, NAP-2, IP-10, fractalkine and CCL14 (all reported to be involved in atherosclerosis or to be regulated by shear stress (26, 28, 30)), on low and oscillatory shear stress stimuli at different time points. From the 10 chemokines investigated in this study, 4 (MCP-1, GRO-α/KC, IP-10, and fractalkine) were upregulated in response to alterations in shear stress at different time points. No shear stress responsive upregulation in the expression of the other chemokines (RANTES, eotaxin, ELC, NAP-2, SDF-1α and CCL14) was observed. After 1
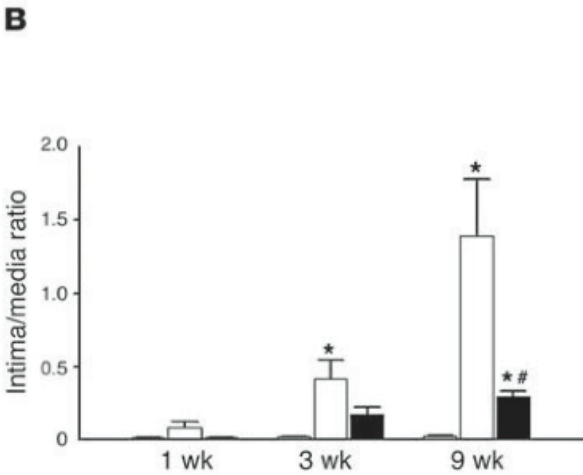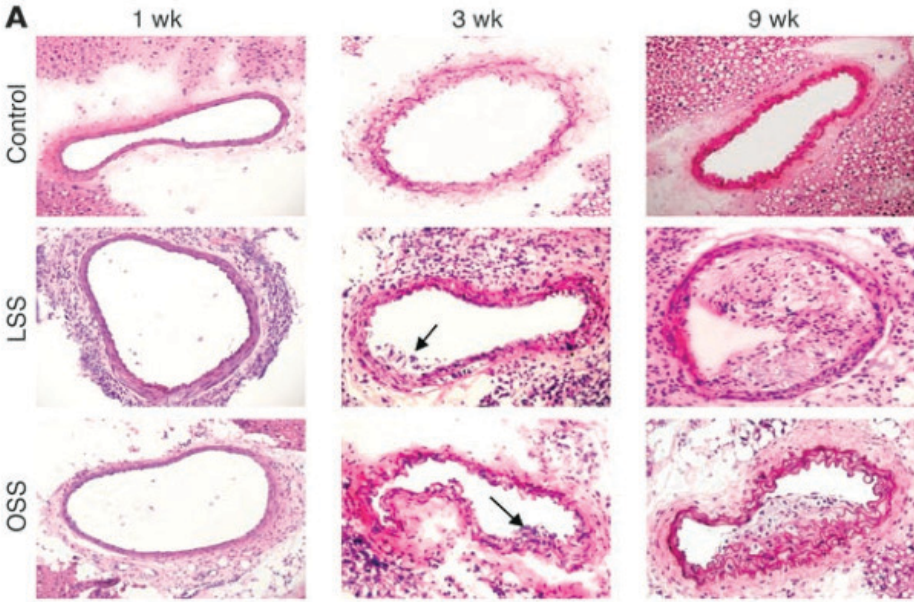
Figure 1. *Representative hematoxylin and eosin-stained cross-sections of murine carotid arteries at different time points after cast placement in mice on a Western diet.*
(A) Sections from the oscillatory shear stress region (OSS), low shear stress region (LSS) and undisturbed region (control) after one, three, and nine weeks of cast placement. The arrows in the pictures indicate accumulations of macrophages in fatty streaks (original magnification, 200X.). (B) Intima/media ratio in the control regions (hatched bars), the low shear stress regions (white bars), and the oscillatory shear stress regions (black bars) at the three different time points. *P<0.05 versus control. #P<0.05 versus low shear stress.
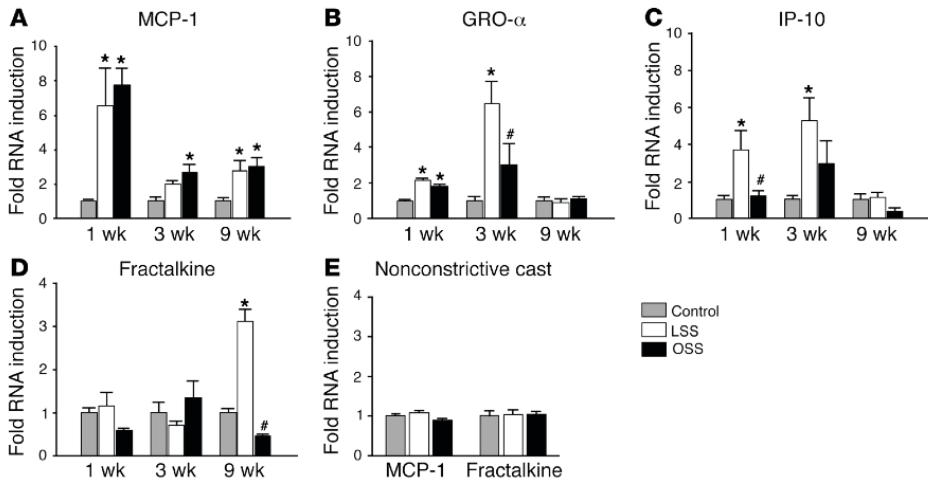
Figure 2:. *Validation of the expression levels of the upregulated chemokines.* MCP-1 (Panel A), GRO-α/ KC (Panel B), IP-10 (panel C), and fractalkine (panel D) expression levels were measured by QPCR using pooled non-amplified cDNA samples (5 animals per pool, N=3) at different time points (1, 3, and 9 weeks), and different locations (low, control and oscillatory shear stress regions). *P<0.05 versus control. #P<0.05 versus low shear stress. (E) Placement of a non-constrictive, control cast that does not alter the laminar shear stress, did not induce changes in gene expression.

week, QPCR showed an increase in expression of the chemokines, MCP-1 and GRO-α/KC in the altered shear stress regions compared to control. In addition, IP-10 was more expressed in the low shear stress than in the oscillatory shear stress region. After 3 weeks of cast placement, the increased gene expression levels in MCP-1 were maintained in both low shear stress and oscillatory shear stress regions, while GRO-α/KC and IP-10 were only upregulated in the low shear stress region. After 9 weeks of cast placement the expression of MCP-1 and IP-10 returned to baseline levels. Of interest, fractalkine was only upregulated at this time point, and exclusively in the low shear stress regions.

Validation experiments

To verify the results obtained from the linearly amplified samples, we repeated the QPCR experiments with pooled samples of non-amplified RNA for those chemokines that were differentially upregulated. Essentially the same expression patterns were observed for MCP-1, GRO-α/KC, IP-10, and fractalkine (Figure 2 A, B, C, D) when we compared data from non-amplified RNA with data obtained with linearly amplified RNA. In particular the expression pattern of fractalkine were highly similar.

In order to exclude possible non-shear stress related effects of the cast on chemokine expression, we performed control experiments with sham casts. These sham casts
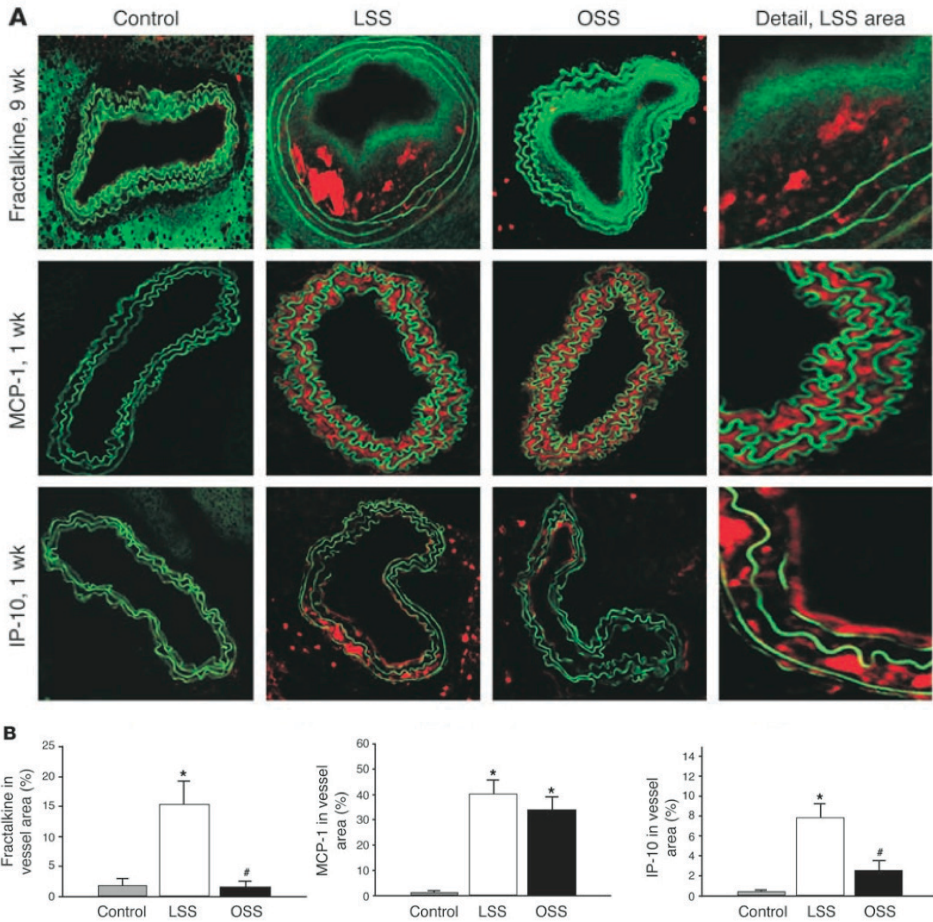
Figure 3. *Confirmation of gene expression results of selected chemokines by immuno-histological analysis of the protein levels in carotid arteries at different time points after cast placement in mice on a Western diet.* (A) Representative cross-sections of murine carotid arteries stained for fractalkine after 9 weeks of cast placement, and MCP-1 and IP-10 after 1 week of cast placement, in the control, low and oscillatory shear stress regions (original magnification, 200X). Chemokine expression is represented by a red signal. Green auto-fluorescence is from the elastic laminae and demarcates the intimal and medial areas. (B) Immuno-histological quantification of the chemokine signals of the low shear stress (LSS), the oscillatory shear stress (OSS) regions and control regions are shown. N=5. *P<0.05 versus control. #P<0.05 versus low shear stress.
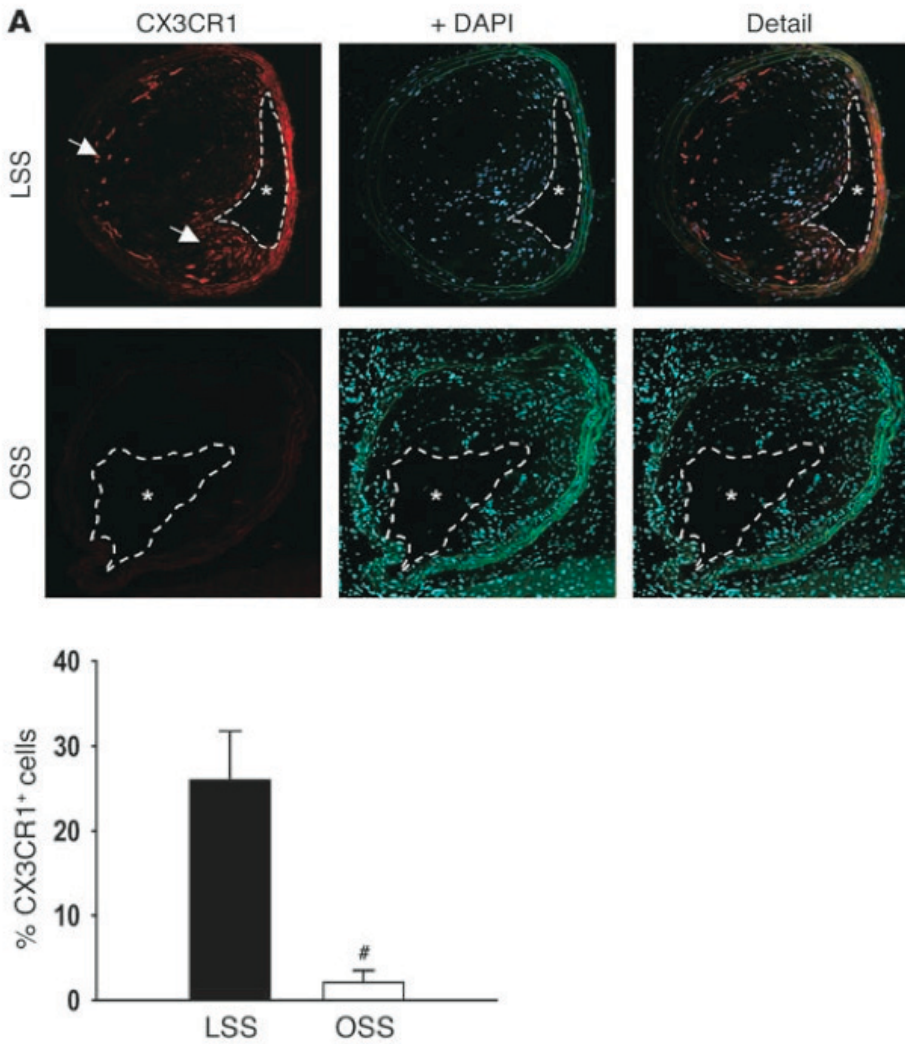
Figure 4. *Accumulation of CX3CR1+ cells in the different by shear stress induced mature athersclerotic lesions after 9 weeks of cast placement.*

(A) Representative cross-sections of murine carotid arteries stained for CX3CR1 (red signal) and nuclei (blue signal). Arrows indicate CX3CR1 positive cells. Asterisks indicate the position of the lumen, while the white dotted lines demarcate the boundaries between lumen and intima. (B) Immuno-histological quantification of the chemokine-receptor signal in the low (LSS) and the oscillatory shear stress (OSS) region. N=5. #P<0.05 versus low shear stress.
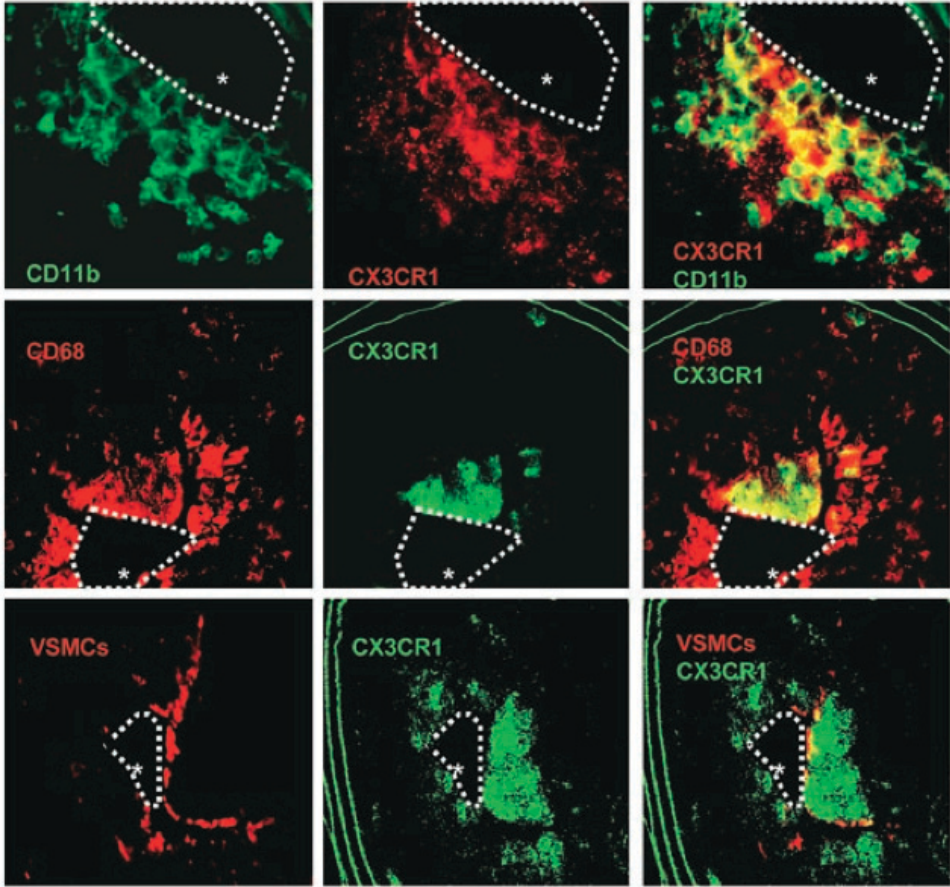
Figure 5. *CX3CR1 expressing cells located in the advanced lesions are mainly monocytes and macrophages.* Representative cross-sections of murine carotid arteries stained for CX3CR1 and CD11b (upper panels), CD68 (middle panels), and VSMC α-actin (lower panels), respectively. In the third panels, overlays show the co-localization signal in yellow. Asterisks indicate the position of the lumen, while the white dotted lines demarcate the boundaries between lumen and intima. Double staining for the identification of CX3CR1 expressing cell types has been repeated in 4 different experiments.

were made of the same material as the real cast, but did not induce the alterations in shear stress due to a non-constrictive luminal geometry. Placement of the sham casts failed to cause lesion formation in both the upstream or downstream location from the device even after 9 weeks of instrumentation. Gene expression analysis on cDNA obtained from both locations did not reveal upregulation of MCP-1 or fractalkine (Figure 2E).

Total cholesterol levels in plasma were increased in animals on the atherogenic Western type diet (1 week = 27.3± 2.0 mmol/l, 3 weeks = 22.4± 0.9 mmol/l, 9 weeks = 24.3± 2.4   mmol/l) compared to animals on chow (10.9± 3.0 mmol/l). However, total cholesterol concentrations between animals treated with the cast or the non-constrictive sham cast were not different (9 weeks cast = 24.3± 2.4 mmol/l versus 9 weeks sham cast = 25.5± 3.0 mmol/l). Therefore, the observed variations in chemokine expression cannot be attributed to differences in plasma cholesterol levels.

Protein levels follow gene expression levels of selected chemokines

We evaluated the protein levels of a selected group of responsive chemokines. Fractalkine was studied, because it was the only chemokine with elevated expression in the atherosclerotic lesions induced by low shear stress that showed the interesting plaque composition. Indeed, a more intense fractalkine staining was found in the low shear stress region compared to the oscillatory shear stress and control regions (Figure 3A, B, upper panels) at 9 weeks, which is in accordance with the mRNA expression data. We also evaluated MCP-1, as the relevance of this chemokine for the pathology of atherosclerosis is well-known(25). Immunohistological analysis of vessel segments at 1 week, which is the time-point with the highest MCP-1 expression (see Figure 2), confirmed the upregulation of MCP-1 under both shear stress conditions (Figure 3A, B, middle panels). In addition, we selected one of the chemokines that were upregulated during early atherosclerosis development induced by low shear stress. The differences in protein level of IP-10 between the low shear stress and the oscillatory shear stress areas at 1 week of cast placement closely resemble the mRNA expression pattern. (Figure 3A, B, lower panels).

Figure 6, right page: *Fractalkine function was inhibited during cast-induced atherogenesis in ApoE-/- mice by administration of a neutralizing antibody from week 6 until week 9.* Representative cross-sections are shown stained for: lesion morphology by hemotoxylin/eosin (A), macrophages (B), lipids (C), VSMCs (D), collagen (E), and fractalkine receptor (CX3CR1) (F). Asterisks indicate the position of the lumen, while the white dotted lines demarcate the boundaries between lumen and intima. Bar diagrams represent the lesion area and quantification of the (immuno-)histological analysis of the different plaque components. The percentages of positive area at time point 9 weeks in the intima in the low (LSS) and the oscillatory shear stress (OSS) region are indicated, comparing the control antibody group (-) with the α-fractalkine antibody group (+). N=8. *P<0.05 versus control antibody group.
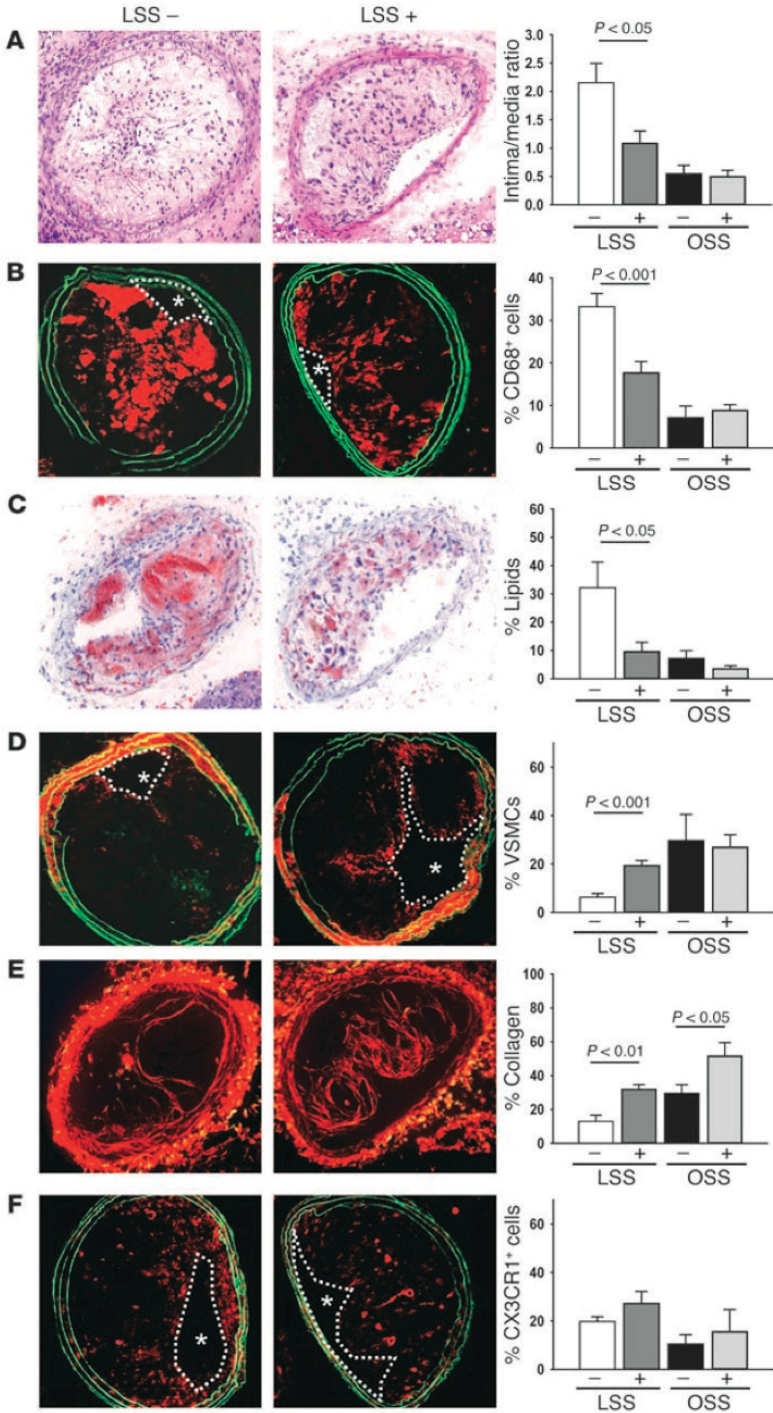
Fractalkine receptor expressing cells are present in the low shear stress-induced atherosclerotic plaques

From the above findings, we concluded that fractalkine is an interesting chemokine for further studies. We therefore assessed the effect of low and oscillatory shear stress on the accumulation of CX3CR1 (i.e. the fractalkine receptor) positive cells in advanced lesions in order to determine its contribution to the pathology of the low shear stress lesions. CX3CR1 expressing cells were detected in the intimal area of lesions situated in the low shear stress region, while in the lesions in the oscillatory shear stress regions CX3CR1 expressing cells were hardly detected (Figure 4A, B). Further analysis of the atherosclerotic lesions located in the low shear stress area showed that many cells positive for CX3CR1 were also positive for the monocyte/macrophage markers CD11b and CD68 in the lesions (Figure 5, upper and middle panels, respectively). Double staining for CX3CR1 and VSMC α-actin, did not show any obvious evidence for smooth muscle cells expressing the fraktalkine receptor (Figure 5, lower panels). Serial cross-sections show no general overlap of these CX3CR1+ cells with the fractalkine+ areas, indicating that most of these receptor positive cells do not produce the fractalkine ligand.

Inhibition of fractalkine function restrains growth and stabilizes atherosclerotic plaques induced by low shear stress

To evaluate the functional implications of above findings, we studied the possible effect of fractalkine inhibition on systemic effects, plaque composition and plaque vulnerability. Microscopic inspections of hematoxilin-eosin stained sections of liver, lung, spleen and draining lymph nodes of the carotid artery did not reveal any abnormalities in animals treated with the rabbit polyclonal IgG neutralizing antibody against fractalkine in the fractalkine group or the rabbit polyclonal IgG control antibody in the control group (data not shown). Furthermore, FACS analysis on spleen-derived and peripheral blood leukocytes showed no differences in the numbers of CD3+ cells or in the CD4+/CD8+ cell ratios between the two groups (data not shown).

Animals in the fractalkine inhibition group showed a 50% reduction of plaque area in low shear stress regions only (Figure 6A), i.e. in the regions with a differential upregulation of fractalkine. In addition, fraktalkine inhibition changed plaque composition –with the exception of collagen– exclusively in the by low shear stress induced plaques: treatment with fractalkine-neutralizing antibodies approximately halved CD68 positive macrophage content and lipid accumulation in these type of atherosclerotic plaques compared with the control group and doubled the number of VSMCs (Figure 6A, B, C, and D). However, in the oscillatory shear stress regions, no differences between the fractalkine and the control group were observed in size and content of the plaques. In both the low shear stress regions and in the oscillatory shear stress regions, treatment with anti-fractalkine antibodies resulted in increased

collagen content (Figure 6E). In both shear stress regions, no effect was found on the number of CX3CR1 positive cells in response to fractalkine antibody treatment (Figure 6F).

Morphometric evaluation of the plaques in the low shear stress and the oscillatory shear stress region show that the relative cap area (cap/intima ratio) and the relative necrotic core size (core/intima ratio) were both ~2 fold smaller in the atherosclerotic lesions induced by low shear stress than by oscillatory shear stress (Figure 7). Treatment with anti-fractalkine antibodies resulted in an increase in cap thickness, and decreased the size of the necrotic core in the by low shear stress induced lesions (Figure 7).

Fractalkine might also affect the infiltration of other types of immune component cells involved in atherogenesis. Therefore, we analyzed the lesions induced by low or oscillatory shear stress from mice treated with the anti-fractalkine antibodies or with control antibodies for the accumulation of CD3+ (pan T cell marker) T cells, mast cells and NK cells. We found that fractalkine inhibition had no effect on CD3+ T cells accumulation (Figure 8A). However, inhibition of fractalkine function strongly reduced the numbers of mast cells in the adventitia of the plaques induced by low shear stress (Figure 8B). For the detection of NK cells, we used the anti-mouse Ly49G2 antibody, 4D11, which has no cross-reaction with macrophages and has been used previously for the detection of NK cells in murine plaque areas(31). In both the atherosclerotic lesions induced by low shear stress or oscillatory shear stress, NK cells were scarce, limited to one to two cells per lesion, and fractalkine inhibition did not show any effects.
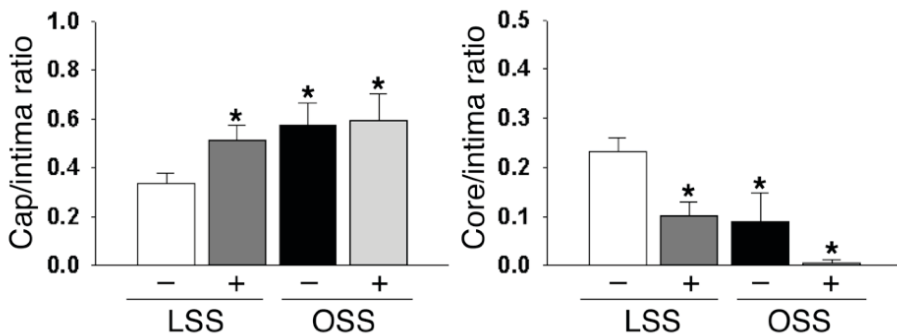
Figure 7. *The effect of fractalkine inhibition on cap thickness and the size of the necrotic core in the low shear stress and oscillatory shear stress lesions.*

Quantification of cap thickness (left panel) and the necrotic core (right panel) relative to total intimal area of the low shear stress (LSS) and the oscillatory shear stress (OSS) regions, comparing the control antibody group (-) with the α-fractalkine antibody group (+). N=8. *P<0.05 versus low shear stress without antibody treatment (-).

Figure 8. *The effect of fractalkine inhibition on T cells (panel A) and mast cells infiltration (panel B, and Il-6 and CRP expression (panel C) in the low shear stress and oscillatory shear stress lesions.*

In the left panels, representative cross-sections taken from the low shear stress lesions (LSS) from ApoE-/- mice after 9 weeks of cast placement with administration of rabbit IgG control antibodies (-) or with the neutralizing antibody against fractalkine (+) are shown. Cross-sections are stained for CD3+ T cells (A) and mast cells using toluidin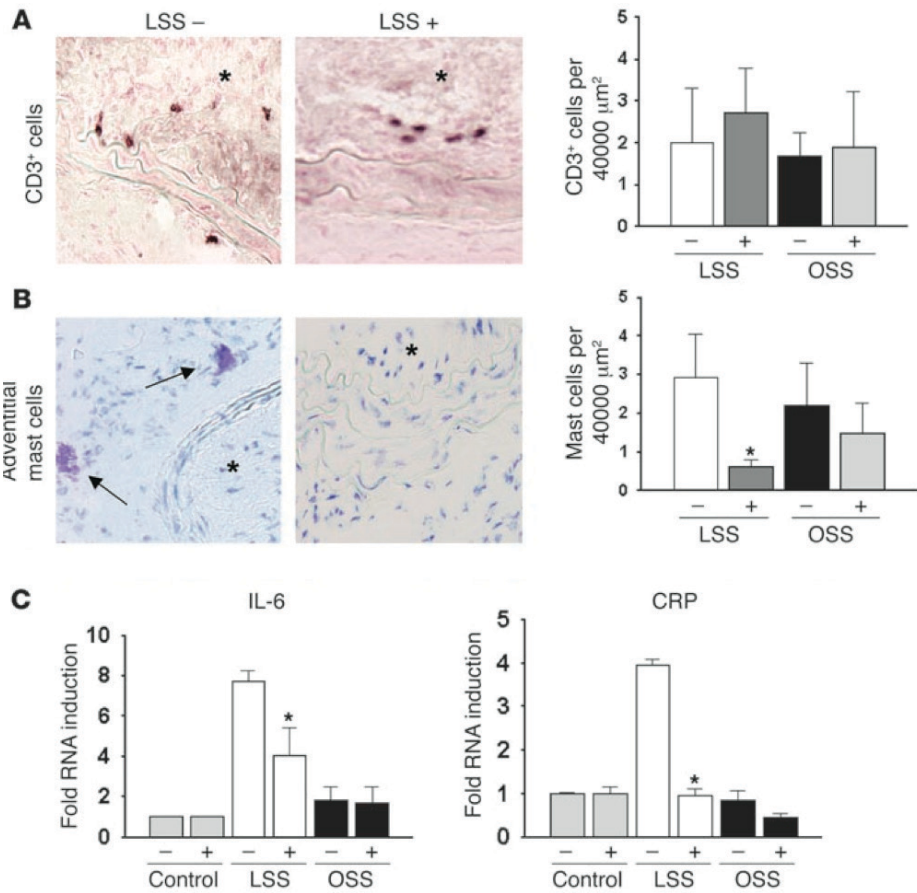e blue (B) (original magnification, 200X). CD3+ T cells and mast cells are indicated by arrows. Asterisks indicate the intimal area. The number of positive cells counted in the intima (CD3+ T cells) and adventitia (mast cells) in the low shear stress (LSS) and oscillatory shear stress (OSS) lesions, with administration of rabbit IgG control antibodies (-) or with the neutralizing antibody against fractalkine (+). N=6. *P<0.05 versus control antibody group. (C) Expression levels of CRP and IL-6 in carotid arteries at 9 weeks after cast placement in mice on a Western diet in response to fractalkine inhibition. Expression profiles were measured by QPCR using amplified RNA samples (10 animals per pool, N=3). In the control group (-), Il-6 and CRP levels in the low shear stress region are significantly upregulated versus control and oscillatory shear stress region. *P<0.05 versus α-fractalkine antibody group (+).

83

Gene expression analysis of the different vessel segments at the 9 weeks time point revealed increased expression of the pro-inflammatory mediators CRP and IL-6 in the low shear stress versus the oscillatory shear stress regions in the control group. Fractalkine inhibition reduced gene expression of CRP and IL-6 as expression of these genes in the low shear stress areas were significantly decreased in response to antibody treatment (Figure 8C).

Subsequently, we investigated whether the effect of fractalkine inhibition is restricted to the lesions induced by the cast model. Therefore, the composition of the atherosclerotic lesions in the brachiocephalic arteries (BCAs) was analyzed. We found indeed effects of fractalkine inhibition on BCA lesions. Treatment with neutralizing antibodies against fractalkine reduced lipid and macrophage accumulation in the intimal area. It also increased the collagen content in these BCA lesions (Figure 9). No significant differences in the percentage of intimal VSMCs and lesion size were found, but a trend was observed towards a reduction in intimal area in response to the treatment (control group = 0.11 ± 0.01 mm^2 versus fractalkine inhibition group 0.08 ± 0.01 mm^2). Discussion

The main findings of this study are: (i) the development of atherosclerotic plaques induced by low shear stress is characterized by a specific expression of GRO-α/KC, IP-10, and fractalkine. (ii) Fractalkine determines the growth and the composition of this type of atherosclerotic lesion.

The high mortality accompanying atherosclerosis can be ascribed to a large extent to rupture of vulnerable plaques (32, 33). The morphology of vulnerable plaques consists of a characteristic triad: a large lipid core, a thin fibrous cap and an accumulation of inflammatory leukocytes. This inflammatory component is prominent in plaques with a vulnerable phenotype, and it has been postulated that activation of the immune system is an important condition for the development of vulnerable plaques (7-11). Accumulation of inflammatory cells into plaques has been examined extensively and a cascade model has emerged from these studies. This model describes rolling, arrest and migration as a sequential process (9). Arrest of inflammatory cells on the endothelial layer in an arterial flow field, as occurs in our experiments, is due to an increased clustering on the cell surface (avidity) and increased affinity of integrins for their ligands (20, 21). Both processes are strongly modulated by chemokines (17, 24). However, the role of shear stress in the expression of chemokines largely unknown.

We studied the effect of shear stress on chemokine expression, and thus potential leukocyte recruitment during plaque formation, performing a screening of 10 chemokines that are known to be involved in the pathology of atherosclerosis or are known to be responsive to shear stress. Interestingly, 4 of the selected genes, MCP-1, GRO-α/KC, IP-10 and fractalkine, were upregulated. These were studied in more detail.
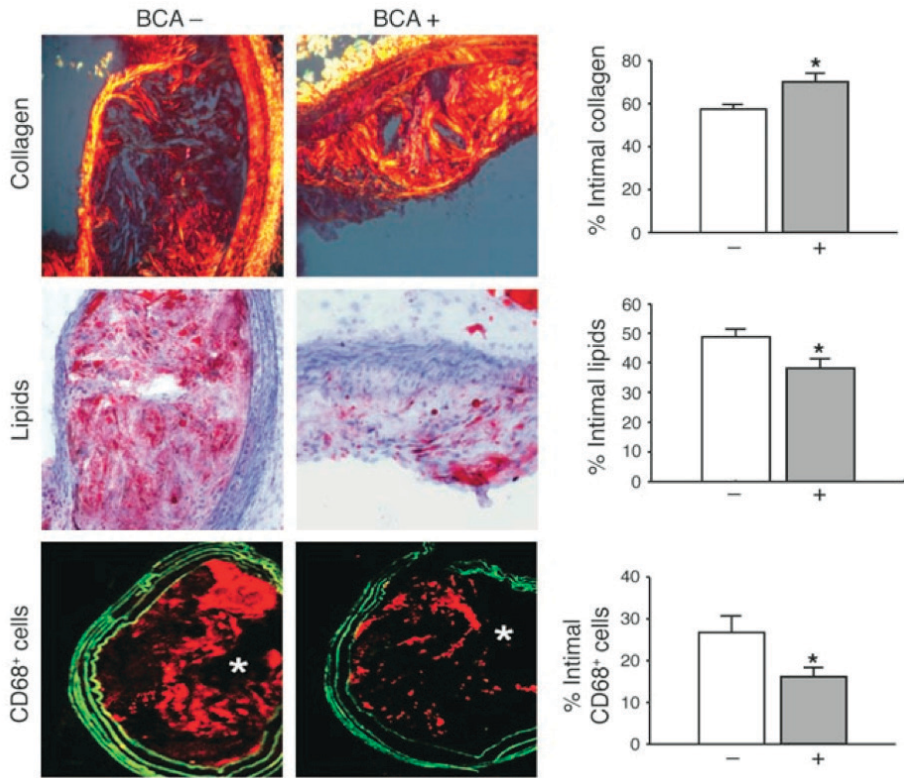
Figure 9: Fractalkine function was inhibited during atherosclerosis development in the BCAs in ApoE-/- mice on Western diet by administration of a neutralizing antibody from week 6 until week 9. Representative cross-sections are shown stained for: collagen (upper panels), lipids (middle panels), and macrophages (lower panels). Asterisks indicate the position of the atherosclerotic lesions. Bar diagrams represent quantification of the (immuno-)histological analysis of the different plaque components. The percentages of positive area at time point 9 weeks in the intima in the BCAs are indicated, comparing the control antibody group (-) with the fractalkine antibody group (+). N=6. *P<0.05 versus control antibody group.

MCP-1 accumulation has been demonstrated in human atherosclerotic lesions and in plaques induced in animal models (34, 35). It is involved in monocyte/macrophage recruitment and knock out studies indicate an important role in atherogenesis (25). In the present study, MCP-1 expression levels did not differ between low and oscillatory shear stress stimuli. These findings are in accordance with in vitro studies showing a role for both low and oscillatory shear stress in MCP-1 production by endothelial cells (26, 27). This lack in differential expression and the decline in MCP-1 expression after the first week of shear stress stimulation may imply that the MCP-1/CCR2 (MCP-1 receptor) interaction is important

predominantly during early atherogenesis, and may not play an important role in determining the phenotype of the advanced atherosclerotic lesion. Recent studies with CCR2 deficient mice indicate that early reconstitution of CCR2 positive cells prevent the effects of CCR2 deficiency, while this effect is absent during later phases(36), similar to the present findings.

Two other genes (IP-10 and GRO-α/KC) were upregulated in the early phase of low shear stress induced plaque formation. IP-10 is a chemoattractant for monocytes (37) and T-lymphocytes (38) and is induced by production of interferon-g (IFN-γ) (39). Only a small number of studies have identified this chemokine in relation with vascular disease. However, as IFN-g has been associated with vulnerable plaque formation (40), this chemokine may be of importance. Indeed, increased serum levels of IP-10 have been associated with coronary artery disease in patients (41).

GRO-α/KC and its receptor CXCR-2 are involved in the accumulation of macrophages during atherogenesis, and high level expression of CXCR-2 by macrophages is detected in advanced lesions of patients and LDL receptor deficient mice (42). Surprisingly, increased GRO-α/KC expression was only detected at earlier time points (1 and 3 weeks). This implies that GRO-α/KC/CXCR2 interaction is mainly involved during the early events of low shear stress induced plaque formation.

From the upregulated chemokines, fractalkine is the only one that is exclusively expressed in the low shear stress-induced atherosclerotic plaque. Fractalkine is a unique chemokine that not only acts as a chemoattractant, but also as an adhesion molecule expressed on endothelial cells upon stimulation (43). The fractalkine receptor CX3CR1 is expressed on monocytes, macrophages, lymphocytes, VSMCs (44) and ECs, where its expression is regulated by IFN-γ (45, 46). Functional studies in mice indicate that CX3CR1 or fractalkine deficiency results in smaller atherosclerotic lesions, associated with a reduction in the number of macrophages and foam cells (47-49). In the present study, we observed more CX3CR1 positive cells in the plaques with the distinct composition located in the low shear stress region as compared to the plaques found in the oscillatory shear stress regions, suggesting that there is an effect of fractalkine expression on cell recruitment. Subsequent qualitative analysis of CX3CR1 positive cells identified predominantly monocytes and macrophages, and few VSMCs co-localizing with the fractalkine receptor. It is postulated that monocytes may enter the atherosclerotic lesion from the adventitial side. However, in the lesions induced by low shear stress, cells positive for CD11b, which is a cell surface marker for monocytes that is downregulated during their differentiation into macrophages (50), were mainly detected just underneath the endothelium (Figure 5). Additional studies in which we stained the lesions for the myeloid-committed progenitor cell marker er-mp53(51), showed er-mp53+ cells mainly located in

close proximity of the lumen (data not shown). We conclude from these data that plaque macrophages enter the lesions that are induced by low shear stress via the luminal side.

Inhibition of fractalkine/CX3CR1 interaction decreased plaque growth, and altered the composition of the atherosclerotic plaques within the low shear stress regions. The exact mechanism is presently unknown, but might include a reduced accumulation of macrophages and foam cells, derived from CX3CR1[high] monocytes. In addition, the lesions contained increased amounts of extracellular matrix (collagen) and VSMCs, thereby increasing collagen synthesis, when compared with the lesions of the control group. Importantly, inhibition of fractalkine/CX3CR1 interaction had only minor effects on the lesions induced by oscillatory shear stress. This might indicate a role for low shear stress in the fractalkine-mediated effects. However, as fractalkine upregulation was only observed in the low shear stress plaques after 9 weeks of cast placement, other factors may be involved. For instance, extreme narrowing of the luminal area during later phases of plaque growth might have increased shear stress locally, and this increase in shear stress might have provided the trigger for fractalkine expression. In addition inflammatory mediators (e.g. IFN-γ) released from within the vessel wall during atherogenesis induced by low shear stress might also be responsible for the upregulation of fractalkine. Nevertheless, expression of fractalkine remains a distinct (indirect) effect of low shear stress-induction of atherosclerosis, and the results of the functional experiments presented in this study are important, as they clearly show the critical role of fractalkine in determining the composition of advanced atherosclerotic lesions.

Recent in vitro findings obtained from flow chamber assays indicate that fractakine contributes to platelet activation and adhesion, and could therefore play an important role in increasing thrombogenesis in atherosclerosis(52). We studied platelet aggregation in the different shear stress lesions in response to fractalkine inhibition by immunohistochemistry, staining for P-selectin. Platelet aggregations were detected in both the low shear stress and oscillatory shear stress induced lesions. However, these vascular pathologies were also observed in fractalkine antibody treated animals. The platelets were activated, as platelet-leukocyte conjugates were formed lining the endothelium. Occasionally, large platelet-rich thrombi were detected in the lumen. As activated endothelial cells also produce P-selectin, we double-stained with antibodies directed against von Willebrand factor (green signal). The results show that these defined histological structures positive for P-selectin were indeed platelet aggregations lying on top of von Willebrand factor positive endothelial cells. These data indicate that fractalkine might not play a significant role in (micro) thrombogenesis in vivo in the context of atheroschlerosis. It also seems not to be a prominent mechanism to explain the fractalkine effects.

The finding that fractalkine inhibition results in a decreased accumulation of mast cells in the adventitia of the by low shear stress induced lesions, is interesting as it

has been shown by Virmani and co-workers that mast cells infiltrate the adventitia of atherosclerotic vessel segments during plaque development in humans(53). Accumulation of mast cells in the adventitia is also increased in the coronary arteries of patients who died of acute myocardial infarction(54). It was speculated that the release of histamine and leukotrienes by activated mast cells in the adventitia could cause constriction of the atherosclerotic vessels, leading to acute coronary syndrome(55). Fractalkine has been shown to be involved in the recruitment of mast cells in skin tissue(56) and in the airway of patients with asthma(57). Our study now shows that chemotaxis of mast cells into the adventitia of atherosclerotic vessel segments is (partly) regulated by fractalkine. The inhibition of fractalkine function could therefore potentially provide an additional therapeutical advantage.

In the studies conducted on the atherosclerotic lesions of the BCA, we show that the effect of fractalkine blockage is not restricted to lesions induced by the cast and that this chemokine is also involved in the progression of the disease at natural occurring predilection sites. The effects of fractalkine are mostly on atherosclerotic plaques with a distinct composition supporting a less "stable" phenotype, as both the low shear stress induced lesions(6) and the BCA lesions(58) show the occurrence of spontaneous intra plaque hemorrhages which are rare at other atherosclerosis-prone locations of the arterial tree, whereas the effects of fractalkine inhibition on the lesions induced by oscillatory shear stress were limited.

A limitation to the current study is that by using whole homogenates from vessel tissue, we cannot distinguish in the mRNA data between changes in activation/ expression level per individual cell and changes in the number of cells expressing the chemokine of interest. Although the clear relation and effect of these identified chemokines on plaque composition prevail, it would be interesting to assess whether increased chemokine expression is derived from an activated subpopulation of intimal cells. Currently, we are conducting a large study in which we isolate specific cell types and subpopulations in the low and oscillatory shear stress lesions to evaluate their state of activation. In this study, we used an in house developed model for shear stress alteration to induce two types of atherosclerotic lesions. Although the lesions triggered by low shear stress show a less "stable" phenotype than the lesions induced by oscillatory shear stress, no plaque rupture was detected. Until now, actual plaque rupture has not been demonstrated unambiguously in any animal model. We did observe however that the atherosclerotic lesions in the low shear stress area in our model are more or susceptible to intraplaque hemorrhages. In addition, morphometric analysis of the low shear stress and the oscillatory shear stress regions indicate that they differ in fibrous cap thickness and necrotic core size. Taken together with the distinct difference in plaque composition between the atherosclerotic lesions induced by the two types of shear stress, we conclude that the cast model is suitable to

investigate the role of chemokines in determining plaque phenotype.

In conclusion, the present study indicates that different shear stress fields have yielded different plaque compositions associated with different responses in chemokine expression. Low shear stress induces the development of larger lesions which characteristics point towards a less "stable" phenotype. These lesions are characterized by increased expression of multiple chemokines (GRO-α/KC, fractalkine and IP-10) compared to the oscillatory shear stress induced lesions. Fractalkine appears to be crucial in development of the distinct plaque phenotype that is induced by low shear stress triggering. Therefore, stabilization of this type of atherosclerotic plaques in patients by inhibiting fractalkine-fractalkine receptor interaction might provide an effective therapy.

Materials and Methods

Mice

Mice deficient in apolipopotein E (apoE-/-) in a C57BL/6J background were obtained from Jackson Laboratory. Animals 15-20 weeks of age were assigned randomly to one of the 3 time points (see below). During the experimental period, all animals were fed a Western type diet consisting of 15% (w/w) cacoa butter and 0.25% (w/w) cholesterol (diet W, Hope Farms). After a two weeks period of Western diet, shear stress in the right common carotid artery was altered by cast placement as previously described(5). In short, the animals were anesthetized with isoflurane and the anterior cervical triangles were accessed by a sagittal anterior neck incision. Both halves of the cast were placed around the right common carotid artery and fixed with a suture, wounds were closed and the animals were allowed to recover. Animals with cast implants were sacrificed at 1, 3, and 9 weeks after surgery.

To study the effects of fractalkine blockage on plaque development, apoE-/- animals were injected three times a week in the tail artery with 25mg of neutralizing rabbit a-mouse fractalkine antibody (Ebioscience) or rabbit IgG isotype control antibody (Ebioscience). Mice received the injections after six weeks of cast placement up until the 9 weeks time point at which the animals were sacrificed. The Erasmus MC institutional review board approved all animal studies described in this manuscript.

Gene expression analysis

Freshly isolated vessel segments were each divided into three different regions (0.5 mm proximal from the cast, 1 mm in the cast, and 0.5 mm distal to the cast) and pooled per region (n=10). Total RNA from the samples was extracted using the RNeasy kit (Qiagen) and was linearly amplified following an Eberwine T7

protocol(59) or directly reversed transcribed into cDNA as indicated. Quantitative real-time PCR (QPCR) reactions were performed using a real-time fluorescent determination in the iCycler iQ Detection System (Biorad). Primers were designed for MCP-1, GRO-α, regulated upon activation, normal T cell expressed and secreted (RANTES/CCL5), eotaxin-1/CCL11, EBI-1-ligand chemokine (ELC/CCL19), stromal cell-derived factor 1a (SDF-1α/CXCL12), neutrophil activating protein 2 (NAP-2/CXCL7), interferon inducible protein-10 (IP-10/CXCL10), fraktalkine/CX3CL1, and CC chemokine ligand-14 (CCL14). Target gene mRNA levels were expressed relatively to the housekeeping gene hypoxanthine guanine phosphoribosyl transferase (HPRT) as an endogenous control.

Cholesterol analysis
Blood samples were taken under anaesthesia by orbital puncture at the time of sacrifice. Total plasma cholesterol concentrations were measured enzymatically using a commercially available kit (kit 236691, Boehringer Mannheim GmbH).

Histology
6 μm cryosections of the right and the left common carotid arteries or brachiocephalic arteries were obtained as described before(6). Sections equally spaced throughout the arteries at 120 μm intervals were used for analyses. Macrophages were detected using anti CD68 antibodies (Santa Cruz Biotechnology), and smooth muscle cells by antibodies against VSMC α-actin (Sigma, Chemical Co.,). Lipid deposition was analyzed with Oil red O staining and collagen with picrosirius red. Fraktalkine, MCP-1, IP-10 (Sigma Chemical Co.), and CX3CR1 polyclonal antibodies (Santa Cruz Biotechnology) and R594 or FITC labeled secondary antibodies (Molecular Probes) were used for analysis with a Zeiss LSM510LNO inverted laser scanning confocal microscope (Carl Zeiss).

Quantification and statistics
Data analysis was performed using a microscopy image analysis system (Impak C, Clemex Vision Image Analysis System; Clemex Technologies). Intimal/media ratio was analyzed on haematoxylin/eosin stained sections. In order to quantify the expression of different chemokines in the vessel, the area positive for the specific staining was expressed as a percentage of the total area enclosed by the external elastic lamina and the lumen. To assess the percentage of the different plaque components, the area within the intimal positive for each staining was expressed as a percentage of the total intimal area. All cross sections stained were averaged per region of shear stress, i.e. low, oscillatory and high shear stress. For the morphometric analysis, the fibrocellular cap region was determined from collagen staining by picrosirius red and was expressed as a percentage of the total intimal area (cap/intima ratio)(60). The necrotic core region was determined

as an acellular area of the lesion (core/intima ratio)(60). Area was determined as acellular, lacking in nuclei and cytoplasm, from H&E stained sections. The necrotic core area was differentiated from regions of dense fibrous scars by the presence of macrophage debris. Statistical analysis was performed using one ANOVA analysis of variance followed by the Tukey test. Data are presented as mean ± SEM. P values <0.05 were considered significant.

References

1. Cheng, C. 2006. Atherosclerotic lesion size and vulnerability are determined by patterns of fluid shear stress. in review.

2. Williams, H., Johnson, J.L., Carson, K.G., and Jackson, C.L. 2002. Characteristics of intact and ruptured atherosclerotic plaques in brachiocephalic arteries of apolipoprotein E knockout mice. Arterioscler Thromb Vasc Biol 22:788-792.

3. Pedersen, E.M., Oyre, S., Agerbaek, M., Kristensen, I.B., Ringgaard, S., Boesiger, P., and Paaske, W.P. 1999. Distribution of early atherosclerotic lesions in the human abdominal aorta correlates with wall shear stresses measured in vivo. Eur J Vasc Endovasc Surg 18:328-333.

4. Wentzel, J.J., Kloet, J., Andhyiswara, I., Oomen, J.A., Schuurbiers, J.C., de Smet, B.J., Post, M.J., de Kleijn, D., Pasterkamp, G., Borst, C., et al. 2001. Shear-stress and wall-stress regulation of vascular remodeling after balloon angioplasty: effect of matrix metalloproteinase inhibition. Circulation 104:91-96.

5. Buchanan, J.R., Jr., Kleinstreuer, C., Truskey, G.A., and Lei, M. 1999. Relation between non-uniform hemodynamics and sites of altered permeability and lesion growth at the rabbit aorto-celiac junction. Atherosclerosis 143:27-40.

6. Stone, P.H., Coskun, A.U., Kinlay, S., Clark, M.E., Sonka, M., Wahle, A., Ilegbusi, O.J., Yeghiazarians, Y., Popma, J.J., Orav, J., et al. 2003. Effect of endothelial shear stress on the progression of coronary artery disease, vascular remodeling, and in-stent restenosis in humans: in vivo 6-month follow-up study. Circulation 108:438-444.

7. Cheng, C., van Haperen, R., de Waard, M., van Damme, L.C., Tempel, D., Hanemaaijer, L., van Capellen, G.W., Bos, J., Slager, C.J., Duncker, D.J., et al. 2005. Shear stress affects the intracellular distribution of eNOS: direct demonstration by a novel in vivo technique. Blood.

8. de Nooijer, R., von der Thusen, J.H., Verkleij, C.J., Kuiper, J., Jukema, J.W., van der Wall, E.E., van Berkel, J.C., and Biessen, E.A. 2004. Overexpression of IL-18 decreases intimal collagen content and promotes a vulnerable plaque phenotype in apolipoprotein-E-deficient mice. Arterioscler Thromb Vasc Biol 24:2313-2319.

9. Dickson, B.C., and Gotlieb, A.I. 2003. Towards understanding acute destabilization of vulnerable atherosclerotic plaques. Cardiovasc Pathol 12:237-248.

10. Libby, P., Geng, Y.J., Aikawa, M., Schoenbeck, U., Mach, F., Clinton, S.K., Sukhova, G.K., and Lee, R.T. 1996. Macrophages and atherosclerotic plaque stability. Curr Opin Lipidol 7:330-335.

11. Chyu, K.Y., and Shah, P.K. 2001. The role of inflammation in plaque disruption and thrombosis. Rev Cardiovasc Med 2:82-91.

12. Shah, P.K. 1998. Role of inflammation and metalloproteinases in plaque disruption and thrombosis. Vasc Med 3:199-206.

13. Shah, P.K., Falk, E., Badimon, J.J., Fernandez-Ortiz, A., Mailhac, A., Villareal-Levy, G., Fallon, J.T., Regnstrom, J., and Fuster, V. 1995. Human monocyte-derived macrophages induce collagen breakdown in fibrous caps of atherosclerotic plaques. Potential role of matrix-degrading metalloproteinases and implications for plaque rupture. Circulation 92:1565-1569.

14. Mach, F., Schonbeck, U., and Libby, P. 1998. CD40 signaling in vascular cells: a key role in atherosclerosis? Atherosclerosis 137 Suppl:S89-95.

15. Johnston, B., and Butcher, E.C. 2002. Chemokines in rapid leukocyte adhesion triggering and migration. Semin Immunol 14:83-92.

16. Vestweber, D., and Blanks, J.E. 1999. Mechanisms that regulate the function of the selectins and their ligands. Physiol Rev 79:181-213.

17. Konstantopoulos, K., Kukreti, S., and McIntire, L.V. 1998. Biomechanics of cell interactions in shear fields. Adv Drug Deliv Rev 33:141-164.

18. Laudanna, C., Kim, J.Y., Constantin, G., and Butcher, E. 2002. Rapid leukocyte integrin activation by chemokines. Immunol Rev 186:37-46.

19. McEver, R.P., and Cummings, R.D. 1997. Perspectives series: cell adhesion in vascular biology. Role of PSGL-1 binding to selectins in leukocyte recruitment. J Clin Invest 100:485-491.

20. Chan, J.R., Hyduk, S.J., and Cybulsky, M.I. 2001. Chemoattractants induce a rapid and transient upregulation of monocyte alpha4 integrin affinity for vascular cell adhesion molecule 1 which mediates arrest: an early step in the process of emigration. J Exp Med 193:1149-1158.

21. Sugihara-Seki, M. 2000. Flow around cells adhered to a microvessel wall. I. Fluid stresses and forces acting on the cells. Biorheology 37:341-359.

22. Gaver, D.P., 3rd, and Kute, S.M. 1998. A theoretical model study of the influence of fluid stresses on a cell adhering to a microchannel wall. Biophys J 75:721-733.

23. Mohan, S., Mohan, N., Valente, A.J., and Sprague, E.A. 1999. Regulation of low shear flow-induced HAEC VCAM-1 expression and monocyte adhesion. Am J Physiol 276:C1100-1107.

24. Chappell, D.C., Varner, S.E., Nerem, R.M., Medford, R.M., and Alexander, R.W. 1998. Oscillatory shear stress stimulates adhesion molecule expression in cultured human endothelium. Circ Res 82:532-539.

25. Weber, C. 2003. Novel mechanistic concepts for the control of leukocyte transmigration: specialization of integrins, chemokines, and junctional molecules. J Mol Med 81:4-19.

26. Charo, I.F., and Taubman, M.B. 2004. Chemokines in the pathogenesis of vascular disease. Circ Res 95:858-866.

27. Shyy, Y.J., Hsieh, H.J., Usami, S., and Chien, S. 1994. Fluid shear stress induces a biphasic response of human monocyte chemotactic protein 1 gene expression in vascular endothelium. Proc Natl Acad Sci U S A 91:4678-4682.

28. Bao, X., Lu, C., and Frangos, J.A. 1999. Temporal gradient in shear but not steady shear stress induces PDGF-A and MCP-1 expression in endothelial cells: role of NO, NF kappa B, and egr-1. Arterioscler Thromb Vasc Biol 19:996-1003.

29. Kato, H., Uchimura, I., Nawa, C., Kawakami, A., and Numano, F. 2001. Fluid shear stress suppresses interleukin 8 production by vascular endothelial cells. Biorheology 38:347-353.

30. Cheng, C., de Crom, R., van Haperen, R., Helderman, F., Gourabi, B.M., van Damme, L.C., Kirschbaum, S.W., Slager, C.J., van der Steen, A.F., and Krams, R. 2004. The role of shear stress in atherosclerosis: action through gene expression and inflammation? Cell Biochem Biophys 41:279-294.

31. Weber, C., Schober, A., and Zernecke, A. 2004. Chemokines: key regulators of mononuclear cell recruitment in atherosclerotic vascular disease. Arterioscler Thromb Vasc Biol 24:1997-2008.

32. Whitman, S.C., Rateri, D.L., Szilvassy, S.J., Yokoyama, W., and Daugherty, A. 2004. Depletion of natural killer cell function decreases atherosclerosis in low-density lipoprotein receptor null mice. Arterioscler Thromb Vasc Biol 24:1049-1054.

33. Burke, A.P., Farb, A., Pestaner, J., Malcom, G.T., Zieske, A., Kutys, R., Smialek, J., and Virmani, R. 2002. Traditional risk factors and the incidence of sudden coronary death with and without coronary thrombosis in blacks. Circulation 105:419-424.

34. Farb, A., Burke, A.P., Tang, A.L., Liang, T.Y., Mannan, P., Smialek, J., and Virmani, R. 1996. Coronary plaque erosion without rupture into a lipid core. A frequent cause of coronary thrombosis in sudden coronary death. Circulation 93:1354-1363.

35. Takeya, M., Yoshimura, T., Leonard, E.J., and Takahashi, K. 1993. Detection of monocyte chemoattractant protein-1 in human atherosclerotic lesions by an anti-monocyte chemoattractant protein-1 monoclonal antibody. Hum Pathol 24:534-539.

36. Rayner, K., Van Eersel, S., Groot, P.H., and Reape, T.J. 2000. Localisation of mRNA for JE/MCP-1 and its receptor CCR2 in atherosclerotic lesions of the ApoE knockout mouse. J Vasc Res 37:93-102.

37. Guo, J., de Waard, V., Van Eck, M., Hildebrand, R.B., van Wanrooij, E.J., Kuiper, J., Maeda, N., Benson, G.M., Groot, P.H., and Van Berkel, T.J. 2005. Repopulation of apolipoprotein E knockout mice with CCR2-deficient bone marrow progenitor

cells does not inhibit ongoing atherosclerotic lesion development. Arterioscler Thromb Vasc Biol 25:1014-1019.

38. Taub, D.D., Longo, D.L., and Murphy, W.J. 1996. Human interferon-inducible protein-10 induces mononuclear cell infiltration in mice and promotes the migration of human T lymphocytes into the peripheral tissues and human peripheral blood lymphocytes-SCID mice. Blood 87:1423-1431.

39. Loetscher, M., Gerber, B., Loetscher, P., Jones, S.A., Piali, L., Clark-Lewis, I., Baggiolini, M., and Moser, B. 1996. Chemokine receptor specific for IP10 and mig: structure, function, and expression in activated T-lymphocytes. J Exp Med 184:963-969.

40. Luster, A.D., and Ravetch, J.V. 1987. Biochemical characterization of a gamma interferon-inducible cytokine (IP-10). J Exp Med 166:1084-1097.

41. Libby, P., Schoenbeck, U., Mach, F., Selwyn, A.P., and Ganz, P. 1998. Current concepts in cardiovascular pathology: the role of LDL cholesterol in plaque rupture and stabilization. Am J Med 104:14S-18S.

42. Kawamura, A., Miura, S., Fujino, M., Nishikawa, H., Matsuo, Y., Tanigawa, H., Tomita, S., Tsuchiya, Y., Matsuo, K., and Saku, K. 2003. CXCR3 chemokine receptor-plasma IP10 interaction in patients with coronary artery disease. Circ J 67:851-854.

43. Boisvert, W.A., Santiago, R., Curtiss, L.K., and Terkeltaub, R.A. 1998. A leukocyte homologue of the IL-8 receptor CXCR-2 mediates the accumulation of macrophages in atherosclerotic lesions of LDL receptor-deficient mice. J Clin Invest 101:353-363.

44. Mizoue, L.S., Bazan, J.F., Johnson, E.C., and Handel, T.M. 1999. Solution structure and dynamics of the CX3C chemokine domain of fractalkine and its interaction with an N-terminal fragment of CX3CR1. Biochemistry 38:1402-1414.

45. Lucas, A.D., Bursill, C., Guzik, T.J., Sadowski, J., Channon, K.M., and Greaves, D.R. 2003. Smooth muscle cells in human atherosclerotic plaques express the fractalkine receptor CX3CR1 and undergo chemotaxis to the CX3C chemokine fractalkine (CX3CL1). Circulation 108:2498-2504.

46. Ludwig, A., Berkhout, T., Moores, K., Groot, P., and Chapman, G. 2002. Fractalkine is expressed by smooth muscle cells in response to IFN-gamma and TNF-alpha and is modulated by metalloproteinase activity. J Immunol 168:604-612.

47. Hatakeyama, M., Imaizumi, T., Tamo, W., Yamashita, K., Yoshida, H., Fukuda, I., and Satoh, K. 2004. Heparin inhibits IFN-gamma-induced fractalkine/CX3CL1 expression in human endothelial cells. Inflammation 28:7-13.

48. Lesnik, P., Haskell, C.A., and Charo, I.F. 2003. Decreased atherosclerosis in CX3CR1-/- mice reveals a role for fractalkine in atherogenesis. J Clin Invest 111:333-340.

49. Combadiere, C., Potteaux, S., Gao, J.L., Esposito, B., Casanova, S., Lee, E.J.,

Debre, P., Tedgui, A., Murphy, P.M., and Mallat, Z. 2003. Decreased atherosclerotic lesion formation in CX3CR1/apolipoprotein E double knockout mice. Circulation 107:1009-1016.

50. Teupser, D., Pavlides, S., Tan, M., Gutierrez-Ramos, J.C., Kolbeck, R., and Breslow, J.L. 2004. Major reduction of atherosclerosis in fractalkine (CX3CL1)-deficient mice is at the brachiocephalic artery, not the aortic root. Proc Natl Acad Sci U S A 101:17795-17800.

51. Gray, J.L., and Shankar, R. 1995. Down regulation of CD11b and CD18 expression in atherosclerotic lesion-derived macrophages. Am Surg 61:674-679; discussion 679-680.

52. de Bruijn, M.F., Ploemacher, R.E., Mayen, A.E., Voerman, J.S., Slieker, W.A., van Ewijk, W., and Leenen, P.J. 1996. High-level expression of the ER-MP58 antigen on mouse bone marrow hematopoietic progenitor cells marks commitment to the myeloid lineage. Eur J Immunol 26:2850-2858.

53. Schafer, A., Schulz, C., Eigenthaler, M., Fraccarollo, D., Kobsar, A., Gawaz, M., Ertl, G., Walter, U., and Bauersachs, J. 2004. Novel role of the membrane-bound chemokine fractalkine in platelet activation and adhesion. Blood 103:407-412.

54. Atkinson, J.B., Harlan, C.W., Harlan, G.C., and Virmani, R. 1994. The association of mast cells and atherosclerosis: a morphologic study of early atherosclerotic lesions in young people. Hum Pathol 25:154-159.

55. Galli, S.J. 2000. Mast cells and basophils. Curr Opin Hematol 7:32-39.

56. Laine, P., Naukkarinen, A., Heikkila, L., Penttila, A., and Kovanen, P.T. 2000. Adventitial mast cells connect with sensory nerve fibers in atherosclerotic coronary arteries. Circulation 101:1665-1669.

57. Papadopoulos, E.J., Fitzhugh, D.J., Tkaczyk, C., Gilfillan, A.M., Sassetti, C., Metcalfe, D.D., and Hwang, S.T. 2000. Mast cells migrate, but do not degranulate, in response to fractalkine, a membrane-bound chemokine expressed constitutively in diverse cells of the skin. Eur J Immunol 30:2355-2361.

58. El-Shazly, A., Berger, P., Girodet, P.O., Ousova, O., Fayon, M., Vernejoux, J.M., Marthan, R., and Tunon-de-Lara, J.M. 2006. Fraktalkine produced by airway smooth muscle cells contributes to mast cell recruitment in asthma. J Immunol 176:1860-1868.

59. Moll, P.R., Duschl, J., and Richter, K. 2004. Optimized RNA amplification using T7-RNA-polymerase based in vitro transcription. Anal Biochem 334:164-174.

60. von der Thusen, J.H., van Vlijmen, B.J., Hoeben, R.C., Kockx, M.M., Havekes, L.M., van Berkel, T.J., and Biessen, E.A. 2002. Induction of atherosclerotic plaque rupture in apolipoprotein E-/- mice after adenovirus-mediated transfer of p53. Circulation 105:2064-2070.

variables
role smooth
macrophage
patients lesions development atherosclerotic
disease
inflammatory atherosclerosis
mouse
plaque
shown collagen
formation human
cholesterol might
found data
quartiles
concentration control
unstable cells
levels
inhibition vs plaques
Figure
also SMC
device
findings lesion
content
CXCL10
necrotic
mice
used staining
increase
model study T-cells vulnerable
concentrations measured treated

Chapter 5

Atherosclerotic Plaque Stability is Affected by the Chemokine CXCL10 in Both Mice and Humans

D. Segers, J.A. Lipton, P.J.M. Leenen, C. Cheng, D. Tempel,

H.J. Duckers, G. Pasterkamp, F.L. Moll, R. de Crom, R. Krams.

Abstract

Background
We previously found the chemokine CXCL10 gene to be specifically upregulated early during experimental development of plaque with an unstable phenotype. In this study we evaluated the functional consequences of these findings in mice and subsequently investigated whether these findings expressed importance for human vulnerable plaque development.

Methods and Results
In ApoE-/- mice, we induced unstable plaque with using a flow-altering device around the carotid artery. From week 1-4, mice were injected with a bioactivity-neutralizing CXCL10 antibody. After 9 weeks, lesion compositions of plaques were evaluated. CXCL10 inhibition resulted in a more stable plaque phenotype: collagen increased by 58% (p=0.002), smooth muscle cell content increased 2-fold (p=0.03), while macrophage activation as indicated by MHC class II expression decreased by 50% (p=0.005). Also, the size of necrotic cores decreased by 41% (p=0.01). Next, in 106 human carotid endarterectomy specimens we measured concentrations of CXCL10 protein and tested for association with plaque morphology. We found that increasing concentrations of CXCL10 strongly associate with an increase in atheromatous plaque phenotype (ANOVA, p=0.003), with high macrophage, low smooth muscle cell and low collagen content.

Conclusions
In the present study we show that a causal relationship exists between local production of CXCL10 and development of vulnerable plaque. Inhibition of CXCL10 in a mouse model showed its functional involvement, while human endarterectomy analysis indicated an association between lesion morphology and the concentration of CXCL10. We conclude that CXCL10 might provide a new lead towards plaque-stabilizing therapy.

Introduction

Atherosclerosis is a progressive inflammatory disease of the arterial vasculature with lesions that may turn unstable, which may lead to lesion rupture. The high mortality of these ruptures has been associated with atherosclerotic plaques that display a specific histological phenotype, characterized by a large pool of lipids and necrotic cell debris covered by a thin fibrous cap and the presence of inflammatory cells in the plaque shoulders[1].

Previously, we developed an experimental animal model in which plaques with stable and unstable characteristics are simultaneously induced in a single straight arterial segment[2]. We subsequently identified specific expression profiles of various chemokine genes in vulnerable plaque developement[3]. In these, the chemokine CXCL10 was specifically upregulated during the early phase in the development of the vulnerable plaque segment.

CXCL10 is a member of the CXC-family of chemokines. Upon stimulation with interferon-gamma (IFN-γ) it is expressed by many cell types, e.g. monocytes/macrophages, endothelial cells, fibroblasts and natural killer-cells[4, 5]. Effects of CXCL10 are mediated by the G-protein coupled receptor CXCR3, which is known to be expressed by resting and activated T-cells, NK-cells as well as a subset of peripheral blood monocytes[5-7]. Furthermore, CXCL10 plays a variety of roles in inflammatory disease, like in the initiation and maintenance of T-helper-1 (Th1)-polarized immune responses[8, 9], migration of activated T-cells[10], but also of natural killer cells[11], of monocytes[12, 13] and of smooth muscle cells (SMC)[14].

Despite these compelling findings described in literature, in atherosclerosis CXCL10 has been less completely characterized. In human atherosclerosis, but not in healthy arteries, endothelial cells, smooth muscle cells and macrophages express CXCL10[15]. Functional observations in CXCL10 gene knockout mice indicated that CXCL10 exerts pro-atherogenic effects, probably related to the specific recruitment and retention of activated Th1 cells and downregulation of a regulatory T cell response[16]. While these findings indicate that CXCL10 plays a role in atherogenesis, its effect on plaque composition is unclear. Based on our previous observations on gene expression in the mouse model, we hypothesized that CXCL10 mediates development of vulnerable atherosclerotic plaque. Hence, we assessed whether CXCL10 plays a critical role in unstable plaque development by evaluating the effect of antibody-mediated functional inhibition of CXCL10 on lesion phenotype in our vulnerable plaque mouse model. To provide evidence that the findings in the mouse bear relevance for human atherosclerosis, we also investigated the association between CXCL10 concentrations and plaque composition in human carotid endarterectomy lesions.

Materials & Methods

Animals and surgical procedures

Apolipoprotein-E deficient mice, 15-20 weeks of age, were obtained from the Jackson Laboratories (Bar Harbor, ME, USA). They were fed a high fat, high cholesterol diet consisting of 15% (wt/wt) cocoa butter and 0.25% cholesterol (wt/wt) (Diet W, Hope Farms, Woerden, The Netherlands). Two weeks after this diet was initiated, the mice were instrumented with a shear stress-altering device around the right common carotid artery under 2% isoflurane anesthesia, as described previously[2]. Briefly, this device gradually narrows the vessel lumen to ~70% of its original diameter. As a consequence, shear stress is lowered upstream of the device, gradually increases inside the device and is oscillating just downstream of the device[17]. After surgery, the mice were kept on the high fat, high cholesterol diet for the remainder of the experiment. The device remained in situ for 9 weeks. Intervention and control groups consisted of at least 10 animals per group. All animal experiments were approved by the institutional animal ethical committee and performed in compliance with institutional and national guidelines.

CXCL10 inhibition

Mice were intravenously injected three times a week in week 2-4 post-surgery with an anti-mouse bioactivity-neutralizing monoclonal CXCL10 antibody (MAB466, R&D Systems, Abingdon, United Kingdom) in a dose of 25 μg in 0.2 ml sterile PBS. Untreated cast-instrumented mice served as control.

Isolation and analysis of murine tissues

Following sacrifice, blood was collected and mice were flushed systemically with PBS. Next, the common carotid artery was isolated, embedded in OCT compound (Tissue-Tek, Sakura, Japan), and snap-frozen in liquid nitrogen. For histology, 8 μm cryosections were cut and stained for routine histology (Hematoxilin-Eosin, HE), lipids (Oil Red O), collagen (Picrosirius Red), macrophages (anti-CD68, AbD-Serotec, Oxford, UK), macrophage activation (anti-Major Histocompatibility Complex (MHC) class II, clone M5/114, ATCC TIB-120) and smooth muscle cells (anti-SMC α-actin, Sigma-Aldrich, The Netherlands). Subsequently, high-resolution images ware taken using an Olympus BX-40 microscope or a Zeiss LSM5 Meta confocal microscope (Zeiss Jena, Germany). Collagen stainings were assessed using crossed circular polarization filters. To calculate lesion size and cellular content relative to the plaque area, all images were analyzed after digitalization by automated image analysis software (Clemex Technologies Inc, Canada) applying thresholding of the stained areas. Necrotic cores (defined as hypocellular plaque cavities devoid of collagen, containing cholesterol clefts) were assessed based on HE and Picrosirius Red stained sections and measured relative to the lesion area. Total cholesterol levels were measured in serum samples by an

enzymatic colorimetric method (Cholesterol E, Wako Diagnostics, USA).

Endarterectomy procedures

All patients in this study were participants of a prospective study aimed at investigating the predictive value of plaque characteristics for long-term outcome (AtheroExpress), of which the study methods have been described extensively before[18]. In short, all patients underwent carotid endarterectomy, during which arterial wall tissue was obtained. Next, the culprit lesion, defined as the segment with the largest plaque burden, was processed for histological examination. In addition to HE staining, sections were stained for collagen (Picrosirius Red), SMC (α-actin), and macrophage (CD68) content. Histological assessment was performed in a semi-quantitative fashion (none; minor; moderate; heavy), on basis of two independent observers. When results contradicted, a third independent observer was consulted. Subsequently, plaques were designated as fibrous (lipids constitute <10% of lesion surface area), fibro-atheromatous (10-40% lipids) or atheromatous (>40% lipids) based on collagen and HE stainings. Besides, plaques were also designated as SMC-dominant or macrophage-dominant based on the prevailing cell type obtained from the specific stainings.

A 5 mm segment directly adjacent to the culprit lesion was crushed in liquid nitrogen, and subsequently total protein was extracted using 1 mL of Tripure Isolation Reagent (Boehringer Mannheim, Germany), according to the manufacturer's protocol. Then, CXCL10 concentration was measured by Enzyme-Linked Immuno Sorbent Assay (ELISA) according to manufacturers instructions (Quantikine human CXCL10 immunoassay, R&D Systems, Abingdon, United Kingdom), and blinded from histological and clinical data.

Statistical analysis

SPSS (version 15.0, SPSS Inc., USA) was used for all analyses. To test the differences between the treated and the control mice at 9 weeks of cast placement, a student's T test was used. When these data had a non-Gaussian distribution, a non-parametric T-test was used. For the endarterectomy samples, to compare CXCL10 levels between categorical baseline and plaque morphology variables, Kruskal-Wallis and Mann-Whitney tests for non-Gaussian distributed data were used. To investigate the differences between continuous baseline variables and CXCL10, patients were categorized into quartiles, named 1 through 4 based on increasing CXCL10 concentration. Subsequently, these quartiles were used to sort all other variables. One-way ANOVA was used to compare continuous variables. The quartiles were also used to visualize the relationship between CXCL10 concentration and plaque morphology. Data are described as mean ± SD or median (Inter Quartile Range) as appropriate. A p-value of <0.05 was considered statistically significant.

Results

Suppression of CXCL10 bioactivity inhibits experimental vulnerable plaque formation

As we previously found that CXCL10 is expressed specifically in developing unstable lesions[3], we investigated if CXCL10 is also functionally involved in the development of plaque vulnerability using a mouse model that we developed before[2]. ApoE-deficient mice, in which a shear stress-altering device was applied, were injected with a bioactivity-neutralizing antibody during the onset of plaque formation. As expected, serum total cholesterol levels did not differ between treated and control mice (30.13 ± 4.6 vs. 29.92 ± 6.7 mmol/L, p=0.92). Short-term inhibition of CXCL10 did not influence the extent of plaque development, since we found no difference in lesion size between the treated and the control mice after 9 weeks of shear stress alteration. Because macrophage foam cells are characteristic of atherosclerosis, we measured both plaque lipid (31.3 ± 8.0% treated vs. 29.5 ± 7.0% control) and macrophage content (31.7 ± 7.6% treated vs. 27.8 ± 7.0 control; Figure 1A), where both remained unchanged upon CXCL10 inhibition.

To assess plaque vulnerability, we determined the amount of collagen in the lesions, which is the main stabilizing component of the plaque. Interestingly, we found a 57% increase in the relative amount of collagen in the plaques following CXCL10 suppression (17.8 ± 6.5% vs. 11.3 ± 5.5%, p=0.002; Figure 1B). The amount of plaque collagen is essentially the result of a balance between collagen deposition and breakdown. Therefore, the increase in collagen may be the result of decreased breakdown predominantly by proteinases secreted by activated macrophages. To determine the extent of immune activation, we measured MHC class II by immunohistochemistry. The cellular morphology, location in the plaque and spatial association of MHC class II staining with macrophage staining by CD68 antibodies in adjacent sections (Fig.1A, C) strongly suggests

Figure 1, right page: *Anti-CXCL10 treatment in atherosclerosis susceptible mice results in a change into a more stable lesion phenotype.*

A flow-altering device around the common carotid artery induced atherosclerosis in ApoE-/- mice. From week 1-4 of lesion development, a bioactivity-neutralizing anti-CXCL10 antibody was injected. After 9 weeks, lesions were compared to untreated controls by histology. The pictures show representative histological sections of treated and control mice. All photographs have been made with the same magnification (100x). Scale bars are provided in E and represent 100 μm. Data in bar diagrams are the mean values ± SD of at least 8 sections from at least 10 different animals per group. CXCL10 inhibition resulted in a more stable morphology evidenced by: unchanged amounts of lesion macrophages (A), increased amounts of collagen (B), decreased macrophage activation (C), increased numbers of SMC (D) and reduced necrotic core size (E). *p<0.05, **p<0.01.
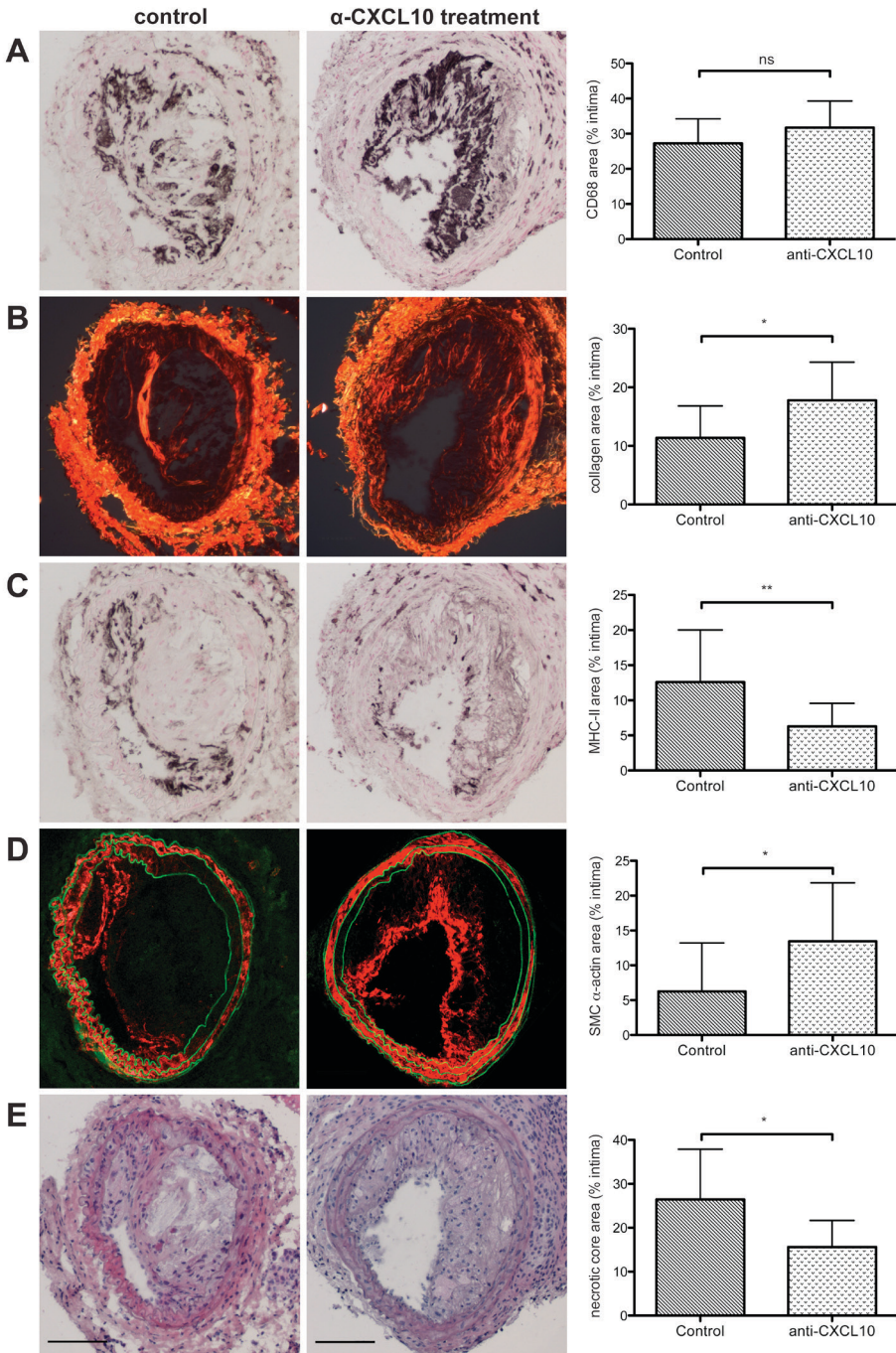
that MHCII-positive cells are the prime cells expressing this activation marker. We found a 50% reduction in the plaque MHC class II levels following CXCL10 inhibition (6.3 ± 3.3% vs. 12.6 ± 7.4%, p=0.005; Figure 1C). In addition, the amount of SMC, which are known to produce collagen, nearly doubled in the CXCL10-suppressed group (13.5 ± 8.4% vs. 6.3 ± 7.0%, p=0.03; Figure 1D), suggesting that the differences in collagen content may be explained by several factors.

The necrotic core is a hallmark component of the vulnerable plaque. To test whether CXCL10 inhibition reduces necrotic core formation, we analyzed both the number of necrotic cores in the lesions as well their relative size. We found that CXCL10 inhibition resulted in fewer necrotic cores: 38.9 ± 22.1% vs. 57.7 ± 20% of the sections covering the entire lesion contained a necrotic core (p=0.02). Moreover, also the relative size of the necrotic cores decreased following antibody treatment from 26.4 ± 11.4% to 15.6 ± 6.1% of the plaque surface area (p=0.01; Figure 1E).
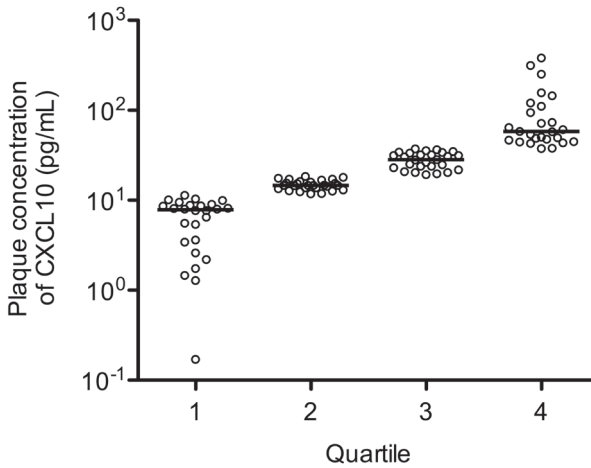
Figure 2. *Distribution of CXCL10 measurements from each patient across quartiles.* Atherosclerotic plaques were obtained from 106 patients during carotid endarterectomy. In the plaque segment directly adjacent to the culprit lesion, the content of the chemokine CXCL10 was measured by ELISA. Based on these measurements, patients were divided into one of four quartiles according to the CXCL10 concentration. Quartile 1 represents the lesions with the lowest CXCL10 values, whereas quartile 4 contains the highest. This figure shows the individual measurements for all patients and the distribution across each quartile of plaque CXCL10. Horizontal bars represent the median concentration of each quartile.

Patient characteristics

For this study endarterectomy specimens of 106 patients were analyzed. An overview of the patient characteristics is provided in Table 1. Histological examples of the lesions are shown in a previous publication by Verhoeven et al[18]. The CXCL10 concentration in the specimens ranged from undetectable to 384.8 pg/mL, with a median (interquartile range) of 38.34 pg/mL (14-39 pg/mL). To compare continuous CXCL10 levels to the categorical variables, patients were categorized into quartiles (Figure 2). The variables were then tested for changes across the quartiles. No differences were found comparing risk factors for atherosclerotic disease. The use of medication did not differ significantly between the quartiles.

Clinical Characteristics	Total	Quartile of CXCL10 concentration				p-value[*]
		1	2	3	4	
CXCL10 pg/mL	38.3 (14-40)[†]	0-11.3	11.8-18.4	19.3-37.2	37.6-382.6	0.000
Age (years)[†]	68.4 ± 8.9	66.0 ± 8.0	68.3 ± 10.2	67.7 ± 8.2	71.2 ± 8.5	0.157
Male (%)	73.6	73.1	70.4	66.7	84.6	0.316
Hypertension (%)	71.7	80.0	70.4	66.7	79.2	0.764
Smoker (%)	24.5	30.8	18.5	32.0	19.2	0.476
Symptomatic disease (%)	86.8	84.6	85.2	92.6	84.6	0.762
Statin (%)	56.6	66.7	55.6	55.6	56.0	0.530
β-blocker (%)	39.6	37.5	33.3	56.0	41.7	0.321
ACE-inhibitor (%)	39.6	42.3	33.3	40.7	42.3	0.881
Serum values[†]						
Total cholesterol (mmol/L)	4.9 ± 1.3	4.8 ± 0.9	5.2 ± 1.3	4.8 ± 1.7	4.6 ± 1.2	0.564
HDL (mmol/L)	1.2 ± 0.4	1.2 ± 0.4	1.4 ± 0.3	1.1 ± 0.3	1.1 ± 0.4	0.156
LDL (mmol/L)	3.0 ± 1.1	2.7 ± 0.8	3.3 ± 1.0	3.2 ± 1.4	2.7 ± 1.0	0.392
Triglycerides (mmol/L)	1.9 ± 0.9	2.3 ± 1.0	1.8 ± 0.8	2.0 ± 1.1	1.7 ± 0.7	0.434
ApoB (mmol/L)	0.9 ± 0.2	0.9 ± 0.2	1.0 ± 0.2	1.0 ± 0.3	0.9 ± 0.3	0.787
Glucose (mmol/L)	6.6 ± 1.9	5.8 ± 0.7	7.0 ± 2.0	7.0 ± 2.3	6.4 ± 1.9	0.129
CRP (mg/mL)	3.40 (1.6-7.3)	3.13 (1.4-5.8)	2.96 (1.8-5.8)	4.81 (1.7-9.1)	4.52 (1.6-7.3)	0.221

Table 1. *Patient baseline measurements for carotid endarterectomy specimens.*

Baseline data of 106 patients were stratified into four quartiles according to plaque CXCL10 concentration. [†]Values are represented as mean ± SD or median (Inter Quartile Range) as appropriate. [*]p-values based on ANOVA test between CXCL10 quartiles for continuous variables, and non-parametric Mann-Whitney test for categorical variables.
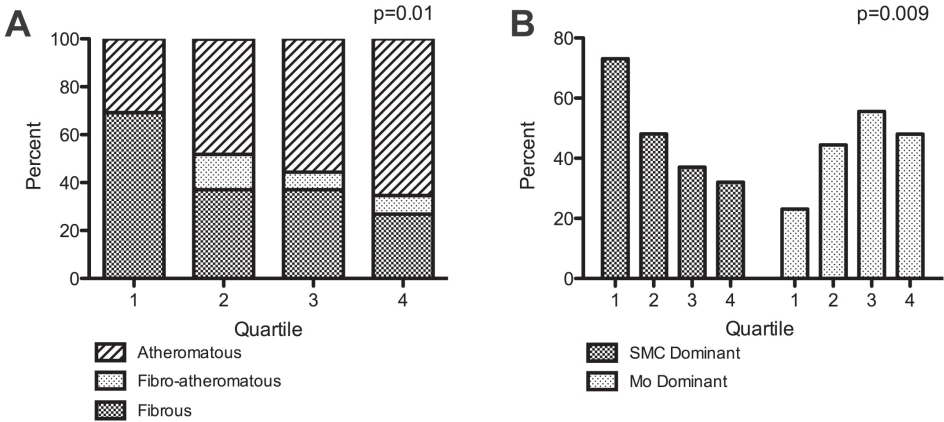
Figure 3. *Plaque concentrations of CXCL10 are associated with lesion morphology.*

Individual values were divided over quartiles (see Fig.1). By using ANOVA, we tested to see if plaque CXCL10 concentrations associated with lesion morphology. Increasing plaque concentrations of CXCL10 were indeed associated with an increase in atheromatous-type lesions (A) and a decrease of SMC dominant lesions and an increase of macrophage dominant lesions (B).

High CXCL10 concentrations identify patients with a more vulnerable plaque phenotype

Several significant associations were found between plaque composition and CXCL10 levels. Atheromatous lesions were more prominent at higher CXCL10 concentrations than those classified as fibrous (Rank 53 vs. 45, p=0.003). Also, higher CXCL10 concentrations were associated with more macrophage-dominant plaques (Rank 56 vs. 41, p=0.009), and fewer smooth muscle cells (Rank 39 vs. 74, p=0.001) and less collagen (Rank 37 vs. 63, p=0.003).

Subsequently, we analyzed the association between plaque composition and CXCL10 levels, by dividing patients into quartiles based upon CXCL10 concentration. More atheromatous lesions were represented in the higher quartiles, while fibrous lesions were more frequently present in the lower quartiles (Figure 3A). Macrophage-dominant lesions were mostly found in the top quartiles of CXCL10 content, while SMC-dominance associated with lower CXCL10 concentrations (Figure 3B). However, no differences were seen in the macrophage staining between the quartiles (Figure 4A). This paradox was the result of an inverse relation between smooth muscle cell staining and increasing CXCL10 concentrations (Figure 4B). Additionally, more collagen staining was seen in the plaques in the lower quartiles (Figure 4C).
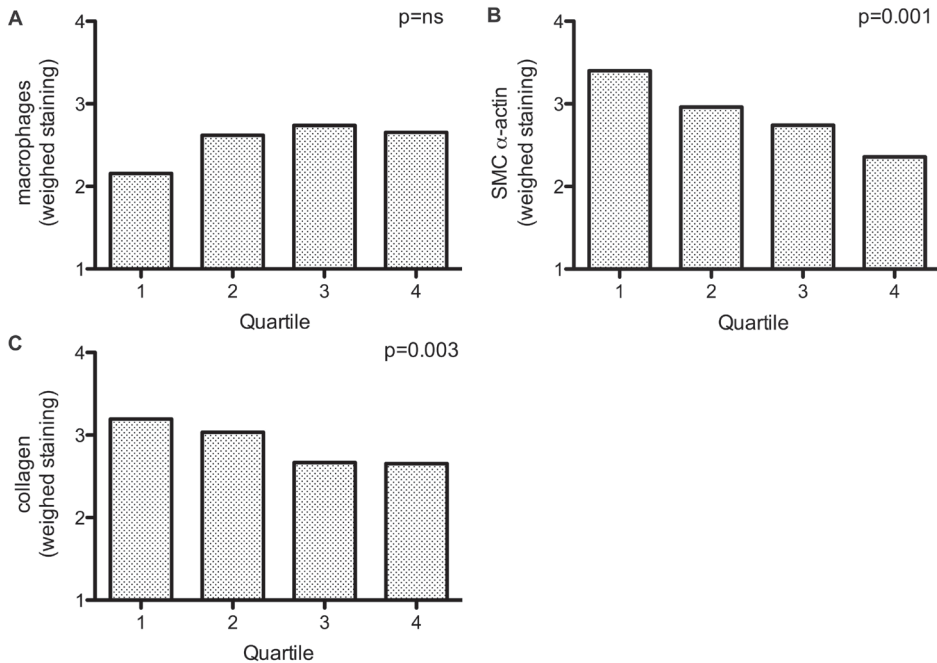
Figure 4. *Increasing carotid plaque CXCL10 concentrations are associated with a less fibrous phenotype.*

Plaque concentrations of CXCL10 were associated with histological qualities of the lesion by ANOVA. Staining for macrophages, SMC or collagen was quantified as none, minor, moderate or high. Based on these qualifications a weighed value for average staining intensity was calculated (1, none; 2, minor; 3, moderate; 4, heavy staining). Macrophage staining was not associated with plaque CXCL10 (A), whereas high plaque concentrations of CXCL10 were associated with decreasing amounts of smooth muscle cells (SMC) (B) and decreasing collagen (C).

Discussion

This study may be summarized by its two main findings. First, we showed a functional role of CXCL10 in vulnerable plaque formation in an experimental mouse model for unstable atherosclerotic disease. We observed that inhibiting CXCL10 with a bioactivity-neutralizing antibody resulted in plaques with less macrophage activation, with more SMC and a subsequent increase in collagen content compared to controls. A decreased number and size of necrotic cores in the lesions of the treated animals further substantiated these findings. This resulted in a lesion phenotype with increased intrinsic stability.

Second, we found that in human carotid plaques, CXCL10 levels are associated with lesion morphology. This is evidenced by an increased number of atheromatous plaques with increasing CXCL10 concentrations, and by the association with unstable plaque characteristics, such as macrophage dominance and reduced

presence of smooth muscle cells and collagen.

Previous studies have shown that inhibition of CXCL10 by antibodies in an intestinal inflammation animal model is an effective way to inhibit its function[19, 20]. The findings in those studies have been ascribed to the reduced amount of Th1 cells that were recruited to the diseased sites and either reduced production of inflammatory cytokines[19] or resulted in inflammatory disease exacerbation[20], depending on the role of T-cells in the pathogenesis of the disease.

The lesion-stabilizing effect we observed by inhibiting CXCL10, might be explained by a similar mechanism as described above, as it has been shown before that inhibition of the CXCL10-CXCR3 pathway decreases the amount of lesional T-cells[16, 21]. Veillard et al reported that genetic deletion of CXCR3 in ApoE knockout mice reduced early lesion formation, which correlated with an increase in lesional FoxP3-positive regulatory T-cells [21]. Recently, it has been reported that genetic deletion of CXCL10 in atherosclerosis-susceptible mice also resulted in smaller lesions, which contained fewer CD4+ T-cells[16]. Surprisingly however, despite the decrease in overall T-cell presence in the lesions, a higher expression of FoxP3 as well as of the anti-inflammatory cytokines IL-10 and TGF-β mRNA was found. This suggests a more prominent role for regulatory T-cells in this model. A similar increase in FoxP3 and TGF-β expression was found in a study using a peptide antagonizing CXCR3 in LDL receptor knockout mice, resulting in smaller lesions in the aortic root and the aorta[22].

A general limitation of our experimental mouse model is that there are few T-cells in the induced lesions after 9 weeks of cast placement, approximately 2-4 per lesion cross section[3]. As a consequence, we have been unable to find a difference in T-cell numbers following CXCL10 inhibition (data not shown). Nevertheless, the reduction in T-cells might have taken place during the early phase of actual inhibition. We performed measurements at only one time point, while the presence of T-cells in a lesion changes over time[23]. Also, the effect of small numbers of T-cells might prove to be very strong[24].

The small numbers of T-cells do not allow to produce sufficiently reliable data to enable making a comparison with the situation in mice that are deficient in CXCL 10 by gene targeting. This cannot be solved by mRNA analyses, as there was no RNA available from the endarterectomy samples that have been used. Besides facilitating recruitment of leukocytes, CXCL10 also induces and sustains a dominant Th1-type response by increasing the production of IFN-γ, providing a positive feedback loop[25]. Neutralization of CXCL10 might therefore result in a decreased concentration of IFN-γ in the lesions, which is considered a key cytokine in disease progression[26] and macrophage activation[27]. This notion is in agreement with our findings regarding macrophage activation status as measured by MHC class II expression[27], SMC presence[27] and collagen accumulation[28].

An alternative or additional mechanism of plaque modification by CXCL10

inhibition might be operative as well. Not only Th1 and NK cells, as major IFN-g producers, are responsive to CXCL10, but also plasmacytoid dendritic cells (PDC) express CXCR3 and are recruited via this receptor[29]. The numbers of circulating PDC are reduced in human atherosclerosis, while immunohistochemical analysis has indicated that they are recruited to advanced plaques[30,31]. PDC are known to produce large quantities of IFN-a upon activation and this cytokine functions as an inflammatory amplifier in the atherosclerotic plaque[32]. Additionally, a minor subset of monocytes has been shown to be recruited via CXCR3 to inflammatory environments[7] and might thus contribute to plaque instability as well.

Further research is needed to understand the mechanisms underlying the effects of CXCL10 inhibition. E.g., apoptosis could have an important role in the observed differences in plaque composition and size. It could be of interest to study the role of SMC in more detail by staining serial sections for proliferation and apoptosis on the one hand and alpha actin on the other hand. In addition, in situ zymography studies could be performed to get a clearer idea of the possible role of collagenolytic activity in the lesions. It would be very interesting to know more about the role of the pro-inflammatory cytokine microenvironment in the plaque in the experiments with CXCL 10 inhibition. From the present data, we cannot exclude that by inhibiting CXCL10 we just postponed the process of the lesion formation and maturation, rather than permanently altering it. For this argument and because of the ongoing discussion on the quality of animal models representing human disease states, we also performed a parallel study in humans. Mach et al[15] were the first to associate CXCL10 with human atherosclerosis, reporting that CXCL10 was expressed in several stages of the disease. CXCL10 was shown to be present on the surface of endothelial cells, suggesting a role in the recruitment and adhesion of CXCR3-positive cells from the circulation. They also showed broad expression of CXCL10 by SMC and macrophages throughout the lesion. Little is known about the effects of CXCL10 on human atherosclerosis development and clinical outcome. Previous studies sought to correlate plasma CXCL10 levels with the occurrence of coronary heart disease (CHD). In a case-control study it was found that CHD risk was associated with an increase in serum CXCL10.[33] A later prospective study showed that indeed increased levels of CXCL10 exist prior to CHD, but was not considered an independent risk factor[34]. Our study is the first one to correlate lesional CXCL10 protein content with plaque morphology in humans and to be a possible predictor of plaque vulnerability. Obviously, this cannot be measured directly in living patients, so it would be of interest to know the correlation between lesional and systemic levels of CXCL10. There were no plasma samples available to measure the systemic CXCL 10 levels and correlate them to the lesional levels, so this has to await future work.

In conclusion, we showed that the chemokine CXCL10 plays a functional role in the destabilization of atherosclerotic plaques in mice and is specifically upregulated in vulnerable plaques in humans. Since the experimental data were paralleled by similar findings in human unstable lesions, CXCL10 might be regarded as a new lead into understanding the process of plaque destabilization.

References

1. Virmani R, Kolodgie FD, Burke AP, Farb A, Schwartz SM. Lessons from sudden coronary death: a comprehensive morphological classification scheme for atherosclerotic lesions. Arterioscler Thromb Vasc Biol. 2000;20(5):1262-1275.

2. Cheng C, Tempel D, van Haperen R, van der Baan A, Grosveld F, Daemen MJ, Krams R, de Crom R. Atherosclerotic lesion size and vulnerability are determined by patterns of fluid shear stress. Circulation. 2006;113(23):2744-2753.

3. Cheng C, Tempel D, van Haperen R, de Boer HC, Segers D, Huisman M, van Zonneveld AJ, Leenen PJ, van der Steen A, Serruys PW, de Crom R, Krams R. Shear stress-induced changes in atherosclerotic plaque composition are modulated by chemokines. J Clin Invest. 2007;117(3):616-626.

4. Luster AD, Ravetch JV. Biochemical characterization of a gamma interferon-inducible cytokine (IP-10). J Exp Med. 1987;166(4):1084-1097.

5. Inngjerdingen M, Damaj B, Maghazachi AA. Expression and regulation of chemokine receptors in human natural killer cells. Blood. 2001;97(2):367-375.

6. Loetscher M, Loetscher P, Brass N, Meese E, Moser B. Lymphocyte-specific chemokine receptor CXCR3: regulation, chemokine binding and gene localization. Eur J Immunol. 1998;28(11):3696-3705.

7. Janatpour MJ, Hudak S, Sathe M, Sedgwick JD, McEvoy LM. Tumor necrosis factor-dependent segmental control of MIG expression by high endothelial venules in inflamed lymph nodes regulates monocyte recruitment. J Exp Med. 2001;194(9):1375-1384.

8. Hyun JG, Lee G, Brown JB, Grimm GR, Mittal N, Luster AD, Barrett TA. Anti-interferon-inducible chemokine, CXCL10, reduces colitis by impairing T helper-1 induction and recruitment in mice. Inflamm Bowel Dis. 2005;11(9):799-805.

9. Fife BT, Kennedy KJ, Paniagua MC, Lukacs NW, Kunkel SL, Luster AD, Karpus WJ. CXCL10 (IFN-gamma-inducible protein-10) control of encephalitogenic CD4+ T cell accumulation in the central nervous system during experimental autoimmune encephalomyelitis. J Immunol. 2001;166(12):7617-7624.

10. Loetscher M, Gerber B, Loetscher P, Jones SA, Piali L, Clark-Lewis I, Baggiolini M, Moser B. Chemokine receptor specific for IP10 and mig: structure, function, and expression in activated T-lymphocytes. J Exp Med. 1996;184(3):963-969.

11. Luster AD. Chemokines--chemotactic cytokines that mediate inflammation. N Engl J Med. 1998;338(7):436-445.

12. Taub DD, Longo DL, Murphy WJ. Human interferon-inducible protein-10 induces mononuclear cell infiltration in mice and promotes the migration of human T lymphocytes into the peripheral tissues and human peripheral blood lymphocytes-SCID mice. Blood. 1996;87(4):1423-1431.

13. Taub DD, Lloyd AR, Conlon K, Wang JM, Ortaldo JR, Harada A, Matsushima K, Kelvin DJ, Oppenheim JJ. Recombinant human interferon-inducible protein 10 is a chemoattractant for human monocytes and T lymphocytes and promotes T cell adhesion to endothelial cells. J Exp Med. 1993;177(6):1809-1814.

14. Wang X, Yue TL, Ohlstein EH, Sung CP, Feuerstein GZ. Interferon-inducible protein-10 involves vascular smooth muscle cell migration, proliferation, and inflammatory response. J Biol Chem. 1996;271(39):24286-24293.

15. Mach F, Sauty A, Iarossi AS, Sukhova GK, Neote K, Libby P, Luster AD. Differential expression of three T lymphocyte-activating CXC chemokines by human atheroma-associated cells. J Clin Invest. 1999;104(8):1041-1050.

16. Heller EA, Liu E, Tager AM, Yuan Q, Lin AY, Ahluwalia N, Jones K, Koehn SL, Lok VM, Aikawa E, Moore KJ, Luster AD, Gerszten RE. Chemokine CXCL10 promotes atherogenesis by modulating the local balance of effector and regulatory T cells. Circulation. 2006;113(19):2301-2312.

17. Cheng C, van Haperen R, de Waard M, van Damme LC, Tempel D, Hanemaaijer L, van Cappellen GW, Bos J, Slager CJ, Duncker DJ, van der Steen AF, de Crom R, Krams R. Shear stress affects the intracellular distribution of eNOS: direct demonstration by a novel in vivo technique. Blood. 2005;106(12):3691-3698.

18. Verhoeven BA, Velema E, Schoneveld AH, de Vries JP, de Bruin P, Seldenrijk CA, de Kleijn DP, Busser E, van der Graaf Y, Moll F, Pasterkamp G. Athero-express: differential atherosclerotic plaque expression of mRNA and protein in relation to cardiovascular events and patient characteristics. Rationale and design. Eur J Epidemiol. 2004;19(12):1127-1133.

19. Singh UP, Singh S, Taub DD, Lillard JW. Inhibition of IFN-{gamma}-Inducible Protein-10 Abrogates Colitis in IL-10-/- Mice J Immunol. 2003;171(3):1401.

20. Narumi S, Kaburaki T, Yoneyama H, Iwamura H, Kobayashi Y, Matsushima K. Neutralization of IFN-inducible protein 10/CXCL10 exacerbates experimental autoimmune encephalomyelitis. Eur J Immunol. 2002;32(6):1784-1791.

21. Veillard NR, Steffens S, Pelli G, Lu B, Kwak BR, Gerard C, Charo IF, Mach F. Differential influence of chemokine receptors CCR2 and CXCR3 in development of atherosclerosis in vivo. Circulation. 2005;112(6):870-878.

22. van Wanrooij EJ, de Jager SC, van Es T, de Vos P, Birch HL, Owen DA, Watson RJ, Biessen EA, Chapman GA, Van Berkel TJ, Kuiper J. CXCR3 antagonist NBI-74330 attenuates atherosclerotic plaque formation in LDL receptor-deficient mice. Arterioscler Thromb Vasc Biol. 2008;28(2):251-257.

23. Khallou-Laschet J, Caligiuri G, Groyer E, Tupin E, Gaston AT, Poirier B, Kronenberg M, Cohen JL, Klatzmann D, Kaveri SV, Nicoletti A. The proatherogenic role of T cells requires cell division and is dependent on the stage of the disease. Arterioscler Thromb Vasc Biol. 2006;26(2):353-358.

24. Schleicher U, Hesse A, Bogdan C. Minute numbers of contaminant CD8+ T cells or CD11b+CD11c+ NK cells are the source of IFN-gamma in IL-12/IL-18-stimulated mouse macrophage populations. Blood. 2005;105(3):1319-1328.

25. Gangur V, Simons FE, Hayglass KT. Human IP-10 selectively promotes dominance of polyclonally activated and environmental antigen-driven IFN-gamma over IL-4 responses. FASEB J. 1998;12(9):705-713.

26. Harvey EJ, Ramji DP. Interferon-gamma and atherosclerosis: pro- or anti-atherogenic? Cardiovasc Res. 2005;67(1):11-20.

27. Schroder K, Hertzog PJ, Ravasi T, Hume DA. Interferon-{gamma}: an overview of signals, mechanisms and functions. J Leukoc Biol. 2004;75(2):163.

28. Amento EP, Ehsani N, Palmer H, Libby P. Cytokines and growth factors positively and negatively regulate interstitial collagen gene expression in human vascular smooth muscle cells. Arterioscler Thromb. 1991;11(5):1223-1230.

Cella M, Jarrossay D, Facchetti F, Alebardi O, Nakajima H, Lanzavecchia A, Colonna M. 1999. Plasmacytoid monocytes migrate to inflamed lymph nodes and produce large amounts of type I interferon. Nat Med 5:919-23.

Van Vre EA, Bosmans JM, Van Brussel I, Maris M, De Meyer GR, Van Schil PE, Vrints CJ, Bult H. 2011. Immunohistochemical characterisation of dendritic cells in human atherosclerotic lesions: possible pitfalls. Pathology 43:239-47.

Van Vre EA, Hoymans VY, Bult H, Lenjou M, Van Bockstaele DR, Vrints CJ, Bosmans JM. 2006. Decreased number of circulating plasmacytoid dendritic cells in patients with atherosclerotic coronary artery disease. Coron Artery Dis 17:243-8.

Niessner A, Shin MS, Pryshchep O, Goronzy JJ, Chaikof EL, Weyand CM. 2007. Synergistic proinflammatory effects of the antiviral cytokine interferon-alpha and Toll-like receptor 4 ligands in the atherosclerotic plaque. Circulation 116:2043-52.

33. Rothenbacher D, Müller-Scholze S, Herder C, Koenig W, Kolb H. Differential expression of chemokines, risk of stable coronary heart disease, and correlation with established cardiovascular risk markers. Arterioscler Thromb Vasc Biol. 2006;26(1):194-199.

34. Herder C, Baumert J, Thorand B, Kolb H, Koenig W. Chemokines and incident coronary heart disease: results from the MONICA/KORA Augsburg case-cohort study, 1984-2002. Arterioscler Thromb Vasc Biol. 2006;26(9):2147-2152.

time Ingenuity
device
atherosclerotic

plaque
group
SMC
USA
Figure
also
data
analysis
weeks
shear
amplification

expression

used
technical
expressed
genetic Germany
results
RNA
phenotype
pathways
mice
development performed
differences
arrays California
samples
atherosclerosis
segments
groups
two using
segment
high cDNA
structures
LSSOSS
differentially
genes stress may
lnc
single cap

Chapter 6

Gene Expression Profiling of Unstable Plaque Development in Atherosclerotic Mice

D. Segers, K. Brand, D. Tempel, M. Pescatori, A. Stubbs, P.J.M. Leenen,
S. Bauerschmidt, A. van Gool, R. Krams, R. de Crom
Work in progress

Abstract

Background

Underlying mechanisms of the differential development of atherosclerotic plaques into stable or unstable lesions are currently unclear.
Aim: To evaluate whole genome genetic expression profiles of stable and unstable plaques during their development in order to gain further insight into plaque growth in general, but also into the differentiation mechanisms of lesions.

Methods and Results

Using a flow altering device, both stable and unstable lesions were developed in atherosclerosis susceptible mice in oscillatory (OSS) and low shear stress (LSS) conditions respectively. After either 6 or 9 weeks, plaque tissue was harvested by laser microdissection and RNA was extracted, linearly amplified and analyzed by whole genome microarrays. Highly expressed genes were stained by immunohistological techniques. Results: Differentially expressed genes were only found between LSS and OSS segments after 6 weeks of plaque development, most of them involved in neuronal pathways. Immunohistological staining was unable to confirm the genetic data.

Conclusion

These data should be considered inconclusive. Repeating experiments are necessary, combined with validation by qPCR.

Introduction

Vulnerability of atherosclerotic lesions and the inherent risk of plaque rupture are a major clinical problem. An unstable lesion characteristically has a large lipid core and a thin overlying fibrous cap. Loss of fibrous cap material is mediated by breakdown of collagenous structures due to the proteolytic activity of matrix metalloproteinases (MMP). Vascular smooth muscle cells (SMC) play an essential role in the formation of the fibrous cap. During lesion progression, contractile SMC migrate from the tunica media to the newly formed neointima. The SMC will dedifferentiate from their contractile phenotype into a synthetic phenotype, and start to produce extracellular matrix components like collagen. Thus, cap thickness results from the balance between collagen synthesis by the SMC and degradation by MMP.

Previously, we developed an experimental animal model in which both plaques with stable and unstable characteristics are simultaneously induced in a single straight arterial segment. This model is based on a device that alters the blood flow and therefore induces different shear stress patterns. Briefly, this device gradually narrows the vessel lumen to ~70% of its original diameter. As a consequence, shear stress is lowered upstream of the device (low shear stress; LSS), gradually increases inside the device (high shear stress; HSS) and is oscillating (oscillatory shear stress; OSS) just downstream of the device[1]. Nine weeks after placement of the device in atherosclerosis-susceptible mice, the lesions in the LSS segment had the characteristics of an unstable plaque with a necrotic core and thin fibrous cap, whereas the OSS segment displayed a stable phenotype with increased presence matrix-producing SMC and collagen and reduced gelatinolytic activity. The HSS segment remained free of atherosclerosis.

Since the underlying mechanisms resulting in these two distinct morphologies are unclear, we evaluated the genetic expression profiles of the lesions from LSS and the OSS segments during their development, by whole genome microarray analysis. Using this approach we aim to get further insight into plaque growth in general, but also what mechanisms may play a role in the differentiation of the two plaque phenotypes. The results could lead to new hypotheses with regard to atherosclerosis, which can be studied in the future. Hence, the aim of this study was not to explore the newly found mechanisms in depth.

Materials and Methods

Animals and surgical procedures

Apolipoprotein-E deficient mice, 15-20 weeks of age, were obtained from the Jackson Laboratories (Bar Harbor, ME, USA), and fed a high fat, high cholesterol diet consisting of 15% (wt/wt) cocoa butter and 0.25% cholesterol (wt/wt) (Diet W, Hope Farms, The Netherlands). Two weeks after this diet was initiated, the

mice were anesthetized with 2% isoflurane and instrumented with a shear stress-altering device around the right common carotid artery, as described previously[2]. Mice were kept on the high fat, high cholesterol diet for the remainder of the experiment. The device remained in situ until sacrifice after 6 or 9 weeks. At each time point, six mice were used for genetic analysis and another three for histological validation of expression results.

All animal experiments were approved by the institutional animal ethical committee and performed in compliance with institutional and national guidelines.

Tissue preparation

Following sacrifice, blood was collected and mice were flushed systemically with PBS treated with the RNase inhibitor diethylpyrocarbonate (DEPC). Subsequently, the common carotid artery was quickly isolated, embedded in OCT compound (Tissue-Tek, Sakura, Japan), and snap-frozen in liquid nitrogen. 20 µm cryosections of both the LSS and the OSS segment were cut and mounted on 1mm PALM pen-membrane slides. Next, the sections were fixed for 30 seconds in 70% ethanol, stained with hematoxylin for 3 minutes, were rinsed with water and dehydrated by several rinses in 100% ethanol. All solutions used during the staining procedure were treated with DEPC.

Laser microdissection and RNA purification

To avoid interference by medial or adventitial structures, we exclusively isolated the neointima by Laser Microdissection and Pressure Catapulting (LMPC) using the PALM Microlaser system (Carl Zeiss Micro-Imaging, Germany). Isolated neointimas were dissolved immediately in lysis buffer (Qiagen, Germany) and stored at −80 °C for subsequent RNA purification. RNA was purified using the RNeasy Micro kit with DNase treatment (Qiagen, Germany) according the manufacturer's protocol, except that 20 ng of 16S/23S bacterial ribosomal RNA (Roche Applied Science, Germany) was used as carrier and an additional elution was performed in the final step to maximize RNA yield. RNA eluted with RNase free water was vacuum evaporated for immediate amplification and cDNA generation.

Amplification and labeling of purified RNA samples

Quality of the freshly purified RNA was assayed using the BioAnalyzer 2100 in combination with the RNA 6000 Pico chip (Agilent Technologies, USA). When intact 18S/28S ribosomal RNA peaks were evident, the sample was considered acceptable for further processing. Amplification and cDNA labeling with biotin was accomplished using the Ovation RNA Amplification System V2 and FL-Ovation cDNA Biotin Module V2 respectively according to the manufacturers protocols (Nugen Technologies Inc, San Carlos, California, USA). Efficiency of

the amplification was assayed quantitatively by 260/280nm estimation of cDNA concentration, where a total yield of at least 4.85 μg cDNA was deemed sufficient for specific amplification of the RNA template. In order to prevent technical induction of differences, the amplification of the samples was performed in two randomly composed groups of all samples.

Hybridization of biotin labeled cDNA samples

4 groups were analyzed, which represent two plaque locations (LLS and OSS) at 6 and 9 weeks after cast placement. Each group consisted of 6 arrays. All samples were hybridized to the arrays in a single batch. Biotin labeled cDNA samples were combined with hybridization cocktail including DMSO according to the manufacturer's protocol (Nugen Technologies Inc, San Carlos, California, USA) and hybridized to GeneChip Mouse Genome 430 2.0 arrays for 18 hours (Affymetrix Inc, Santa Clara, California, USA). Post-hybridization washing, scanning and image analysis were performed according to the manufacturer's protocols (Affymetrix Inc, Santa Clara, California, USA). All arrays were run as a single batch, in order to prevent batch-effects.

Analysis of microarray expression data

All analyses were performed using BRB-ArrayTools developed by Dr. Richard Simon and BRB-ArrayTools Development Team[3] (http://linus.nci.nih.gov/BRB-ArrayTools.html). Raw expression data was imported and normalized using the GC Robust Multi-array Averaging (gcRMA) method[4]. Next, the data was filtered such that if a probe set expression values differed at least 1.5-fold from the median in at least 20% of the arrays, they were kept for analysis. The overall difference between the two groups was visualized by multidimensional scaling analysis. This is a method to graphically display high-dimensional data in three dimensions. Samples with similar gene expression profiles will lie close together in the three-dimensional space to form a cluster.

Following multidimensional scaling, lists of differentially expressed genes were calculated using a multivariate permutation test, to provide a false-discovery rate of <10% with 95% confidence (BRB array Tools, class comparison). The multivariate test is fully non-parametric and therefore does not require the assumption of Gaussian distribution of the data.

Also, instead of only looking at differentially expressed genes it may be very interesting to determine how genes between the two locations interact as parts of pathways or gene networks. Therefore, we also performed analysis of our data using Ingenuity Pathway Analysis (Ingenuity Systems, Inc, Redwood City, California, USA). Ingenuity Pathway Analysis (IPA) allows researchers to construct knowledge-based structural networks of expression data in the context of known functional interrelationships of different genes.

Histological validation

8 μm cryosections were cut and stained for the markers bassoon (Synaptic Systems, Germany), tyroxine hydroxylase and dopamine beta hydroxylase (both, Santa Cruz Biotechnology Inc., USA). Non-relevant rabbit immunoglobulins were used for control stainings.

Results & Discussion

In this study we performed genetic analysis by whole-genome microarrays on atherosclerotic plaques. We compared expression profiles at 6 and 9 weeks after surgical placement of a shear stress modifier, which induces a low shear stress and an oscillatory shear stress segment in a single arterial segment. The former will develop into a plaque with an unstable phenotype at 9 weeks, whereas the latter will become stable at that time point. We search for differential expression of genes between the segments at the two different time points and between the segments at one time point (Table 1).

Surprisingly, despite technical success of the experiment (see Table 2 for results) we did not identify differentially expressed genes within the following comparisons:
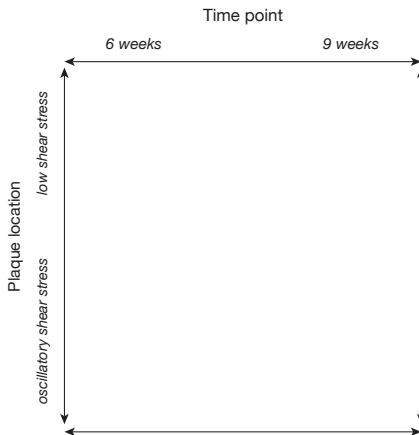
Table 1. *Performed comparisons with the expression data.*

LSS 6 weeks vs. LSS 9 weeks, OSS 6 weeks vs. OSS 9 weeks and LSS 9 weeks vs. OSS 9 weeks. Maybe the differentiation into the two plaque phenotypes occurs in an earlier phase of plaque development, and therefore could not be detected in this study. Another possible explanation is that the genetic differences are too small to be detected by the techniques we performed. This might be due to the very small amounts of RNA isolated by the laser microdissection, for which strong amplification is needed. This induces noise into the data, which might obscure delicate differences.

On the other hand, the genome-wide expression patterns between the LSS and

OSS segments after 6 weeks of plaque development did show large differences, which might underlie the distinct differences found in plaque morphology after 9 weeks of cast placement. Since it is impossible to see from the raw expression data if the samples within a group are comparable, the data is graphically represented. The result is shown in the multidimensional scaling plot (Figure 1). In this image shows each group (LSS or OSS) is color-coded and each dot represents the data of a single sample. Our results show that all six samples from each group nicely cluster together at opposite end of the axis, evidencing large differences between the groups and similarity within each group. This is an important step, because it shows possible sample effects (e.g. due to technical failure or biological variation), which may obscure further analysis prior to statistical processing of the expression data.

After performing the multivariate test we found 2329 probe-sets to be differentially expressed between the LSS and the OSS plaque segments at 6 weeks, with a minimum 2-fold difference. Of these, the majority was overexpressed in the OSS segment (2225 probe-sets), many of these genes were very weakly expressed in the LSS segment. This resulted in huge fold differences between these segments. In Table 3, we listed the probe-sets that differed more than 50-fold.

When these differentially expressed genes were further analyzed by visual examination, by gene ontology analysis and by Ingenuity networks analysis, curiously enough we did not find any clear vascular or immunological pathways in

A

Group	ng/ul	A260	260/280	260/230
6wk LSS	214,32	6,49	1,93	2,41
6wk OSS	227,87	6,91	1,92	2,40
9wk LSS	221,10	6,70	1,92	2,37
9wk OSS	212,13	6,43	1,92	2,38

B

%Present	GAPDH 5'	GAPDH 3'	GAPDH 3' 5' ratio
65,48	1027,89	1682,40	1,69

Table 2. *Average quality control data of samples pre and post-hybridization.*

A. Result of quality control of RNA yield following linear amplification with the Ovation RNA Amplification System V2 and FL-Ovation cDNA Biotin Module V2 (Nugen Technologies Inc, San Carlos, California, USA). Average yield in each group was equal. The high 260/280 and 260/230 ratios show that the solutions are free contaminants. LSS=low shear stress, OSS=oscillatory shear stress.

B. Post hybridization quality data show good % present (over 50%) and good 3' 5' ratio's (< 3).
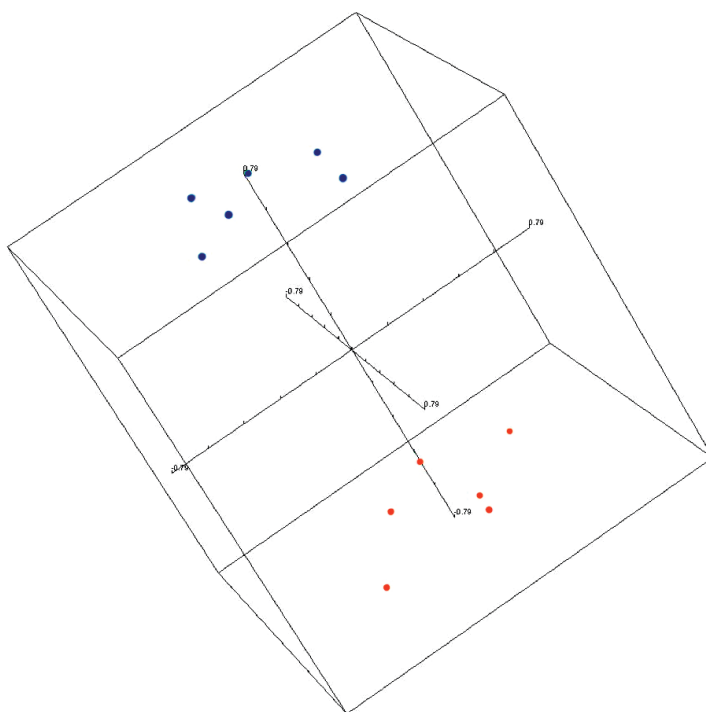
Figure 1: *Multidimensional Scaling plot of all samples (n=12) at 6 weeks.*

Multidimensional scaling aims to visualize the total variation between all the genes in three main components along three axes, which contain the first three principal components of the data set. Each sample is represented as a single point. If all the dots are scattered across the 3D-space represented by the axes, large variation between the samples exists. If samples are clustered together at a single location along the axes, they are very similar. If clustered dots have the same colors, this depicts they belong to the same experimental group. The two groups of samples clearly differentiate from each other along one of the axes, which represents the large differences between the groups (especially since the first principal component already describes the separation) as well as the reproducibility within the groups. Blue: OSS samples, Red: LSS samples.

this data. This is unexpected since we already know from histological and qPCR analysis that there are differences in the expression of several factors including fractalkine[5]. Moreover, most of the differentially expressed genes were in some way related to neurological pathways and mechanisms. This also is difficult to explain, since neuronal growth into lesions has not been described before. For example, one of the strongly expressed genes links to the neuronal protein bassoon. This is a zinc-finger CAG/glutamine-repeat protein selectively localized at the active zone of presynaptic nerve terminals[6]. It's a structural component of the neuron, which to as far as our knowledge has never been described in non-neuronal structures and as such a strange find in our data. We stained for bassoon in sections, where
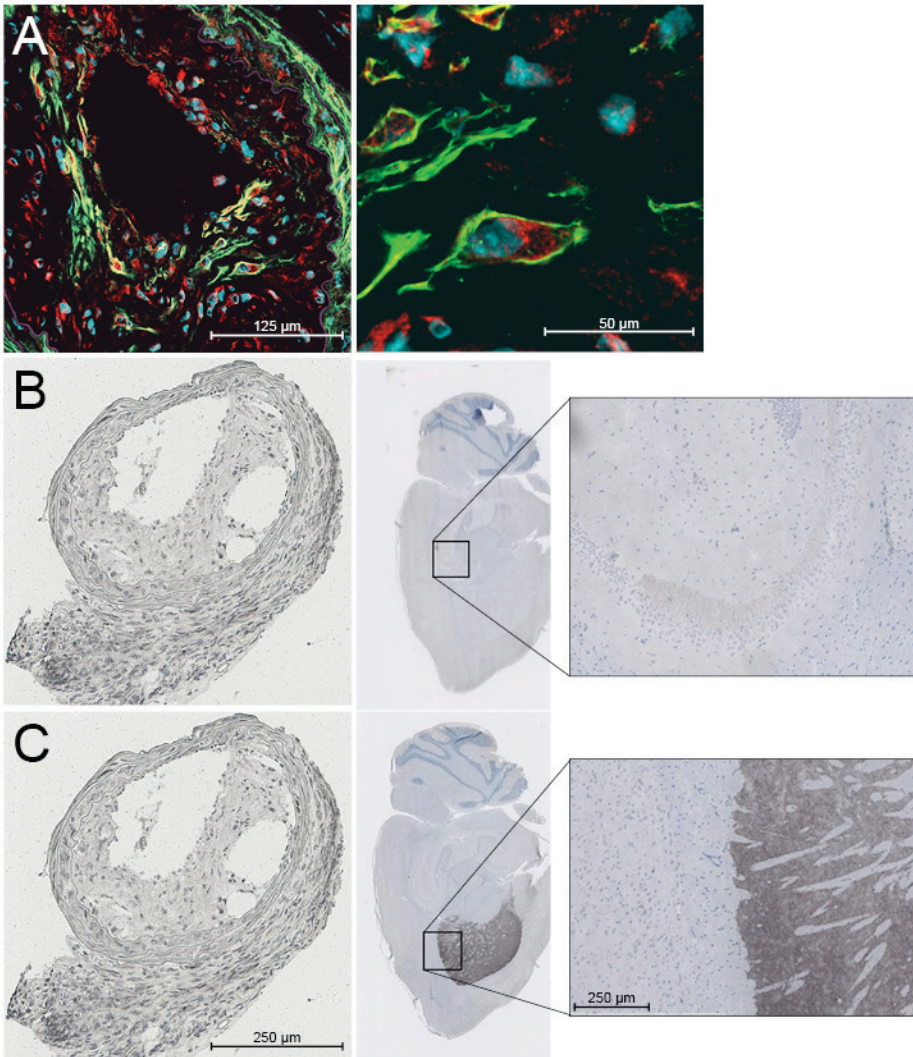
Figure 2: *Immunohistological staining.*
A: left panel shows 200x image of atherosclerotic plaque after bassoon (red) and SMC alpha-actin (green) double staining. Nuclei were stained with DAPI (blue). Right panel shows 1000x magnification. There is clear intracellular staining of bassoon in an α-actin positive SMC. The left panel shows many bassoon positive cells without α-actin positivity, on morphological grounds most probably SMC as well, since double staining with CD68 (macrophage marker) was negative (data not shown). B: dopamine beta hydroxylase staining of atherosclerotic plaque, mouse brain and brain magnification (left to right). C: Tyrosine hydroxylase staining staining of atherosclerotic plaque, mouse brain and brain magnification (left to right)

tissue expression was very limited. Morphologically we did not stain structures resembling neuronal origin. The only positive signal was obtained from a part of the plaque smooth muscle cells, which showed nice intracellular staining (Figure 2).

Next, we used Ingenuity Pathway Analysis to overlay our gene lists with functional data. One of the pathways that is almost fully expressed in these analysis is the phox2a pathway (Figure 3). Phox2a is a transcription factor that acts early in development to help promote the formation of neurons and regulate neuron differentiation[7]. It also regulates the expression of tyrosine hydroxylase and dopamine beta-hydroxylase, two catecholaminergic biosynthetic enzymes essential for the differentiation and maintenance of the noradrenergic neurotransmitter phenotype. We tried to immunostain some of the enzymes from this pathway in mouse sections from the same location and time point. The genes encoding these enzymes were among the most highly expressed genes on our arrays. Notably, we were unable to show clear positive staining for the following markers: dopamine beta-hydroxylase (DBH), tyrosine hydroxylase (TH) and DOPA decarboxylase (DDC) (Figure 2). The lack of positive staining for the proteins encoded by these genes indicate that high RNA expression is not matched by protein expression in atherosclerotic plaque, casting doubts on the significance of the findings by microarray.

In general, we can conclude that the relevance of the findings above for the development of atherosclerosis is unknown and that these data are inconclusive as such. Since we use such small quantities of RNA to start out with, there is a risk of inducing variations due to technical issues. On the other hand, we processed our samples in combined batches containing samples of each group. And since the samples from the 6 weeks groups are very similar in respect to each other (Figure 1), this evidences that we are indeed facing true effects of the biology and ruling out a technical result. Hypothetically, these data give handles for some possible new insights into plaque destabilization. With the emerging field of neuro-immunology[8,9], one could hypothesize that a neuronal control of the atherosclerotic plaque may emerge during development. It is known that effector nerve endings in inflamed tissues may alter the expression of pro and anti-inflammatory cytokines[8]. The role of this mechanism in atherosclerosis is still elusive, but is very interesting with respect to the occurrence of atherosclerotic events with a circadian rhythm[10], or during strenuous exercise (high catecholamine expression)[11]. Before such hypotheses based on these data can be justified, the experiments should be repeated. This is needed because technological developments have resulted into superior techniques to those used in these studies, allowing the collection of more reliable data. Furthermore, hypotheses mentioned above should be supported by conclusive validation experiments, which are currently lacking.

Gene name	Fold-change	Parametric p-value
5-hydroxytryptamine (serotonin) receptor 3A	398	< 1e-07
dopamine beta hydroxylase	386,5	< 1e-07
synaptosomal-associated protein 25	348,6	0,0000002
neurensin 1	347,5	< 1e-07
solute carrier family 10 (sodium/bile acid cotransporter family), member 4	342,8	< 1e-07
Ras-like without CAAX 2	322,3	< 1e-07
NA	306,8	< 1e-07
synaptotagmin IV	254,6	< 1e-07
dopa decarboxylase	243,3	< 1e-07
sparc/osteonectin, cwcv and kazal-like domains proteoglycan 3	239,1	< 1e-07
tyrosine hydroxylase	235	< 1e-07
neurofilament, light polypeptide	232,8	< 1e-07
peripherin	231,9	< 1e-07
ELAV (embryonic lethal, abnormal vision, Drosophila)-like 2 (Hu antigen B)	228,8	0,0000001
secretogranin V	227,2	< 1e-07
dopamine beta hydroxylase	223,7	< 1e-07
synaptotagmin I	213,8	< 1e-07
cholinergic receptor, nicotinic, alpha polypeptide 3	208,4	< 1e-07
neurofilament, light polypeptide	208,2	< 1e-07
guanine nucleotide binding protein (G protein), gamma 3	197	< 1e-07
follistatin-like 5	185,9	< 1e-07
complexin 1	181,8	< 1e-07
sulfotransferase family 4A, member 1	179,2	< 1e-07
ELAV (embryonic lethal, abnormal vision, Drosophila)-like 2 (Hu antigen B)	175,1	< 1e-07

Table 3: *Fold change differences in expression of the highest expressed genes. Continued on the next pages*

Gene name	Fold-change	Parametric p-value
nuclear receptor interacting protein 3	171,6	< 1e-07
RIKEN cDNA A530088H08 gene	168,1	< 1e-07
paired-like homeobox 2b	167,4	0,0000001
complexin 1	161	< 1e-07
synaptotagmin IV	159,7	< 1e-07
RIKEN cDNA 4930488B01 gene	156,9	< 1e-07
Ca2+-dependent secretion activator	155,5	< 1e-07
myelin transcription factor 1	153,3	< 1e-07
secretogranin II	152	< 1e-07
regulated endocrine-specific protein 18	151,6	< 1e-07
sphingosine-1-phosphate phosphotase 2	151,2	< 1e-07
mitogen-activated protein kinase 10	144,8	0,0000001
microtubule-associated protein 4	135,3	< 1e-07
sodium channel, voltage-gated, type IX, alpha	129,9	0,0000001
contactin 1	129,8	< 1e-07
ELAV (embryonic lethal, abnormal vision, Drosophila)-like 4 (Hu antigen D)	129,7	< 1e-07
RIKEN cDNA A530088H08 gene	128,7	< 1e-07
cholinergic receptor, nicotinic, alpha polypeptide 3	125,3	< 1e-07
tetraspan transmembrane protein, hair cell stereocilia	123,7	< 1e-07
follistatin-like 5	122,4	< 1e-07
NA	118,4	< 1e-07
solute carrier family 7 (cationic amino acid transporter, y+ system), member 14	117,8	< 1e-07
protein phosphatase 2 (formerly 2A), regulatory subunit B (PR 52), gamma isoform	116,9	< 1e-07
brain expressed X-linked 2	116,8	< 1e-07
kinesin family member 5A	115,5	< 1e-07
transmembrane protein 130	114,1	< 1e-07

Gene name	Fold-change	Parametric p-value
cholinergic receptor, nicotinic, beta polypeptide 4	109,9	< 1e-07
piggyBac transposable element derived 5	105,4	< 1e-07
internexin neuronal intermediate filament protein, alpha	103,4	< 1e-07
synapsin II	101,8	< 1e-07
NA	100,6	< 1e-07
creatine kinase, mitochondrial 1, ubiquitous	98,4	< 1e-07
NA	96,9	0,0000002
hippocalcin-like 4	96,8	< 1e-07
NA	95,6	< 1e-07
glutamate receptor, metabotropic 7	93,8	0,0000001
synapsin II	90,7	< 1e-07
RIKEN cDNA A230106N23 gene	90,2	< 1e-07
hypothetical protein B830032F12	88,4	< 1e-07
N-ethylmaleimide sensitive fusion protein attachment protein beta	88	< 1e-07
N-ethylmaleimide sensitive fusion protein attachment protein beta	87,5	< 1e-07
Ras-like without CAAX 2	85,9	< 1e-07
RAB3B, member RAS oncogene family	85,5	< 1e-07
transmembrane protein 179	85,4	< 1e-07
neurofilament, medium polypeptide	84,7	< 1e-07
protein phosphatase 2 (formerly 2A), regulatory subunit B (PR 52), beta isoform	84	< 1e-07
chromogranin B	83,7	0,0000001
expressed sequence AW121567	82,8	< 1e-07
amphiphysin	82,2	< 1e-07
ELAV (embryonic lethal, abnormal vision, Drosophila)-like 4 (Hu antigen D)	81,5	< 1e-07
endothelin 3	79,6	< 1e-07
glutamate receptor, ionotropic, AMPA2 (alpha 2)	78,9	< 1e-07

Gene name	Fold-change	Parametric p-value
ganglioside-induced differentiation-associated-protein 1	77,3	0,0000004
mitogen-activated protein kinase 10	76	< 1e-07
sodium channel, voltage-gated, type IX, alpha	76	< 1e-07
RIMS binding protein 2	75,5	< 1e-07
bruno-like 6, RNA binding protein (Drosophila)	75,4	< 1e-07
insulinoma-associated 2	75,3	< 1e-07
reticulon 1	75,3	< 1e-07
NA	72,4	< 1e-07
nerve growth factor receptor (TNFR superfamily, member 16)	72,4	< 1e-07
astrotactin 1	72,3	< 1e-07
stathmin-like 3	70,5	< 1e-07
ELKS/RAB6-interacting/CAST family member 2	69,6	< 1e-07
solute carrier family 29 (nucleoside transporters), member 4	68,3	< 1e-07
G protein-coupled receptor 22	63,6	< 1e-07
mitogen-activated protein kinase 8 interacting protein 2	63,3	< 1e-07
5-hydroxytryptamine (serotonin) receptor 3B	63,2	< 1e-07
acetylcholinesterase	61,2	< 1e-07
adducin 2 (beta)	61,2	< 1e-07
transmembrane protein 59-like	61,1	< 1e-07
RIKEN cDNA A730017C20 gene	61	0,000002
neuronatin	60,9	< 1e-07
UbiE-YGHL1 fusion protein	60	< 1e-07
SH3-domain GRB2-like 2	59,7	< 1e-07
synaptosomal-associated protein 91	59,7	0,0000001
synaptotagmin IX	59,7	< 1e-07
synapsin II	59	< 1e-07

Gene name	Fold-change	Parametric p-value
solute carrier family 6 (neurotransmitter transporter, noradrenalin), member 2	58,8	< 1e-07
sparc/osteonectin, cwcv and kazal-like domains proteoglycan 1	58,8	0,0000001
synaptotagmin II	58,8	< 1e-07
potassium inwardly-rectifying channel, subfamily J, member 3	58,4	< 1e-07
sodium channel, voltage-gated, type IX, alpha	57,8	< 1e-07
transcription factor AP-2 beta	57,6	< 1e-07
RIKEN cDNA A030001O10 gene	57,2	< 1e-07
cyclin-dependent kinase 5, regulatory subunit 2 (p39)	57	< 1e-07
homeo box C4	57	< 1e-07
NA	56,3	0,0000002
ELAV (embryonic lethal, abnormal vision, Drosophila)-like 4 (Hu antigen D)	56,2	< 1e-07
NA	56,2	< 1e-07
leucine rich repeat containing 3	56,1	< 1e-07
protocadherin alpha 1	55,1	0,0000001
contactin associated protein-like 2	53,7	< 1e-07
NA	53,4	< 1e-07
protein phosphatase 1, regulatory (inhibitor) subunit 1C	53,1	< 1e-07
microtubule-associated protein tau	52,2	< 1e-07
mitogen-activated protein kinase 8 interacting protein 2	51,8	< 1e-07
transgelin 3	51,6	< 1e-07
VGF nerve growth factor inducible	51,5	< 1e-07
paired-like homeobox 2a	50,9	< 1e-07
zinc finger, CCHC domain containing 18	50,5	< 1e-07
solute carrier family 7 (cationic amino acid transporter, y+ system), member 14	50,2	< 1e-07
growth associated protein 43	50,1	< 1e-07

References

1. Cheng C, van Haperen R, de Waard M, van Damme LC, Tempel D, Hanemaaijer L, van Cappellen GW, Bos J, Slager CJ, Duncker DJ, van der Steen AF, de Crom R, Krams R. Shear stress affects the intracellular distribution of enos: Direct demonstration by a novel in vivo technique. Blood. 2005;106:3691-3698

2. Cheng C, Tempel D, van Haperen R, van der Baan A, Grosveld F, Daemen MJ, Krams R, de Crom R. Atherosclerotic lesion size and vulnerability are determined by patterns of fluid shear stress. Circulation. 2006;113:2744-2753

3. Simon R, Lam A, Li M, Ngan M, Menenzes S, Zhao Y. Analysis of gene expression data using brb-array tools. Cancer Informatics. 2007;2:11-17

4. Wu Z, Irizarry RA, Gentleman R, Martinez-Murillo F. A model-based background adjustment for oligonucleotide expression arrays. Journal of the American Statistical Association. 2004

5. Cheng C, Tempel D, van Haperen R, de Boer HC, Segers D, Huisman M, van Zonneveld AJ, Leenen PJ, van der Steen A, Serruys PW, de Crom R, Krams R. Shear stress-induced changes in atherosclerotic plaque composition are modulated by chemokines. J Clin Invest. 2007;117:616-626

6. Tom Dieck S, Sanmarti-Vila L, Langnaese K, Richter K, Kindler S, Soyke A, Wex H, Smalla KH, Kampf U, Franzer JT, Stumm M, Garner CC, Gundelfinger ED. Bassoon, a novel zinc-finger cag/glutamine-repeat protein selectively localized at the active zone of presynaptic nerve terminals. J Cell Biol. 1998;142:499-509

7. Brunet JF, Pattyn A. Phox2 genes - from patterning to connectivity. Curr Opin Genet Dev. 2002;12:435-440

8. Di Comite G, Grazia Sabbadini M, Corti A, Rovere-Querini P, Manfredi AA. Conversation galante: How the immune and the neuroendocrine systems talk to each other. Autoimmun Rev. 2007;7:23-29

9. Habbal OA, Al-Jabri AA. Circadian rhythm and the immune response: A review. Int Rev Immunol. 2009;28:93-108

10. Muller JE, Tofler GH, Stone PH. Circadian variation and triggers of onset of acute cardiovascular disease. Circulation. 1989;79:733-743

11. Tofler GH, Muller JE. Triggering of acute cardiovascular disease and potential preventive strategies. Circulation. 2006;114:1863-1872

Chapter 7

General Discussion and Future Perspectives

The mechanisms behind the development of atherosclerotic plaques and their transition to clinically significant lesions are currently not fully clear. It is of essential importance to gain knowledge on this matter, in order to develop better diagnostic and therapeutic strategies for this disease. Grossly, the studies presented in this thesis encompass two main issues in understanding atherosclerosis. The first chapters cover the spatial heterogeneity of atherosclerotic lesions. The second part describes studies of the inflammatory mechanisms that take place during disease development. Both will be discussed consecutively, followed by a vision for future experiments.

Plaque heterogeneity

One of the main issues is that developing lesions are morphologically heterogeneous when assessed longitudinally. A single plaque may have multiple appearances depending on which segment is examined. This heterogeneity is not just a phenotypical feature; it has important clinical consequences as well. It has been shown that most plaque ruptures occur in the proximal plaque segment[1, 2].

Since it is currently impossible to accurately study natural history in patients, researchers often turn to animal experiments to test their hypotheses. In this thesis, both rabbits and mice have been used, and results in both models do not always correspond. In chapter 2 of this thesis we showed that there is a correlation between the level of shear stress and the histological qualities of the plaque in experimental atherosclerosis in rabbits. We showed that matrix degrading gelatinolytic activity was highest in the upstream segment and colocalized with a subgroup of macrophages and smooth muscle cells, which were associated with oxidized LDL.

Following the above study, we further assessed the heterogeneity of atherosclerotic plaques in a mouse model in which the development of atherosclerosis is directly coupled to differences in shear stress (chapter 3). In these animals, atherosclerotic lesions with characteristics of unstable plaques develop in a segment primed by low shear stress, resembling the preferential location for human plaque development. In just over half the number of animals studied we found evidence of plaque disruption, mainly intraplaque hemorrhage. All disruptions were located in the upstream part of the lesion, resembling findings in human. With respect to our findings in rabbits, we were unable to obtain similar results. In rabbits macrophages were mostly present in the upstream part of the plaques, whereas in mice the macrophages were equally distributed. Nevertheless, the immunological activity of macrophages in mice was strongly focussed in the upstream segment, something we did not test for in rabbits. Gelatinolytic activity in mouse plaques was most prominent in the downstream segment, which contradicts the previous results in rabbits. A possible explanation for this discrepancy may be the big difference in approach of creating atherosclerosis in each model. Atherosclerosis in rabbits can only develop with a combination of balloon endothelial denudation and a high

cholesterol diet. The former removes the endothelial cells from the artery wall, removing the natural barrier between blood and vascular wall, allowing lipids and inflammatory cells to enter the arterial wall. The endothelial denudation creates a physically altered endothelial barrier, whereas in mice the plaque development endothelial dysfunction is based on an accepted pathophysiological mechanism of altered shear stress. In that sense, the rabbit is a more extreme model of human atherosclerotic disease.

There has not been much research studying the mechanisms behind intraplaque heterogeneity, though many papers describe the non-uniform appearance of lesions. Recently, work has been published describing the predominant upstream localization of plaque ruptures in humans, though the strong upstream localization seems to be strongest in the left anterior descending coronary artery (LAD), whereas in the right coronary artery a more equal distribution of ruptures is seen[1, 2]. Currently, the PREDICTION trial is ongoing, prospectively monitoring coronary segments of low shear stress and expansive remodeling to see if these regions show rapid progression of atherosclerosis and eventually plaque rupture. Ideally, the results of this study may provide anatomical plaque features, used to determine high-risk lesions. This might lead to interventions in a pre-rupture state, reducing the occurrence of acute coronary events.

With the recent development and improvement of micro-imaging techniques, such as micro-CT[3] and micro-MRI[4-6], opportunities arrive to downscale the experimental concept of the rabbit study to smaller animal models better representing the human situation. Also, with the development of high resolution imaging techniques, the door is open to characterize histological and functional characteristics of a plaque without the need to examine the tissues under a microscope. Much effort is currently put into developing molecular imaging techniques as well as improving existing imaging techniques to detect specific plaque components. The first will employ contrast agents labelled with a specific protein that will accumulate in the cell or structure under investigation, enabling detection of heterogeneity[7, 8]. A second approach is to use common imaging modalities like CT, MRI and IVUS and optimize imaging protocols to try to predict plaque composition. These techniques by themselves will not be able to show details on a cellular level, but for that matter they may be combined with molecular imaging techniques. Another advantage of both these approaches is that they may be performed repeatedly over time, giving more insight in the natural history of plaque development.

Inflammatory response

In chapter 4 we describe the differential expression of chemokines during the development of atherosclerosis induced by two different patterns of shear stress. We found differences both in the early and late phases of development, reflecting a continuously changing immunological environment. The morphological qualities

of lesions induced by either low or oscillatory shear stress are partially an effect of the differential expression of CXCL10 (IP-10) and CX3CL1 (fractalkine).

CXCL10 is a chemokine expressed in low levels in immune structures like lymph nodes, but can be highly expressed by monocytes, endothelial cells and SMC after stimulation with the pro-inflammatory cytokine IFN-gamma. The receptor for CXCL10, CXCR3, is known to be primarily expressed on activated Th1 cells, which is considered the key Tcell in atherosclerosis. It has been shown that CXCL10 is highly expressed in atherosclerotic plaques in humans, and that loss of function studies in mice resulted in decreased atherosclerosis. In our studies CXCL10 was shown to be primarily present in the early phases of unstable plaque development in the low shear stress segment. Besides, we've shown that inhibition of CXCL10 during it's highest expression result in smaller and more stable lesions. Finally we found that a more stable lesion phenotype correlates with lower levels of CXCL10 in carotid plaques in humans. Since CXCL10 is considered a Tcell related chemokine, which is highly expressed in our mouse model, it is surprising that we find little Tcells in our lesions. We do find strong lymphadenopathy of the lymph nodes draining the carotid artery, suggesting clonal expansion of the Tcell population. So far, we did not analyze these lymph nodes, but it's plausible that much of the Tcell effects take place there.

Monocytes in general are a very multiform inflammatory cell type and known to play a key role in atherogenesis. Though monocytes come in a sliding gradient of appearances, grossly they are categorized into two main subsets. The first develops into inflammatory macrophages (dubbed M1) following vascular extravasation. In mice, they highly expresses CCR2 and Ly6C and has low expression of CX3CR1 (Ly6C^{hi}, CCR2^{hi}, CX3CR1^{lo}) and is the main circulating subset in hypercholesterolemic mice[9]. The second main subset (M2) gives rise to resident type macrophages and dendritic cells and are characterized by a Ly6C^{lo}, CCR2^{lo} CX3CR1^{hi} phenotype. In humans similar subsets have been described and though dissimilarities are present[10], it appears to be a highly evolutionary preserved phenomenon. It must be kept in mind though, that results from the mouse studies cannot be directly translated to human disease.

It is thought that this differential expression of chemokine receptors lies at the basis of the different phases of disease progression. It was expected that the CCR2-CCL2 and the CX3CR1-CX3CL1 axes were the differentiating factors in subset accumulation into the plaque, determining the fate of plaque development. A lower prevalence of atherosclerotic events was described in humans carrying a genetic polymorphism of the CX3CR1 gene, resulting in a loss of function[11]. Possibly this is due to a lower dendritic cell presence in the arterial wall, resulting in less immune activation[12]. Moreover, in our own studies we find differential expression of chemokines, further supporting that hypothesis. Fractalkine comes

to expression during a later phase in the low shear stress segment, just when the plaque destabilizes. This a key step in the disease progression in this model, since inactivation of fractalkine with antibodies results in the development of a stable phenotype with more collagen and less macrophages. This supports the concept that introduction of a different subset of monocyte derived cell to the plaque drives its destabilization.

Contradicting this concept, it was shown recently that both M1 and M2 subsets use the CX3CR1-CX3CL1 axis gaining access to the vessel wall, be it in combination with other chemokines, like CCL5[13]. This sheds new light on recruitment mechanisms and also may have consequences in the development of pharmacological agents to prevent atherosclerosis development. It may be necessary to inhibit multiple chemokine axes to achieve the desired effects, which may also increase chances of unwanted side effects like increased susceptibility to infections.

Future directions

The studies presented in this thesis comprise the two main concepts described above. Future research should be focussed on combining both concepts into a disease mechanism. In order to achieve that, first the immunologic phenotype of the macrophages accumulating upstream in our mouse model should be further determined, especially with regards to chemokine pathways. The functional relevance of the pathways found, should be studies by using specific chemokine (receptor) inhibition models based on genetic loss-of-function and/or functional inhibition with antibodies or specific peptides. Once these pathways are functionally confirmed, it is necessary to study the kinetics of these macrophages by intravital labelling techniques, for example by applying subset specific targeted liposomes or micelles in conjunction with high resolution imaging techniques like micro-MRI or micro-CT. Also, when using fluorescent labels, intravital microscopy can be used. As a first step, kinetics should be studied in multiple mice at multiple time points. Later, repeated measures in single mice could be added. This approach could also be applied to other atherosclerotic predeliction sites like the brachiocephalic artery to rule out model specific mechanisms.

Another issue that needs to be resolved is the lack of Tcell presence in the lesions of the shear stress mediated plaques. For that, the first step would be to analyze the components of the draining lymph nodes of the plaques by standard FACS techniques, specially focussing on a shift towards a more regulatory Tcell phenotype. Also, the plaques should be analyzed at the currently missing time points (2,4,5 and 7 weeks of cast placement) for presence of Tcells. Although this will probably not yield publishable data, it will provide for a much better understanding of the model in general, which in turn may direct future experiments.

Finally, when the studies above have been performed and a clear monocyte migration mechanism has been resolved, the findings should be translated towards

human atherosclerosis, which might be the biggest challenge. Especially since the biological safety of applying labelled contrast agents in humans is unclear. It will be very difficult to get approval from medical-ethical committees to perform those kinds of studies. Until then, human research will be mostly descriptional with respect to cellular composition of plaques by using post-mortem or surgically obtained specimens. By using blood samples of both symptomatic and asymptomatic patients, we may be able to study plaque dynamics on basis of derived parameters.

In conclusion, the field of (experimental) atherosclerosis research will be an exciting area to operate in for the next decades, hopefully resulting in proper diagnostic and therapeutic possibilities for the generations to come.

References

1. Hong M, Mintz G, Lee C, Lee B, Yang T, Kim Y, Song J, Han K, Kang D, Cheong S. The site of plaque rupture in native coronary arteriesa three-vessel intravascular ultrasound analysis. J Am Coll Cardiol. 2005;46:261-265

2. Tanaka A, Imanishi T, Kitabata H, Kubo T, Takarada S, Kataiwa H, Kuroi A, Tsujioka H, Tanimoto T, Nakamura N, Mizukoshi M, Hirata K, Akasaka T. Distribution and frequency of thin-capped fibroatheromas and ruptured plaques in the entire culprit coronary artery in patients with acute coronary syndrome as determined by optical coherence tomography. The American Journal of Cardiology. 2008;102:975-979

3. Martinez HG, Prajapati SI, Estrada CA, Jimenez F, Quinones MP, Wu I, Bahadur A, Sanderson A, Johnson CR, Shim M, Keller C, Ahuja SS. Images in cardiovascular medicine: Microscopic computed tomography-based virtual histology for visualization and morphometry of atherosclerosis in diabetic apolipoprotein e mutant mice. Circulation. 2009;120:821-822

4. Weinreb DB, Aguinaldo JGS, Feig JE, Fisher EA, Fayad ZA. Non-invasive mri of mouse models of atherosclerosis. NMR Biomed. 2007;20:256-264

5. Jarrett BR, Correa C, Ma KL, Louie AY. In vivo mapping of vascular inflammation using multimodal imaging. PLoS ONE. 2010;5:e13254

6. Ratering D, Baltes C, Lohmann C, Matter CM, Rudin M. Accurate assessment of carotid artery stenosis in atherosclerotic mice using accelerated high-resolution 3d magnetic resonance angiography. Magma (New York, NY). 2010

7. Sanz J, Fayad ZA. Imaging of atherosclerotic cardiovascular disease. Nature. 2008;451:953-957

8. Mulder WJM, Fayad ZA. Nanomedicine captures cardiovascular disease. Arterioscler Thromb Vasc Biol. 2008;28:801-802

9. Swirski FK, Libby P, Aikawa E, Alcaide P, Luscinskas FW, Weissleder R, Pittet MJ. Ly-6chi monocytes dominate hypercholesterolemia-associated monocytosis and give rise to macrophages in atheromata. J Clin Invest. 2007;117:195-205

10. Ingersoll MA, Spanbroek R, Lottaz C, Gautier EL, Frankenberger M, Hoffmann R, Lang R, Haniffa M, Collin M, Tacke F, Habenicht AJR, Ziegler-Heitbrock L, Randolph GJ. Comparison of gene expression profiles between human and mouse monocyte subsets. Blood. 2010;115:e10-19

11. McDermott DH, Fong AM, Yang Q, Sechler JM, Cupples LA, Merrell MN, Wilson PWF, D'Agostino RB, O'Donnell CJ, Patel DD, Murphy PM. Chemokine receptor mutant cx3cr1-m280 has impaired adhesive function and correlates with protection from cardiovascular disease in humans. J Clin Invest. 2003;111:1241-1250

12. Liu P, Yu Y-R, Spencer J, Johnson A, Vallanat C, Fong A, Patterson C, Patel D. Cx3cr1 deficiency impairs dendritic cell accumulation in arterial intima and reduces atherosclerotic burden. Arterioscler Thromb Vasc Biol. 2008;28:243

13. Combadière C, Potteaux S, Rodero M, Simon T, Pezard A, Esposito B, Merval R, Proudfoot A, Tedgui A, Mallat Z. Combined inhibition of ccl2, cx3cr1, and ccr5 abrogates ly6c(hi) and ly6c(lo) monocytosis and almost abolishes atherosclerosis in hypercholesterolemic mice. Circulation. 2008;117:1649-1657

Summary | Samenvatting

Summary

Atherosclerosis is considered a major clinical problem, which underlies most ischemic events of both the heart as well as the brain. From the second decade in life onwards, the disease progresses more rapidly. The clinical silence of atherosclerosis is often broken between the third and fifth decade, when patients present with ischemic complaints of e.g. heart and brain.

Lipid metabolism and inflammation mutually influence each other yielding the complete spectrum of atherosclerotic disease progression. The development of atherosclerosis is strongly associated with conditions like hypertension, diabetes, and hypercholesterolemia and bad life style habits like smoking and lack of physical exercise. They induce an unbeneficial environment for the arterial vasculature, enabling the circulating cholesterol-containing lipoproteins to invade the vascular wall. The vessel wall starts to produce inflammatory signaling molecules like chemokines and adhesion molecules. Subsequently, these attract and bind leukocytes to the vascular wall and enhance the inflammatory process, resulting in atherosclerotic disease progression.

Although the classical risk factors of atherosclerosis are of systemic nature, it has long been observed that plaques are not evenly distributed along the arterial tree. In fact, atherosclerotic lesions appear at specific predilection sites. These sites are at or near side branches or bifurcations, where blood flow is non-uniform, or at the lesser curvature of bends, where blood velocity is relatively low. The effect of blood flow on the vessel wall is mediated through fluid shear stress, which arises from the friction between the flowing blood and endothelial cell layer, the inner lining of arteries. It induces a shearing deformation of the endothelial cells, which will be sensed and followed by a biological response influencing atherosclerosis development. The clinical aspect of atherosclerotic disease progression is not merely the slow narrowing of the vascular lumen, resulting in reduced blood flow to the downstream tissues. Depending on the plaque morphology, it may rupture under the influence of the flowing blood. The freed fatty plaque contents induce a sudden thrombotic response, resulting in acute arterial obstruction. It was previously that shown plaque morphology is dependent on the shear stress pattern the vessel wall was exposed to. Arterial locations exposed to: 1. Low shear stress give rise to unstable plaques prone to rupture, 2. High shear stress protects from atherosclerosis and 3. Oscillatory shear stress results in stable plaque formation.

So, evidence exists that the shear forces on the endothelial cells influence the development of plaque vulnerability. However, the (immunological) mechanisms involved in this shear stress mediated vulnerable plaque development are currently unclear. In this thesis we aimed to clarify some of the immunological mechanisms involved, working towards future therapeutic interventions in treatment and prevention of unstable plaque rupture. Since it is very difficult to perform such

mechanistic studies in humans, we studied experimental atherosclerosis in two specific animal models.

In **Chapter 2**, we studied the spatial organization of atherosclerotic plaques in relation to local variations of shear stress along the vessel wall. By obtaining the arterial geometry by intravascular ultrasound of an atherosclerotic plaque created in rabbits, we were able to calculate the differences of shear stress along the length of the plaque. Next, we superimposed the histological data acquired later onto this geometry. By using elaborate image processing software we were able to show the spatial relation of histological markers like macrophages, smooth muscle cells, lipids, gelatinolytic activity, and oxidized low-density lipoprotein in relation to their local shear stress pattern. Results showed a predominant upstream localization of macrophages and gelatinase activity. Colocalization studies indicated that gelatinase activity was associated with macrophages and smooth muscle cells, and that this was caused by subsets of smooth muscle cells and macrophages, which were associated with oxidized low-density lipoprotein accumulation.

We concluded that localization of a vulnerable plaque phenotype is probably due to an accumulation of oxidized low-density lipoprotein, which activates/induces subsets of smooth muscle cells and macrophages to gelatinase production, which results in plaque degradation and destabilization of the plaque.

Chapter 3 describes further studies of the spatial organization of plaques, this time in plaques induced by a standardized shear stress modifying device (cast) in a mouse model of atherosclerosis. We focused on plaques exposed to low shear stress, which is known to acquire characteristics of vulnerable plaque. We found evidence of plaque disruption (e.g. intraplaque hemorrhage), but only in the upstream segment of the lesions, accompanied by increased macrophage activation compared to the downstream segment. The upstream localization of disruptions is in accordance with findings in humans. We concluded that the vulnerability of atherosclerotic plaque induced by a low shear stress flow pattern is located predominantly in the upstream lesion segment. This is associated with activation of macrophages and relatively low collagen content, but partly dissociated from gelatinase activity.

Following these studies of descriptive nature, we next focused on the immunological mechanisms that underlie the findings described above. Therefore we studied the expression and function of multiple chemokines during different stages of atherosclerotic plaque development in our mouse model using the shear stress modifying cast. In **chapter 4** we first determined which of the chemokines previously mentioned to be critical in disease development are expressed in our lesions. We found clear differences between the plaques induced by low and oscillatory shear stress. We also found differences within the segments over time. So plaque dynamics are both shear stress and time related. We found for example

that MCP-1, a key chemokine involved in monocyte recruitment, was expressed highest during the early phases of plaque development in both low and oscillatory shear stress segments, but expression was much lower at later time point when low shear stress lesions destabilized. Fractalkine, another monocyte recruiting chemokine, was selectively expressed in the low shear stress segment during the destabilization. Since this was such a striking finding, we performed fractalkine inhibition studies, which resulted in much more stable lesions, characterized by an increase in collagen and a decrease in macrophages. We concluded that different shear stress fields yield different plaque compositions associated with different responses in chemokine expression. We also concluded that low shear stress induces the development of larger lesions of which the composition resembles lesions in humans with a less "stable" phenotype and that fractalkine appears to be crucial in the development of the distinct plaque phenotype that is induced by LSS.

A second chemokine that was selectively expressed in low shear stress induced lesions was CXCL10. This particular chemokine was studied in mice in a similar way as fractalkine (**chapter 5**). By inhibiting CXCL10, which is expressed earlier in the plaque development compared to fractalkine, we found that plaques were similar in size, but with much less macrophage activation and more collagen content. This resulted in plaque morphology with a more stable phenotype. We found that there is an association between the plaque concentration of CXCL10 and a more atheromatous phenotype in human carotid artery specimens obtained during endarterectomy. Thus we concluded that CXCL10 is a key chemokine in atherosclerosis and that a functional relationship was shown in mice, whereas clues for a similar relationship in humans were found.

Since the molecular pathways underlying the inflammatory response in artherosclerotic plaque development are extremely complex, we tried to gain further insight by using whole-genome microarrays (**chapter 6**). By laser capture microdissection, we solely obtained plaque tissue with endothelial cells, excluding the muscular arterial wall and its adjacent adventitial structures. This was done to get a clearer signal from mechanisms inside the plaque itself. The extracted RNA from the captured lesions was amplified and run on microarrays. The results were unexpected since no clear vascular or immunological pathways were identified during post-analysis. Moreover, we did find some highly expressed neuronal proteins to be present, but only one of these could be detected by immunostaining. The relevance of these findings for the development of atherosclerosis is unknown and at present these data do not substantiate any firm conclusions. In the light of (technical) advancements in both small quantity RNA processing and bioinformatic analysis methodology, the study should be repeated in order to draw any conclusions.

In **chapter 7** the results of this research project is discussed in a broader perspective

with regard to atherosclerosis development and suggestions for future directions are discussed.

Samenvatting

Atherosclerose, in de volksmond aderverkalking, is een klinisch belangrijk probleem, wat ten grondslag ligt aan ischemische aantasting van zowel het hart als de hersenen. Vanaf de tweede decade van het leven, ontwikkeld de ziekte zich steeds sneller. De klinische stilte ervan wordt vaak doorbroken vanaf middelbare leeftijd, wanneer patiënten klachten krijgen als gevolg van zuurstof tekort in de hartspier en/of het brein.

Vetstofwisseling en ontsteking beïnvloeden elkaar wederzijds, waarbij het hele spectrum van het ziektebeeld tot uiting komt. Progressie van het ziektebeeld is sterk geassocieerd met hoge bloeddruk, diabetes, een verhoogd cholesterol en slechte leefgewoontes zoals roken en gebrek aan beweging. Deze factoren faciliteren een ongunstig milieu voor de arteriële vaatsysteem waarin cholesterol bevattende lipoproteïnen zich in de vaatwand kunnen nestelen. Dit stimuleert de vaatwand tot productie van ontstekingsgebonden signaal moleculen, zoals chemokines en adhesie moleculen. Vervolgens trekken deze signaal moleculen witte bloedlichamen aan welke het ontstekingsproces verder stimuleren, wat leidt tot progressie van de aderverkalking.

Ondanks dat de risicofactoren voor atherosclerose over het gehele lichaam hun effect hebben, is het al lang bekend dat aderverkalking niet gelijkmatig is verdeeld over de vaatboom. In tegenstelling juist, er zijn voorkeurslocaties te beschrijven. Deze locaties bevinden zich bij aftakkingen of splitsingen van bloedvaten (daar waar de bloedstroom niet uniform is), of in binnenbochten (waar de bloedstroom relatief laag is). Het effect van de bloedstroom op de vaatwand wordt gestuurd door de shear stress (afschuifspanning), welke voortkomt uit de wrijving tussen het stromende bloed en de bedekkende cellaag (het endotheel) van het bloedvat. De shear stress zorgt voor een vervorming van de endotheelcellen, welke wordt waargenomen door de cel, wat weer leidt tot een biologische respons welke de aderverkalking beïnvloedt.

Het klinische aspect van atherosclerose is niet slechts het langzaam smaller worden van de vaatdoorgang (lumen), wat leidt tot verminderde bloedstroom naar de weefsels achter de vernauwing. Afhankelijk van de opbouw en samenstelling van de atherosclerotische plaque, kan deze scheuren onder invloed van het stromende bloed. Der vettige plaque inhoud komt dan in contact met het bloed, wat resulteert in een acute stollingreactie gevolgd door plotse verstopping van het bloedvat. Het is bekend dat de samenstelling van de plaque afhankelijk is van de soort shear stress die op de vaatwand wordt uitgeoefend. 1. Lage shear stress geeft instabiele plaques die kunnen scheuren. 2. Hoge shear stress beschermt tegen aderverkalking. 3. Oscillatoire shear stress resulteert in stabiele plaque vorming.

Er is dus wetenschappelijk bewijs dat afschuifkrachten op het endotheel de plaque stabiliteit beïnvloedt. De (immunologische) mechanismen die hieraan

ten grondslag liggen, zijn echter nog onduidelijk. In dit proefschrift hebben we gepoogd enkele van deze immunologische mechanismen verder te ontrafelen, om toekomstige therapeutische interventies en behandeling van instabiele plaques mogelijk te maken. Om dat het zeer moeilijk is om deze mechanismen in mensen te onderzoeken, hebben we hiervoor twee verschillende proefdiermodellen gebruikt.

In **hoofdstuk 2**, hebben we de spatiële organisatie van plaques bestudeerd in relatie met de locale variaties in shear stress over de vaatwand. Met behulp van intravsaculaire ultrageluid (IVUS) opnames werd de geometrie van in konijnen opgewekte atherosclerotische plaques verkregen. Op basis hiervan werd de verdeling van shear stress berekend. Vervolgens werd de histologische data van de plaques hier overheen gelegd. Met behulp van uitgebreide image processing software konden we spatiële relatie tussen histologische markers van macrofagen, gladde spiercellen, lipiden, gelatinolytische activiteit en geoxideerd low-density lipoproteine (oxLDL) vergelijken met de locaal aanwezige shear stress patronen. De resultaten toonde een voorkeur voor stroom opwaartse ophoping van macrofagen en gelatinolytische activiteit. Colocalisatie studies toonde dat gelatinase activiteit geassocieerd was met macrofagen en gladde spiercellen en dat dit werd veroorzaakt door een subgroep van deze cellen welke geassocieerd was met ophoping van oxLDL. We concludeerden dat de lokalisatie van het instabiele plaque fenotype waarschijnlijk het gevolg is van een ophoping van oxLDL, wat een subgroep van gladde spiercellen en macrofagen activeert tot de productie van gelatinase, wat resulteert in de afbraak en destabilisatie van de plaque.

In **hoofdstuk 3** wordt de spatiële organisatie van plaques verder beschreven, dit maal in plaques die zijn opgewekt met behulp van een gestandaardiseerde shear stress veranderende cilinder (cast), in een muis model voor atherosclerose. We richtten ons op de plaque geïnduceerd onder lage shear stress, waarvan bekend is dat ze kenmerken van een instabiele plaque kunnen hebben. We vonden bewijs voor verstoring van de plaque (bijvoorbeeld intraplaque bloedingen), maar alleen in het stroomopwaartse deel. Dit ging gepaard met verhoogde aanwezigheid van macrofagen vergeleken met het stroomafwaartse deel. Deze stroomoopwaartse neiging tot disruptie is in overeenstemming met bevindingen in mensen. We hebben geconcludeerd dat neiging tot instabiliteit van door lage shear stress geïnduceerde plaques zich vooral bevind in de stroomopwaartse delen van de plaque. Dit is geassocieerd met activatie van macrofagen en een relatief lage hoeveelheid collageen, echter zonder verhoging van de gelatinase activiteit.

Na deze twee beschrijvende studies hebben we ons gefocust op de onderliggende immunologische mechanismen. Hiervoor hebben we de expressie en functie van enkele chemokines gedurende verschillende tijdstippen van atherosclerotische plaque ontwikkeling bestudeerd in het muis model met behulp van de shear stress beïnvloedende cast. In hoofdstuk4 hebben we eerst bepaald welke van de eerder

voor atherosclerose relevante beschreven chemokines tot expressie komen in ons model. We vonden opvallende verschillen tussen de plaque segmenten blootgesteld aan lage en oscillatoire shear stress. Daarnaast was er ook een duidelijk verschil in expressie over de tijd. Dus de plaque dynamiek wordt beïnvloed door zowel de locatie als het tijdstip. We beschrijven bijvoorbeeld dat het chemokine MCP-1, welke belangrijk is bij het aantrekken van monocyten, het hoogste is in de vroege fases van plaque ontwikkeling in zowel gebieden van lage als van oscillatoire shear stress, maar dat de expressie later veel lager is als wanneer het lage shear stress segment instabiele kenmerken toont. Fractalkine, een chemokine wat ook monocyten aantrekt, daarentegen was specifiek hoog in expressie in het lage shear stress segment gedurende plaque destabilisatie. Omdat dit zo'n opvallende bevinding was, hebben we vervolgens fractalkine remmingsexperimenten verricht. Dit resulteerde in veel stabielere plaques, gekenmerkt door hogere aanwezigheid van collageen en lagere aantallen macrofagen. We concludeerde dat verschillende shear stress profielen leiden tot morfologisch verschillende plaques wat wordt veroorzaakt door verschillen in chemokine expressie. Daarnaast werd geconcludeerd dat lage shear stress zorgt voor grotere plaques met instabiele kenmerken en dat fractalkine hierin een sleutelrol speelt.

Een tweede chemokine dat specifiek tot expressie kwam in lage shear stress plaques was CXCL10. Dit specifieke chemokine werd op eenzelfde manier bestudeerd als fractalkine (**hoofdstuk 5**). Door remming van CXCL10, wat eerder tot expressie komt in vergelijking met fractalkine, vonden we dat de plaquegrootte niet veranderde, maar dat de hoeveelheid collageen toename en de macrofaag activatie daalde. Dit resulteert in stabielere plaques. Daarnaast beschrijven we dat er in atherosclerotisch materiaal, verkregen tijdens menselijke halsslagader operaties, een associatie is tussen de hoeveelheid CXCL10 in de plaque en een meer atheromateuze plaque morfologie. We hebben geconcludeerd dat CXCL10 een sleutel chemokine is de ontwikkeling van atherosclerose en dat er een functionele relatie is aangetoond in muizen en aanwijzingen voor een gelijk mechanisme in mensen.

Omdat de moleculaire mechanismen die ten grondslag liggen aan de ontstekingsreactie in atherosclerose extreem complex zijn, hebben we met behulp van whole genome microarrays getracht hierin meer inzicht te verkrijgen (**hoofdstuk 6**). Met behulp van laser capture microdissectie, hebben we specifiek het plaque weefsel geïsoleerd om verstoring van de adventitia en spiercellaag van de vaatwand te voorkomen. Het RNA wat hieruit werd verkregen werd vermenigvuldigd en gemeten op microarrays. De resultaten waren onverwacht omdat er geen duidelijk vascular of immunologisch profiel naar boven kwam tijdens de analyse van metingen. Er waren een aantal neuronale eiwitten die sterk vertegenwoordigd waren, echter geen enkele daarvan kon histologisch worden bevestigd in de weefsels. De relevantie van deze bevindingen in het kader van

atherosclerose zijn nog onduidelijk en niet voldoende voor enige conclusies. In het kader van (technische) vooruitgang in het verwerken van zeer minuscule hoeveelheden RNA en bioinformatica analyses die er op volgen, moet deze studies worden herhaald indien we duidelijke conclusies willen trekken.

In **hoofdstuk 7** worden de bevindingen van dit onderzoeksproject in een breder perspectief bediscussieerd met betrekking op ontwikkeling van atherosclerose en worden suggesties gedaan voor toekomstig onderzoek.

List of Publications

Journal Articles

Inflammation and atherosclerosis: mechanisms underlying vulnerable plaque.
Krams R, **Segers D**, Mousavi Gourabi B, Maat W, Cheng C, van Pelt C, van Damme LC, de Feyter P, van der Steen T, de Korte CL, Serruys PW.
J Interv Cardiol. 2003 Apr;16(2):107-113

Monocyte Adhesion in Atherosclerosis: A Biomechanical Approach.
Segers D, Cheng C, de Crom R, Kirschbaum S, Oostlander, A, Helderman F, van Wamel A, Slager C, Serruys PW, van der Steen AF, Krams R.
Vascular Disease Prevention. 2005; 2(3): 227-235

Shear stress is associated with markers of plaque vulnerability and MMP-9 activity.
Krams R, Cheng C, Helderman F, Verheye S, van Damme LC, Mousavi Gourabi B, Tempel D, **Segers D**, de Feyter P, Pasterkamp G, De Klein D, de Crom R, van der Steen AF, Serruys PW.
EuroIntervention. 2006 Aug;2(2):250-256

Gelatinolytic activity in atherosclerotic plaques is highly localized and is associated with both macrophages and smooth muscle cells in vivo.
Segers D, Helderman F, Cheng C, van Damme LC, Tempel D, Boersma E, Serruys PW, de Crom R, van der Steen AF, Holvoet P, Krams R.
Circulation. 2007 Feb 6;115(5):609-616

Shear stress-induced changes in atherosclerotic plaque composition are modulated by chemokines.
Cheng C, Tempel D, van Haperen R, de Boer HC, **Segers D**, Huisman M, van Zonneveld AJ, Leenen PJ, van der Steen A, Serruys PW, de Crom R, Krams R.
J Clin Invest. 2007 Mar;117(3):616-626

Effect of shear stress on vascular inflammation and plaque development.
Helderman F, **Segers D**, de Crom R, Hierck BP, Poelmann RE, Evans PC, Krams R.
Curr Opin Lipidol. 2007 Oct;18(5):527-533

Large variations in absolute wall shear stress levels within one species and between species.
Cheng C, Helderman F, Tempel D, **Segers D**, Hierck B, Poelmann R, van Tol A, Duncker DJ, Robbers-Visser D, Ursem NT, van Haperen R, Wentzel JJ, Gijsen F, van der Steen AF, de Crom R, Krams R.
Atherosclerosis. 2007 Dec;195(2):225-235.

Atherosclerosis: cell biology and lipoproteins-shear stress and inflammation in plaque formation: new evidence.
Segers D, Weinberg P, Krams R.
Curr Opin Lipidol. 2008 Dec;19(6):627-628

A primer on the immune system in the pathogenesis and treatment of atherosclerosis.
Segers D, Garcia-Garcia HM, Cheng C, de Crom R, Krams R, Wentzel JJ, van der Steen AF, Serruys PW, Leenen PJ, Laman JD.
EuroIntervention. 2008 Nov;4(3):378-390

Contrast enhancement by differently sized paramagnetic MRI contrast agents in mice with two phenotypes of atherosclerotic plaque.
van Bochove GS, Paulis LE, **Segers D**, Mulder WJ, Krams R, Nicolay K, Strijkers GJ.
Contrast Media Mol Imaging. 2011 Jan-Feb;6(1):35-45

Atherosclerotic plaque stability is affected by the chemokine CXCL10 in both mice and humans
D. Segers, J.A. Lipton, P.J.M. Leenen, C. Cheng, D. Tempel, H.J. Duckers, G. Pasterkamp, F.L. Moll, R. de Crom, R. Krams.
International Journal of Inflammation, in press

Submitted Journal Articles

Atherosclerotic plaque vulnerability in a mouse model of atherosclerosis is predominantly located in the upstream segment of the lesion
D. Segers, R.Krams, R. de Crom, P.J.M. Leenen.

Fibromodulin deficiency reduces the formation of vulnerable but not stable atherosclerotic lesions in Apolipoprotein E-null mice
A. Shami,R. Gustafsson, S. Kalamajski, R. Krams, **D. Segers**, U. Rauch, G. Roos, J. Nilsson, Å. Oldberg, A. Hultgårdh-Nilsson.

Dankwoord

Als laatste misschien wel het meest gelezen onderdeel van het proefschrift; het dankwoord. Vanzelfsprekend doe je een AIO-project niet in je eentje. Ik denk ook niet dat het mogelijk zou zijn en je moet het ook niet willen. Alle samenwerking is een van de meest waardevolle onderdelen van het hele proces. Vandaar dat een woord van dank dan ook het minste is wat ik kan doen om de mensen te erkennen die me hebben bijgestaan. Het risico bestaat natuurlijk altijd dat je iemand vergeet, gelukkig weten degenen die dank toekomt dat ook zonder een paar regels hieronder.

Professor Krams, beste Rob. Dank je wel voor de mogelijkheden die je me hebt geboden om dit project uit te voeren. Ik denk dat je een zeer goede wetenschapper bent. Je creativiteit en originaliteit zie ik als benijdenswaardige eigenschappen en ben dan ook blij dat je mijn promotor wil zijn. Ook al was de samenwerking na je vertrek uit Rotterdam soms moeizaam, indien nodig kon ik toch een beroep op je doen. Ik heb de gehele ervaring als zeer leerzaam en uitdagend ervaren, dank daarvoor.

Professor Van der Steen, beste Ton. Ondanks het feit dat ons beider werk zich in de uitersten van het spectrum in atherosclerose onderzoek bevinden, werken we toch aan hetzelfde doel. Het is een genoegen om onder je te promoveren. Dank je wel voor de geboden ondersteuning, vooral ook in de laatste fase van het project.

Professor Duncker, Professor Grosveld en Professor Pasterkamp dank aan jullie allen voor het zitting nemen in de kleine commissie en het lezen en beoordelen van mijn proefschrift. Ik ben zeer benieuwd naar jullie commentaren.

Rini de Crom, beste Rini, mijn redder in "verlaten-AIO-nood". Mijn dank is groot. Voor de benchruimte, een kantoorplek, je laboranten, je organisatie (talent), je rust, de financiële ondersteuning. Zo kan ik nog wel even door gaan, maar vooral bedankt voor het beschikbaar zijn waneer het nodig was! Ik zou niet weten hoe het had moeten gaan als je me niet zo had gesteund. Nogmaals heel veel dank.

Pieter Leenen, beste Pieter. Wat ben jij een aanstekelijk enthousiast persoon. Ik heb ècht genoten van alle korte ad hoc- en lange geplande meetings. De manier waarop jij in de wetenschap staat is geweldig. Geen gedachte is gek of onconventioneel genoeg, maar nooit uit de lucht gegrepen. Dank voor alle steun over de afgelopen jaren, zowel wetenschappelijk als persoonlijk. Hopelijk krijg je de mogelijkheid om nog wat langer in het atherosclerose veld te blijven werken.

Alle mensen op de verschillende laboratoria (semi-chronologisch). Luc van Damme, dank je voor je hulp bij de 3D histologie studie. Je beloning komt echt nog een keer; Feyenoord wordt vast wel weer eens kampioen. Caroline Cheng; ik heb je niet altijd begrepen, wel altijd zeer gewaardeerd. Ik heb grote bewondering hoe jij door je wetenschappelijke carrière gaat. Veel succes. Dennie, dank je voor al je antwoorden en hulp op het lab. Veel succes nu met je eigen AIO project. Hang in there, de vruchten aan het eind zijn zoet. Rien, ik vind het jammer dat we elkaar pas op het einde van mijn lab-tijd hebben leren kennen. Je kennis is ongekend, je organisatie methoden trouwens ook. Teus, bedankt voor je analyses van mijn serum samples. Ik zal proberen om de toevoer aan Zweden kalenders voor je veilig te stellen. Adrie/A3, jammer dat onze gezamenlijke inspanningen op de FACS niet zijn gehonoreerd, ik had het graag anders gezien. Jon Laman dank je voor de vele prikkelende vragen die je me hebt gesteld. Marjan van Meurs bedankt voor al jullie hulp bij de kleuringen. Kim, ik zal al je vragen missen. Je neemt mijn rol op de afdeling celbiologie al langzaam over. Veel succes daarmee (en mail me maar als er toch nog een vraagje overblijft).

Al mijn andere lab collega's van de afdelingen Celbiologie en Genetica, (Experimentele) Cardiologie, Immunologie dank voor de praatjes en de inspirerende tijd aan de bench, in de flow-kast of achter de microscoop. Voel je zéker aangesproken!

Beste Sonja, het was fijn om dagelijks met je te lunchen. Even de gedachten verzetten en na de cappuccino weer opgewekt aan de slag. Ik ben het zeker gaan missen.

Beste Mieke, hoofdcoordinator voor mijn promotie plechtigheid, dank je voor al het werk dat je voor me hebt gedaan. Het was fijn om iemand te hebben die alle vragen over de promotie kon beantwoorden.

Karl, thanks mate for all your support in the micrarray study. Your meticulous methods in performing the work were awesome. Also thanks for the nice conversations and the movies. Good luck in your scientific carrere.

Thijs, bedankt kerel. Het was fijn om af en toe mijn pieken en dalen met je te delen, in de wetenschap dat je precies wist wat ik bedoelde omdat je met dezelfde dingen rond liep. Ik heb onze lunches erg gemist de laatste jaren. Het was bijzonder om samen door deze fase heen te gaan. Wij komen er wel. Het was mijn eer om bij jou promotie naast je te staan. Nu is het jou beurt.

Bram, fijn de je mijn paranimf wil zijn. De gesprekken met jou waren een steun in zowel de goede als de lastige tijden. Het is fijn om af en toe te kunnen sparren met iemand met onderzoekservaring in een ander veld. Dank daarvoor. We gaan snel een tafel in Muiderberg reserveren. In een restaurant bedoel ik dan.

Heeren reünisten van D.D.A.M.T. Meridies, jullie jarenlang durende hoon over het gedoe met muisjes was mooi. Precies wat je van dispuutsleden verwacht. Gelukkig proefde ik tussen die hoon genoeg oprechte interesse en steun die zo onmisbaar zijn tijdens een promotie traject. Bedankt. Binnenkort een biertje doen?

Walter, Franka en Irene, ook jullie mag ik zeker niet vergeten. Jullie positieve blik op het leven is inspirerend en was een goede bron van motivatie als het even tegen zat.

Caroline, Stinky, zusje, dank je wel voor je lieve steun en betrokkenheid. Je telefoontjes en onze gezamelijke gekkigheid zijn altijd welkom. Het is maar goed dat er niet overal camera's hangen, anders waren we allang samen ergens opgesloten. Gelukkig kunnen we ook serieus zijn, en da's mooi!

Pappa en mamma, Gert Jan en José. Dank je wel voor jullie onvoorwaardelijke steun en interesse. Het is moeilijk uit te leggen hoe belangrijk dat tot op de dag van vandaag nog is.

Als laatste natuurlijk Mireille, lief Miepje. Wat hebben we het toch goed samen! Het is een genot om iedere dag weer bij je te zijn. Goede dagen worden gekoesterd en slechte dagen zijn zo weer vergeten. Deze fase hebben we in ieder geval samen tot een goed einde gebracht. We hebben nog een geweldige tijd voor de boeg en het is het grootste plezier van mijn leven dat ik dat met jou mag gaan beleven. Ik hou van je, dikke kussie!

Curriculum Vitae

Dolf Segers was born on August 28th in Tilburg, The Netherlands. In 1995 he graduated from HAVO at the Mollerlyceum in Bergen op Zoom. Directly following, he participated in a high school exchange programm for one year in Lancaster, Califormia, USA. It was there and then he decided to become a medical doctor. Upon return he obtained his necessary VWO diploma within the same year.

In 1998, he got admitted to medical school at the Erasmus University Medical Center in Rotterdam, after one year of studying Health Sciences at the Maastricht University. In 2002 he obtained his medicine masters degree, after finishing his master thesis in the department of Experimental Cardiology of the Erasmus University Medical Center, which was headed by professor Dirk Duncker. This research project was supervised by professor Rob Krams and resulted in a position as a PhD candidate in the department of Biomedical Engineering of the Thoraxcenter in Rotterdam. During his PhD studies from 2003 until 2009, he also finished his internships and obtained the MD degree in 2005.

Since April 1st 2009, he is a cardiologist-in-training under supervision of dr. F.J. ten Cate at the Thoraxcenter of the Erasmus University Medical Center. Currently, he is working as a resident at the department of cardiology at the Amphia Hospital in Breda, The Netherlands.

PhD Portfolio

Specific courses offered by COEUR:	Year	ECTS
Congenital heart disease	2004	1.5
Atherosclerosis research	2006	1.5
Molecular biology in atherosclerosis and cardiovascular research	2007	1.5
Cardiovascular imaging and diagnostics	2008	1.5
Erasmus MC courses		
Basiscursus Microchirurgie	2005	1.5
Analysis of microarray gene expression data	2007	1.5
Statistiek basis	2007	1.5
Biomedical writing	2007	4
COEUR Research seminars:	**Year**	**ECTS**
Arrythmia Research	2007	0.4

Other courses followed:	Year	ECTS
Artikel 9, wet op dierproeven	2004	4,5
Dutch Heart Association course Vascular Biology	2005	2.0
Postdoctorale cursus Medische Immunologie	2007	1.5

Symposia and congresses	Year	ECTS
Dutch Atherosclerosis Society symposium	2004, 2005, 2006, 2007	2.1
Shear Stress symposium	2006, 2007, 2008	1.8
AHA Scientific Sessions 2006, Chicago, USA	2006	1.5
NVVI voorjaarssymposium	2006, 2007	1.2
AHA Scientific Sessions 2007, Orlando, USA	2007	1.5

Supervision of students	Year	ECTS
Internship of 4 HLO students (6 months each)	2006-2008	8
Internship of 1 MLO Student (6 months)	2008	2